

WATER CONTAMINATION IN THE AREA OF A LANDFILL COAL ASH

Jean Marie SINZINKAYO

Dissertation submitted in fulfilment of the requirements for the degree of
MASTER IN MINING AND GEO-ENVIRONMENTAL ENGINEERING

Supervisor: Prof. Maria Cristina da Costa Vila

Co-Supervisor: Prof. Renata Maria Gomes dos Santos

Director of Master's Programme: Prof. José Manuel Soutelo Soeiro de Carvalho

Examiner: Prof. Antonio Manuel Antunes Fiuza

NOVEMBER 2017

MASTER IN MINING AND GEO-ENVIRONMENTAL ENGINEERING 2016/2017

DEPARTMENT OF MINING ENGINEERING

Tel. +351 22 0413163/220413164

Edited by:

FACULDADE DE ENGENHARIA DA UNIVERSIDADE DO PORTO

Rua Dr. Roberto Frias

4200-465 Porto

Portugal

Tel. +351 22 508 1400

Fax +351 22 508 1440

Email feup@fe.up.pt

URL <http://www.fe.up.pt>

Partial reproduction of this work is allowed as long as the Author is mentioned together with the Master in Mining and Geo-Environmental Engineering – 2016/2017, Department of Mining and Geo-Environmental Engineering, University of Porto – Faculty of Engineering (*Faculdade de Engenharia da Universidade do Porto - FEUP*), Portugal 2017.

The opinions and information included herein solely represent the views of the Author and the University may not accept legal responsibility or otherwise in relation to errors or omissions that may exist.

This document was produced from an electronic copy provided by the Author.

In God I Trust.

ABSTRACT

Water contamination is a threat to our lives on massive scale because it affects the food chain. With the need of socio-economic development, anthropogenic activities such as, mining and industries are severely affecting the aquatic ecosystem. Former mining plants and industries used to stockpile waste and tailings or ashes on land and discharged leachates or regeants into surface water.

The present work is the part of a broader research project which intended to analyze the potential pollution caused by a landfill of coal ashes originated by an ancient coal power station in northern Portugal.

The run off waters collected from a drainage piping system around the side-hills of the storage (“fibrocimento tube”) are contaminated with heavy metals and its pH is in the range of 2.9-5.4 revealing acid mine drainage generation.

The pollution is analyzed by implementing a transport model with advection, dispersive-diffusion and degradation considering a first-order kinetics. The implementation of the transport and fate model was performed both with Microsoft Excel and Matlab. The simulation allowed to estimate the final concentrations of the contaminant at the discharge point into Douro river. Comparison between these concentrations and the threshold limits for emission of wastewater reveals that only manganese exceeds the threshold limit. The decrease of the concentrations of contaminants is due to natural attenuation by clays natural minerals and sorption into organic matter of the soil in the area.

Keywords: Heavy metals, Pollution, Landfill coal ash, Transport model, Water quality, threshold value.

Résumé

La contamination de l'eau est une menace à grande échelle pour notre vie car elle affecte la chaîne alimentaire. Les anciennes industries minières utilisaient le stockage à découvert sur terre des déchets et résidus et deversaient les lixiviats dans les eaux de surface.

Le présent travail fait partie d'un projet de recherche plus large qui vise à analyser l'évolution de la pollution causée par le dépôt de cendres de charbon d'une ancienne centrale thermoélectrique dans la région de Medas de la municipalité de Gondomar au Portugal.

L'eau provenant de ce dépôt de cendres de charbon (tuyau Fibrocimento) est polluée par des métaux lourds et son pH dans la gamme de 2,9-5,4 révèle la génération d'un drainage minier acide. Cette évolution de pollution est analysée par un modèle de transport de l'eau sur terre en développant la première loi de Fick et en considérant la dégradation de premier ordre de ces métaux lourds. L'application de ce modèle de transport aux logiciels excel et matlab déduit à la concentration finale de chaque métal lourd dans l'eau déversée dans le fleuve Douro. La comparaison de ces valeurs de concentration des métaux lourds avec la valeur limite maximale de l'émission de résidus dans l'eau révèle que seule la concentration du manganèse dépasse la valeur limite admise. Le déclin des valeurs de concentration des autres métaux lourds est dû au phénomène d'atténuation naturelle des minéraux argileux et des composés organiques du sol dans ces milieux.

Mots-clés: Métaux lourds, Pollution, dépôt de Cendres de charbon , Modèle de transport ,Qualité de l'eau, valeur seuil.

ACKNOWLEDGEMENTS

I would like to express my gratitude to my supervisors Prof. Maria Cristina da Costa Vila and Prof. Renata Maria Gomes dos Santos for their useful comments, remarks and scientific rigors they addressed to me during this master thesis work.

Furthermore, I would like to address my special thanks to Prof. José Manuel Soutelo Soeiro de Carvalho, Director of the master degree program for his kind guidance and advice from the beginning of the learning process at University of Porto. I'm grateful to Prof. Antonio Manuel Antunes Fiuza who willingly shared his precious time and knowledge during my postgraduate studies at University of Porto.

I'm also very grateful to Father Paul Zingg of Schoenstatt community of Geneva for helping me and providing me with funding during these days.

A very special gratitude goes to all Erasmus-Mundus/Kite project coordinators from whom I owed the scholarship which allowed me to come to University of Porto.

My deep thanks are addressed to my late father who has gone before harvesting the fruits of his effort to send me to school. I also thank my lovely Mother, my brothers, sisters and nephews for their long prayers.

I thank greatly my family, my wife Gloriose NSHIMIRIMANA and my lovely daughter Laena SINZINKAYO for their patience during my absence.

Student life abroad is not easy but I am lucky to have met Abel Cunha Rodrigues and Jorge Mayer families who supported me during my stay in Portugal, many thanks go to them.

To the community of the Faculty of Engineering of the University of Porto I address my great thanks.

Dedication

I dedicate my dissertation to my wife Gloriose NSHIMIRIMANA and my daughter Laena SINZINKAYO.

I also dedicate my work to my parents, especially my Mom, my brothers NDUWAYO Laurent, GATOTO Audace and my sisters NDUWIMANA Yolande, NDIKUMUREMYI Judith and NDAYIKENGURUKIYE Godeliève, my uncles and nephews.

To my friends and all those who support education for all, I dedicate my dissertation.

CONTENT

ABSTRACT.....	ii
ACKNOWLEDGEMENTS.....	iv
Dedication.....	v
LIST OF FIGURES.....	ix
LIST OF TABLES.....	xi
ACCRONYMS.....	xii
Chapter 1. Introduction.....	1
1.1. General Introduction.....	1
1.2. Objective of the dissertation.....	1
1.3. Dissertation structure.....	2
1.4. Water.....	2
1.5. Water quality.....	3
1.5.1. Water quality threshold limit value.....	4
1.5.2. Portugal water quality threshold value.....	5
1.6. Contamination/pollution.....	6
1.6.1. Water pollution.....	7
1.6.2. Water pollution sources.....	7
1.7. Heavy metals pollution.....	8
1.7.1. Heavy metal definition.....	9
1.7.2. Heavy metals toxicity properties.....	9
1.7.3. Source of heavy metals pollution.....	16
1.7.4. Fate of heavy metals as pollution.....	16
1.7.4.1 Pollution of aquatic life.....	17
1.7.4.2. Acid mine drainage pollution.....	18
1.7.4.2.1. Chemistry of Acid Mine drainage.....	18
1.7.4.2.2. Effects of Acid Mine Drainage on aquatic life.....	19
1.7.5. Heavy metals transport in water.....	20
1.8. Case study.....	21
1.8.1. Douro River.....	23

Chapter 2. DISSERTATION METHODOLOGY	24
2.1. Transport model application from Fibrocimento tube to Douro river	24
2.1.1. Advection/convective process	24
2.1.2. Dispersion process	24
2.1.3. One-dimensional model within surface water	24
2.1.4. Solution of the one-dimensional model	26
2.1.5. Solution of the equation taking into account of degradation	26
2.1.5.1. Kinetic constant study.....	27
2.1.5.1.1.Adsorption kinetic constant determination	28
2.1.5.1.2. Natural clays for heavy metals adsorption	28
2.1.5.1.3.Chitosan as natural occurring for Aluminum adsorption	29
2.1.5.2. Estimating Diffusion Coefficients in Aqueous Systems.....	30
2.2.Transport model implementation	32
2.2.1.Microsoft excel implementation protocol	32
2.2.2.Matlab implementation protocol	33
2.2.2.1. Transport model-Time variable implementation protocol.....	33
2.2.2. 2.Transport model-Distance variable implementation protocol	34
2.3. Available data.....	34
2.3.1 Data from monitoring field	34
2.3.2. Calculated and converted dimensions.....	36
Chapter 3. RESULT AND DISCUSSION.....	37
3.1. Data analysis	37
3.2. Results.....	37
3.2.1. Results from Microsoft excel implementation	38
3.2.1.1. Results from Microsoft excel for transport model-time evolution with degradation from the source.....	38
3.2.1.2.Results from Microsoft excel for transport model- distance evolution with degradation from the source	50
3.2.2. Results from matlab implementation.....	62
3.2.2.1. Matlab results for a transport model- time evolution with degradation from the source	63
3.2.2.2 Matlab results for a transport model-distance evolution with degradation from the source.	67

3.3. Microsoft-Excel and matlab cross validation	71
3.4. Discussion.....	72
3.4.1. Toxicity caused by the concentration of heavy metals in water	72
3.4.2. Acidity of water caused by the AMD	73
3.4.3. Natural attenuation of heavy metals.....	74
3.4.4. Natural attenuation of AMD and pH buffering.....	74
3.4.4. 1. Authigenic secondary minerals formation.....	74
Chapter 4 : CONCLUSION AND RECOMMENDATIONS.....	76
4.1. Conclusion.....	76
4.2. Recommendations for future works.....	76

LIST OF FIGURES

Figure 1: Water distribution in the world.....	3
Figure 2: Acute (a) and chronic (b) poisoning effects of copper	13
Figure 3: Comparison of the effects of zinc intoxication versus deficiency	15
Figure 4 : Source of heavy metals pollution	16
Figure 5: Dead fish by AMD effect	20
Figure 6: Map of the study area	21
Figure 7: Aspect of water collection system on the study area.....	22
Figure 8: Tubular reactor	25
Figure 9: Graphic of aluminum transport model- time evolution	39
Figure 10: Graphic of the fifth curve of the aluminum transport model-time evolution	40
Figure 11: Graphic of copper transport model-time evolution	40
Figure 12: Graphic of the fifth curve of copper transport model-time evolution.....	41
Figure 13: Graphic of iron transport model-time evolution.....	42
Figure 14: Graphic of the fifth curve of iron transport model-time evolution	43
Figure 15: Graphic of manganese transport model-time evolution.....	43
Figure 16: Graphic of the fifth curve of manganese transport model-time evolution	44
Figure 17: Graphic of zinc transport model-time evolution.....	45
Figure 18: Graphic of the fifth curve of zinc transport model-time evolution	46
Figure 19: Graphic of arsenic transport model-time evolution	46
Figure 20: Graphic of the fifth curve of arsenic transport model-time evolution	47
Figure 21: Graphic of nickel transport model-time evolution.....	48
Figure 22 : Graphic of the fifth curve of nickel transport model-time evolution	49
Figure 23: Graphic of lead transport model-time evolution.....	49
Figure 24: Graphic of the fifth curve of lead transport model-time evolution	50
Figure 25: Graphic of aluminum transport model-distance evolution	51
Figure 26: Graphic of the sixth curve of aluminum transport model-distance evolution	52
Figure 27: Graphic of copper transport model- distance evolution	52
Figure 28: Graphic of the sixth curve of copper transport model-distance evolution.....	53
Figure 29: Graphic of iron transport model-distance evolution.....	54
Figure 30: Graphic of the sixth curve of iron transport model-distance evolution	55

Figure 31: Graphic of manganese transport model-distance evolution.....	55
Figure 32: Graphic of the sixth curve of manganese transport model-distance evolution.....	56
Figure 33: Graphic of zinc transport model-Distance evolution.....	56
Figure 34: Graphic of the sixth curve of zinc transport model-distance evolution.....	57
Figure 35: Graphic of arsenic transport model-Distance evolution	58
Figure 36: Graphic of the sixth curve of arsenic transport model-distance evolution	59
Figure 37: Graphic of nickel transport model-distance evolution.....	59
Figure 38: Graphic of the sixth curve of nickel transport model-distance evolution.....	60
Figure 39: Graphic of lead transport model-distance evolution.....	60
Figure 40: Graphic of the sixth curve of lead transport model-Distance evolution	61
Figure 41: Aluminum transport model-time evolution graphic from matlab.....	63
Figure 42: Iron transport model-time evolution graphic from matlab	63
Figure 43: Copper transport model-time evolution graphic from matlab	64
Figure 44: Manganese transport model-time evolution graphic from matlab.....	64
Figure 45: Zinc transport model-time evolution graphic from matlab.....	65
Figure 46: Arsenic transport model-time evolution graphic from matlab	65
Figure 47: Nickel transport model-time evolution graphic from matlab	66
Figure 48: Lead transport model-time evolution graphic from matlab.....	66
Figure 49: Aluminum transport model- distance evolution graphic from matlab.....	67
Figure 50: Copper transport model- distance evolution graphic from matlab	67
Figure 51: Iron transport model- distance evolution graphic from matlab	68
Figure 52: Manganese transport model- distance evolution graphic from matlab.....	68
Figure 53: Zinc transport model- distance evolution graphic from matlab.....	69
Figure 54: Arsenic transport model- distance evolution graphic from matlab.....	69
Figure 55: Nickel transport model- distance evolution graphic from matlab	70
Figure 56: Lead transport model- distance evolution graphic from matlab.....	70

LIST OF TABLES

Table 1: Limit values of emission of some chemicals in water	5
Table 2: First order kinetic constant of heavy metals/chemicals removal in water	30
Table 3 : Diffusivity coefficient estimation	31
Table 4: Concentration and pH of heavy metals and sulfide at Fibrocimento source, in Douro surface water and at 2.5m deep in water.	35
Table 5: Characteristic of the tube	36
Table 6: Simulated residence time and predicted values of concentration from excel implementation of each chemical getting into Douro river	62
Table 7: Simulated residence time and predicted values of concentration of heavy metals and other chemicals discharged into Douro river from matlab implementation	71
Table 8: Excel and Matlab cross validation values	72
Table 9: Comparison of predicted values of concentration discharged into Douro river to the threshold limit values	73

ACCRONYMS

AMD: Acid Mine Drainage

UNEP: United Nation for Environment Protection

UNESCO: United Nations Educational, Scientific and Cultural Organization

WHO: World Health Organization

EPA: Environmental Protection Agency

ACGH: American Conference of Government Industrial Hygienists

EC: European Commission

DL: Diario da Republica

DNA: Deoxyribonucleic Acid

TDS: Total Dissolved Solids

ROS: Reactive Oxygen Species

MCV: Mean Corpuscular Volume

MCH: Mean Corpuscular Hemoglobin

MCHC: Mean Corpuscular Hemoglobin Control

VMA: Valeur minimum admise (in French language)

MAV: Minimum Admitted Value (in English language)

TPP: Thermo-Electric Power Plant

MW: Megawatt

°C: Celsius Degree

N: North

W: West

Å: Angstrom

ARDS: Adult Respiratory Distress Syndrome

Eh: Redox potential

pH: Hydrogen Potential

Chapter 1. Introduction

1.1. General Introduction

With the need of socio-economic development all over the world, adverse effects of anthropogenic activities on natural ecosystem are severely enormous. Anthropogenic activities such as mining and industrial activities threaten the environment.

The main part of the natural ecosystem threatened by such activities are air, soil and water.

Water is the lifeblood of our planet. It is fundamental to the biochemistry of all living organisms. The earth's ecosystems are linked and maintained by water, and provide a permanent habitat for many species, including some 8.500 species of fishes (Acreman, 2004). It is important for human to have an ability to control and protect such systems.

In former mining plants, waste, residues or ashes were stockpiled on land and leachates or reagents were discharged into natural water without taking into consideration their environmental impacts. The stockpiled waste, residues or ash were percolated by rain water and their leachate was directed into surface water.

Some researches and studies should be conducted in order to assess the risk of water pollution.

1.2. Objective of the dissertation

The objective of this work is to analyse the evolution of pollution generated by a landfill coal ash to Douro river.

Using a computational model with microsof-excel and matlab, this work emphasizes on the following specific objectives:

To determine by plotting a transport model, the predicted concentration of heavy metals or chemicals discharged into Douro river;

To compare the concentration of heavy metals or other chemicals in water discharged into Douro river and the maximum admitted value of emission of residues to water decreed by the Government of Portugal; and hence make a conclusion on the potential pollution of Douro river;

To determine the time at which heavy metals or chemicals start to dissolve, at a certain pick of maximal concentration;

To determine the simulated residence time of each heavy metals or chemicals during the pathway from Fibrocimento to Douro river.

To estimate other parameters influencing the transport model such as kinetic and diffusivity constants.

1.3. Dissertation structure

This dissertation is organized in four chapters, references and annex.

The chapter 1 consists of the introduction which relates the objective of this work and provides definitions of some related concepts;

The chapter 2 describes the methodology used in analysing the evolution of pollution of the land fill coal ash to Douro River;

The chapter 3 deals with results and discussion;

The chapter 4 presents conclusion of the dissertation and the recommendations for future works;

The annex presents tables of the results from calculations.

1.4. Water

Of all the water on Earth, only 3% is present as freshwater in lakes, rivers , groundwater (figure 1) and reservoirs systems where it is most easily accessible for use (Krantzberg et al., 2010).

Water covers about 70% of Earth's surface, makes up about 70% of our mass body, and is essential for life (Shakhashiri, 2011).

Water is part of the physiological process of nutrition and waste removal from cell of all living organisms. It is one of the controlling factors for biodiversity and the distribution of Earth's varied ecosystems, communities of animals, plants, bacteria and their interrelated physical and chemical environments (Vandas et al., 2002).

Water on Earth's surface, surface water, exists as streams, rivers, lakes and wetlands, as well as bays and oceans. Surface water also includes the solid forms of water, snow and ice. Water below the surface of the Earth primarily is groundwater, but it also includes soil water (Alley et al., 1998).

Aquatic systems, such as wetlands, streams, rivers and lakes are especially sensitive to changes in water quality and quantity. These ecosystems receive sediments, nutrients, and toxic substances that are produced or used within their watershed, the land area that drains water to stream, river, lake or ocean. Thus, an aquatic ecosystem is indicative of the conditions of the terrestrial habitat in its watershed (Vandas et al., 2002).

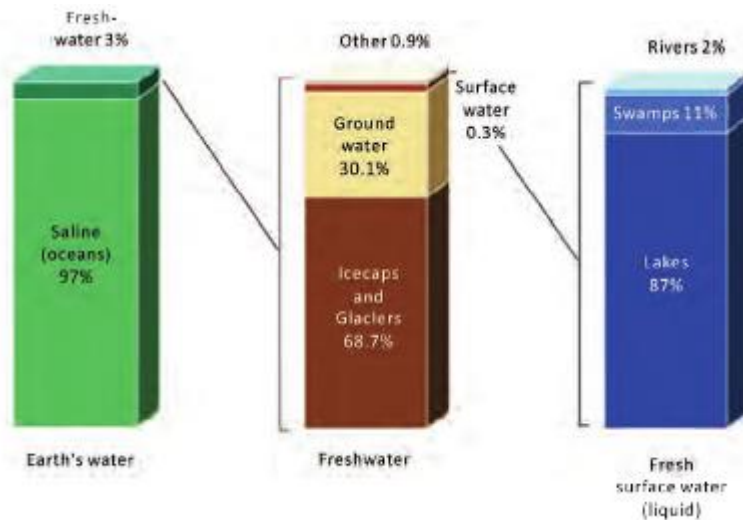


Figure 1: Water distribution in the world (Krantzberg et al., 2010)

1.5. Water quality

Water quality is defined as suitability of water to sustain various uses or processes. Any use will have certain requirements for the physical, chemical or biological characteristics, example, limits on the concentrations of toxic substances, restrictions on temperature and pH ranges for water supporting invertebrate communities. Consequently, water quality can be defined by a range of variables which limit its use (Bartra & Ballance, 1996).

Krantzberg et al., (2010) consider that water quality is commonly defined by its physical, chemical, biological and aesthetical characteristics and reflects its composition as affected by nature and human activities.

A healthy environment is thus one in which water quality supports a rich and varied community of organisms and protects public health.

Many aspects of water quality are developed. Chapman, (1996) considers water quality within the aquatic environment and generally defines aquatic environment as:

- Set of concentrations, speciation, and physical partitions of inorganic or organic substances.
- Composition and state of aquatic biota in the water body.
- Description of temporal and spatial variations due to internal and external factors to water body.

Water quality can hence be defined considering the environmental area because physical, chemical and biological properties vary in space and time due to natural and anthropogenic activities.

With the aim of protection of public health, UNEP, UNESCO, WHO, EPA, environmental experts, government authorities and other organisms over the world created a lot of strategies to combat water quality deterioration. Some are adopted as water quality guidelines, water quality objectives, water quality criteria and water quality standards.

Water quality criteria and water quality standards are related and serve as a baseline for establishing water quality objectives in enforceable environmental control laws or regulations, while water quality objectives are defined as numerical and narrative statements established to support and protect water uses (Helmer & Hespanhol, 1997).

Water quality criteria are synonyms to water quality guidelines and define technically-derived numerical measures of concentrations or descriptive statements to protect aquatic ecosystems and human water uses. They are hence derived from a range of physico-chemical, biological and habitat indicators based on best-available science.

All those strategies are hence base line of water quality guidelines and those numerical values are defined as quantitative measures that protect the environment. Those values are known as threshold values. A definition of threshold value is given below.

1.5.1. Water quality threshold limit value

Threshold limit value started in 1942 when an American Conference of Government Industrial Hygienists (ACGIH) committee was created to compile a listing of state government exposure limits to various chemicals. The committee published then its first annual list of recommended “Maximum allowable concentration” for 144 substances ; thus , the primary source for the term “Threshold limit value” (Ziemen & Castleman, 1989).

Several definitions have been developed after. Based on an ecological point of view, threshold is the point at which there is an abrupt change in an ecosystem quality, property or

phenomenon, where small changes in an environmental driver produce large responses in the ecosystem (Groffman et al., 2006).

1.5.2. Portugal water quality threshold value

Based on the previous definitions of water quality, each country or organization adopts directives to protect water against pollution and deterioration. An example is the Directive 2006/118/EC of European Union which stipulates: “Having regard to the need to achieve consistent levels of protection for groundwater, quality standards and thresholds values should be established, and methodologies based on a common approach developed, in order to provide criteria for the assessment of the chemical status of groundwater bodies” (Directive 2006/118/EC, 2006).

In Portugal, the first regulations in the XXth century related to water quality date from 1904. At the moment the standards that regulate the quality of water are given in a Law (DL 306/2007) that was published in 2007 and transpose the European Directive. That law replaces the standards established in 2001 (DL243/2001) that in turn, replaces the standards established in 1998 (DL 236/98).

The limit value of emission of chemicals used in this work (table1) are found in (DL 236/98).

Table 1: Limit values of emission of some chemicals in water (DL 236/98, 1998).

Chemicals	Limit value of emission (mg/l)
Al	10
Fe	2.0
Mn	2.0
Ni	2.0
As	1.0
Pb	1.0
Cu	1.0
Zn	0.5

The ministry of Environment of Portugal approved also that the minimal limit value of pH of residues allowed to be discharged into water is in the range of 5.0-9.0 (DL 236/98, 1998).

1.6. Contamination/pollution

Contamination and pollution have different meanings even though they have been used as identical terms for a long time. Some environmental experts try to provide different definitions but there is still confusion in using them. It is then necessary to make a distinction between them. What is more important for both terms is that they are applicable to water quality degradation.

Contamination is defined as an introduction into water of any substance in undesirable concentration not normally present in water, e.g. microorganisms, chemicals, waste or sewage, which renders the water unfit for its intended use, and pollution is an addition of pollutant to water while pollutant is defined as substance which impairs the suitability of water for a considered purpose (UNESCO, 1992 in Zaporozec, 2002).

Those definitions are similar and Zaporozec, (2002) continues in the same way by giving a very short and strait definitions. He defines contaminant as a naturally-occurring or human-produced substance that renders water unfits for a given use, and pollution is an addition of pollutant to water which restrains its use.

Based on those definitions, Zaporozec, (2002) considers that those terms are similar and based on degradation of water quality for a given use.

Other environmental experts consider futhermore the harmful effects to human health.

Contamination is simply the presence of a substance where it should not be or at concentration above background. Pollution is contamination that results in or can result in adverse biological effects to communities. All pollutants are contaminants, but not all contaminants are pollutants (Chapman, 2007).

Chapman, (2007) points out that the task of differentiating pollution from contamination is not easy as it can also not be done solely based on chemical analysis because such analyses cannot provide information on bioavailability or on toxicity. Effects based measures such as laboratory or field toxicity tests and measures of the status of resident, exposed communities provide key information, but cannot be used independently to determine pollution status,

because measures cannot easily distinguish between adaptation to contamination (a genetic process) and acclimation¹. Contaminant effects may not be only direct but also indirect.

From Chapman, (2007) consideration, there is distinction between pollution and contamination. But to make it, it is better to consider a large scale of affected communities because there should occur adaptation.

Pollution is hence contamination at large and deep scale with biological effects on affected communities. In this work, pollution is used as an environmental threat.

1.6. 1. Water pollution

Polluted water may have undesirable color, odor, taste, turbidity, organic matter contents, harmful chemical contents, toxic and heavy metals, pesticides, oily matters, industrial waste products, radioactivity, high Total Dissolved Solids (TDS), acids, alkalis, domestic sewage content, virus, bacteria, protozoa, rotifers, worms, etc.

Polluted surface waters (rivers, lakes, and ponds), groundwater, and sea water are all harmful for human, animals and aquatic life (Trivedi, 2003).

In aquatic systems, pollutants are classified in four categories (Rico et al., 1989):

1. Those reaching the environment in enormous quantities;
2. Those which are toxic to aquatic organisms;
3. Those which can be concentrated within organisms to the levels greater than in their living medium and;
4. Those persistent for long period with a high biological half-life.

Among those four categories, heavy metals can be classified into more than one category.

1.6.2. Water pollution sources

All environmental experts point out that water pollutant sources are categorized as point and non-point sources. But there is an ambiguity in making distinction between them. Chapman, (1996) defines a non-point source as a diffuse sources. He argues that a diffuse source on a

¹ According the environmental Engineering Dictionary, acclimation is the response by an animal that enable it to tolerate a change in a single factor (e.g. temperature) in its environment (Mehdi & Agency, 2008), it can also be a tolerance or adaptation of species to toxic metal concentration (Muysen & Janssen, 2001).

regional or even local scale may result from a large number of individual point sources, e.g. an automobile exhausts. The important difference between a point and non-point source is that a point source may be collected, treated or controlled. A diffuse source resulting from many point sources may be controlled provided that all point sources can be identified. He says that the major point sources of pollution to fresh water originate from the collection and discharge of domestic waste water, industrial wastes or certain agricultural activities such as animal husbandry, and most other agricultural activities, such as pesticide spraying or fertilizer application are considered as diffuse sources.

In their distinction, Loague & Corwin, (2016) involve more deeply some other aspects. They characterize a point source as i) easier to control, ii) more readily identifiable and measurable and iii) generally more toxic. They define a non-point source of pollution as the consequence of agricultural activities (e.g. irrigation and drainage, application of pesticides and fertilizers, run off and erosion); urban and industrial run off, erosion associated with construction, mining and forest harvesting activities, lawns, roadways, and golf courses, road salt run off, atmospheric deposition, livestock waste, and hydrologic modification (e.g. dams, diversions, channelization, over pumping of ground water and siltation). They also consider that a point source includes hazardous spills, underground storage tanks, storage piles of chemicals, mine-waste ponds, deep-well waste disposal, industrial or municipal waste outfalls, run off, and leachate from municipal and hazardous waste dumpsites and septic tanks. They characterize a non-point source as i) difficult or impossible to trace ii) enter the environment over an extensive area and sporadic timeframe; iii) are related (at least in part) to certain uncontrollable meteorological events and existing geographic/geomorphologic conditions, iv) have the potential for maintaining a relatively long active presence on the global ecosystem, and v) may result in long-term, chronic (and endocrine) effects on human health and soil-aquatic degradation.

From the previous definitions, it is possible to deduce that point and non-point source can both be more toxic but the main difference between them is that a non-point source is diffuse and a point source is non-diffuse.

1.7. Heavy metals pollution

Some heavy metals have bio-importance as trace elements (Duruibe et al., 2007), but at a certain concentration level, the bio-toxic effects of many of them are harmful to aquatic live and human health.

It is then necessary to know the properties of those natural and anthropogenic occurring and understand their related impact on environment.

1.7.1. Heavy metal definition

Heavy metals refer to any metallic element that has a relatively high density. Heavy metal is a general collective term, which applies to the group of metals and metalloids with a density greater than 4g/cm^3 or five times or more greater than the density of water (Dipak, 2017).

Heavy metals include lead (Pb), cadmium (Cd), zinc (Zn), mercury (Hg), arsenic (As), silver (Ag), chromium (Cr), copper (Cu), iron (Fe), and the platinum group elements. Heavy metals are toxic even at low concentration. They occur as natural constituents of the earth crust, and are persistent environmental pollutant since they cannot be degraded or destroyed. To a small extent, they enter the body system through food, air, and water, and bio-accumulate over a period of time (Duruibe et al.,2007).

1.7.2. Heavy metals toxicity properties

Heavy metals are significant environmental pollutants and their toxicity is a problem of increasing significance for ecological, evolutionary, nutritional and environmental reasons. Heavy metals toxicity can lower energy levels and damage the function of the brain, lungs, kidney, liver, blood composition and other important organs. Long-term exposure can lead to gradually progressing physical, muscular, and neurological degenerative process that initiate diseases such as multiple sclerosis, Parkinson's disease, Alzheimer's disease and muscular dystrophy. Repeated long-term exposure of some heavy metals may even cause cancer (Jaishankar, Tseten, Anbalagan, Mathew, & Beeregowda, 2014).

Symptoms that arise as a result of metal poisoning include intellectual disability in children, dementia in adults, central nervous system disorders, insomnia, emotional instability, depression and vision disturbances (Jan et al., 2015).

The following properties are related to heavy metals which are the main pollutants on which this work emphasizes.

Arsenic(As)

Arsenic is one of the most important heavy metals causing disquiet from both ecological and individual health standpoints. It is prominently toxic and carcinogenic, and extensively available in the form of oxides, sulfides or as a salt of iron, sodium, calcium, copper, etc.

Arsenic is the twentieth most abundant element on earth and its inorganic forms such as arsenate and arsenite compounds are lethal to the environment and human life. Deliberate consumption of arsenic in case of suicidal attempts or accidental consumption by the children may also result in cases of acute poisoning (Jaishankar et al., 2014).

Most common arsenic compounds occur in three oxidation states: trivalent arsenite, pentavalent arsenate and elemental arsenic. Arsenite is ten times more toxic than arsenate, and elemental arsenic is nontoxic. Arsenic also exists in three chemical forms: organic, inorganic and arsine gas. Organic arsenic is having little acute toxicity whereas inorganic arsenic and arsine gas are toxic (Ibrahim et al., 2006).

Arsenic is a protoplasmic poison since it affects primarily the sulfhydryl group of cells causing malfunctioning of cell respiration, cell enzymes and mitosis (Saha et al., 1999).

The inhalation and ingestion of arsenic cause acute effects as mucosal damage, hypovolemic shock, fever, sloughing, gastro-intestinal pain and anorexia. The chronic effects of arsenic are weakness, hepatomegaly, melanosis, peripheral neuropathy, peripheral vascular disease, carcinogenicity, liver, skin and lung cancer. As a health effects, arsenic causes gastro intestinal damage, severe vomiting and death (Jan et al., 2015).

Low levels exposure to arsenic can cause nausea and vomiting, decreased production of red and white blood cells, abnormal heart rhythm, damage to blood vessels, and a sensation of “pins and needles in hands and feet”. Ingestion of very high levels can possibly result in death. Long term low level exposure can cause darkening of the skin and the appearance of small “corns” or “warts” on the palms, soles and torso (Wendy & Sabine, 2009).

Lead(Pb)

Lead has no known beneficial effects in human body. Lead is a highly toxic metal whose widespread use has caused extensive environmental contamination and health problems in many parts of the world. Lead is a bright silvery metal, slightly bluish in a dry atmosphere. It begins to tarnish on contact with air, by forming a complex mixture of compounds, depending on the given conditions. Lead is an extremely toxic heavy metal that disturbs various plants, physiological processes and unlike other metals, such as zinc, copper and manganese, it does not play any biological functions. A plant with high lead concentration speeds up the production of reactive oxygen species (ROS), causing lipid membrane damage that ultimately leads to damage of chlorophyll and photosynthetic process and suppresses the overall growth of the plant (Hou et al., 2013).

Lead enters in the human body by inhalation and ingestion. Lead has the acute effects of nausea, vomiting, thirst, diarrhea, constipation, abdominal pain, hemoglobinuria, oliguria leading to hypovolemic shock. The chronic effects of lead are colic, palsy and encephalopathy. Its health effects are anemia, hypertension, kidney damage, disruption of nervous systems, brain damage and intellectual disorders (Jan et al., 2015).

For pregnant women, exposure to high level of lead may cause miscarriage, and for men it causes damage of organs responsible for sperm production and finally causes infertility (Wendy & Sabine, 2009).

Aluminum(Al)

Investigations on environmental toxicity revealed that aluminum may present a major threat to humans, animals and plants in causing many diseases. Many factors, including pH of water and organic matter content, greatly influence the toxicity of aluminum. With decreasing pH, its toxicity increases. Aluminum in high concentrations is very toxic for aquatic animals, especially for gill breathing organisms such as fish, causing osmoregulatory failure by destroying the plasma and hemolymph ions. The activity of gill enzyme, essential for the uptake of ions, is inhibited by monomeric form of aluminum in fish. Living organisms in water, such as seaweeds and grassfish, are also affected by its toxicity (Jaishankar et al., 2014).

The aluminum toxicity in human body is related to renal osteodystrophy and dialysis encephalopathy (King et al., 1981).

Iron(Fe)

Iron is an essential nutrient for most living organisms because it is a component or cofactor of many critical proteins and enzymes. Iron toxicity is related to the generation of free radicals. Both normal and pathogenic cellular processes produce superoxide (O_2^-) and hydrogen peroxide (H_2O_2) byproducts, whereas enzymes such as superoxide dismutase, glutathione peroxidase, and catalase normally metabolize and neutralize these free radicals. One of the effects of (O_2^-) is the release of stored iron from ferritin. The free iron reacts with (O_2^-) and (H_2O_2) to produce other more reactive and toxic free radicals such as hydroxyl radical. The hydroxyl radical can depolymerize polysaccharides, cause DNA strand breaks, inactivate enzymes, and irritate lipid peroxidation which amplifies damaging cellular and subcellular membranes. If the damage is not repaired, it can lead to cell death (Jeffrey, 2000).

The abundance of species such as periphyton, benthic invertebrates and fish diversity are greatly affected by the direct and indirect effects of iron contamination. The iron precipitate causes considerable damage by means of clogging action and hinder the respiration of fishes. (Jaishankar et al., 2014).

Copper (Cu)

Even copper is an essential trace metal and micronutrient for cellular metabolism on living organisms in account of being a key constituent of metabolic enzymes (Badiye et al., 2013), it can however be extremely toxic to human body and cause acute and chronic poisoning (figure 2 a and b respectively).

It is also toxic to intracellular mechanisms in aquatic animals at high concentrations when it exceeds the threshold level. Fish can accumulate copper via diet or ambient exposure. Even at low environmental concentrations, copper shows distinct affinity to accumulate in fish liver. The typical patho-anatomical appearance includes a large amount of mucus on body surface, under the gill covers and in between gill filaments. Higher doses of copper cause visible external lesions such as discoloration and necrosis on livers of *cuprinus carpo*, *carassius auratus* and *corydoras paleatus*. There is also vacuolization of endothelial cells in fish liver after copper exposure. Hepatocyte vacuolization, necrosis, shrinkage, nuclear pyknosis and increase of sinusoidal spaces were the distinct changes observed in the liver of copper-exposed fish. During copper poisoning, the release of erythroblast usually results from an increase rate of red blood cells catabolism. Reproductive effects are noted at low levels of copper and include blockage of spawning, reduce egg production per female, and other effects. Chronic toxic effects may induce poor growth, decrease immune response, shortened life span, reproductive problems, low fertility and change in appearance and behavior (Authman et al., 2015).

The effects of copper on a human body are hair loss, anemia, kidney damage and headache (Carolin et al., 2017).

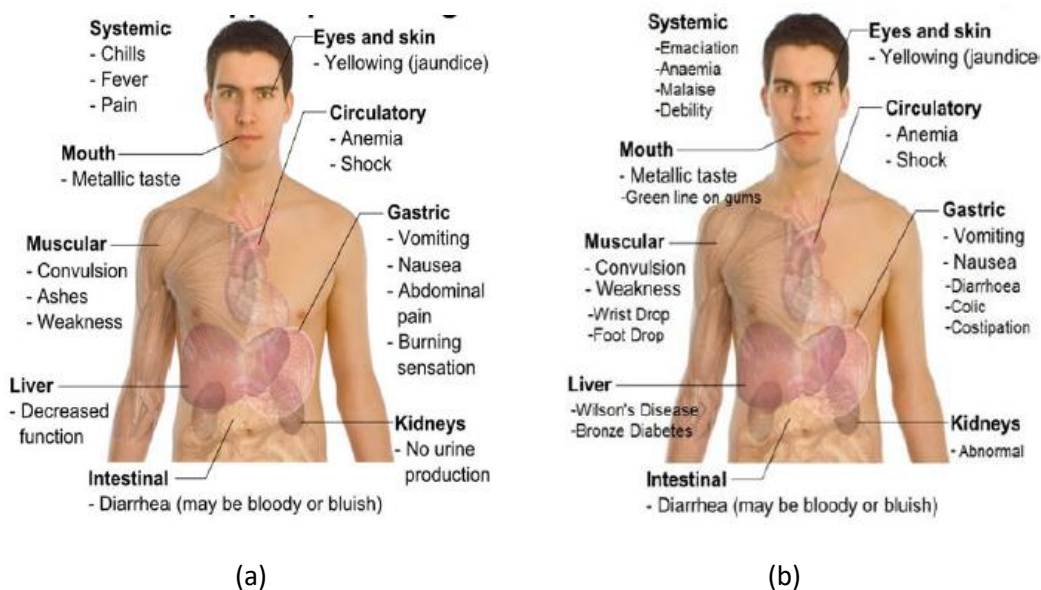


Figure 2: Acute (a) and chronic (b) poisoning effects of copper (Badiye et al., 2013)

Nickel (Ni)

Even nickel is an essential element at low concentrations for many organisms, it is toxic at higher concentrations (Authman et al., 2015).

Exposure to nickel may lead to various adverse health effects, such as nickel allergy, contact dermatitis and oral epithelium damage. Industrial dust from Ni refineries contains water insoluble Ni compounds including Ni_3S_2 and NiO , which are carcinogenic. Breathing in Ni contaminated dust from mining and tobacco smoking leads to significant damage of lungs and nasal cavities, resulting in diseases such as lung cancer and nasal cancer (Kim et al., 2015).

Nickel is known as a haematotoxin, immunotoxin, neurotoxic, genotoxic, reproductive toxic, pulmonary toxic, nephrotoxic, hepatotoxic and carcinogenic agent (Das et al., 2008).

As with the toxicity of other metals, the toxicity of nickel compounds to aquatic organisms is markedly influenced by the physicochemical properties of water. The toxicity of nickel may be due to nickel being in contact with the skin, penetrating the epidermis and combining with body protein. After toxic exposure to nickel compounds, the gill chambers of the fish are filled with mucus and the lamellae appeared dark red in color. Some effects are histological changes in fish gill structure which include hyperplasia, hypertrophy, shortening of secondary lamellae and fusion of adjacent lamellae. *Cyprinus carpio* exposed to nickel showed decreased blood parameters (erythrocyte, leucocytes, hematocrit and hemoglobin count) and lowered values of mean corpuscular volume, (MCV), mean corpuscular hemoglobin (MCH)

and mean corpuscular hemoglobin concentration (MCHC) when compared with the control values. (Authman et al., 2015).

Zinc (Zn)

Compared to other metal ions, zinc is relatively harmless. Only exposure to high doses has toxic effects making acute intoxication. The entry of zinc to human body can be through inhalation, by skin and through ingestion. Inhalation can cause development of adult respiratory distress syndrome (ARDS) which shows that zinc is the main cause for the respiratory symptoms. The acute exposure cause fever, muscle soreness, nausea and vomiting, fatigue, fever, skin inflammation , anemia, chest and caught and dyspnea, (Plum et al., 2010, Carolin et al., 2017).

As it is also essential to human organism, deprivation of zinc by malnutrition or medical conditions have detrimental effects on different organisms. The figure 3 make a comparison of the effects of zinc intoxication versus deficiency (Plum et al., 2010).

Zinc can have a direct toxicity to fish at increased waterborne levels, and fisheries can be affected by either zinc alone or more other together with copper and other metals. The main target of waterborne zinc toxicity are the gills, where the zn^{2+} uptake is disrupted, leading to hypocalcemia and eventual death. Also, fish kidney is considered as a target organ for zinc accumulation. Zinc causes mortality, growth retardation, respiratory and cardiac changes, inhibition of spawning, and a multitude of additional detrimental effects which threaten survival of fish. Gill, liver, kidney, and skeletal muscle are damaged. The first sign of gill damage is detachment of chloride cells from underlying epithelium. *Oreochromis niloticus* fish exposed to zinc sulphate, showed pale and congested gills. The epithelial covering of the gill filaments was hyperplastic and edematous with vacuolated epithelial covering of gill rakers. Zinc exposure has been shown to induce histopathological alterations in ovarian tissue of *Tilapia nilotica* (degeneration and hyperaemia) and liver tissue of *oreochromis mossambicus* (hyalinizations, hepatocyte vacuolation, cellular swelling and congestion of blood vessels (Authman et al., 2015).

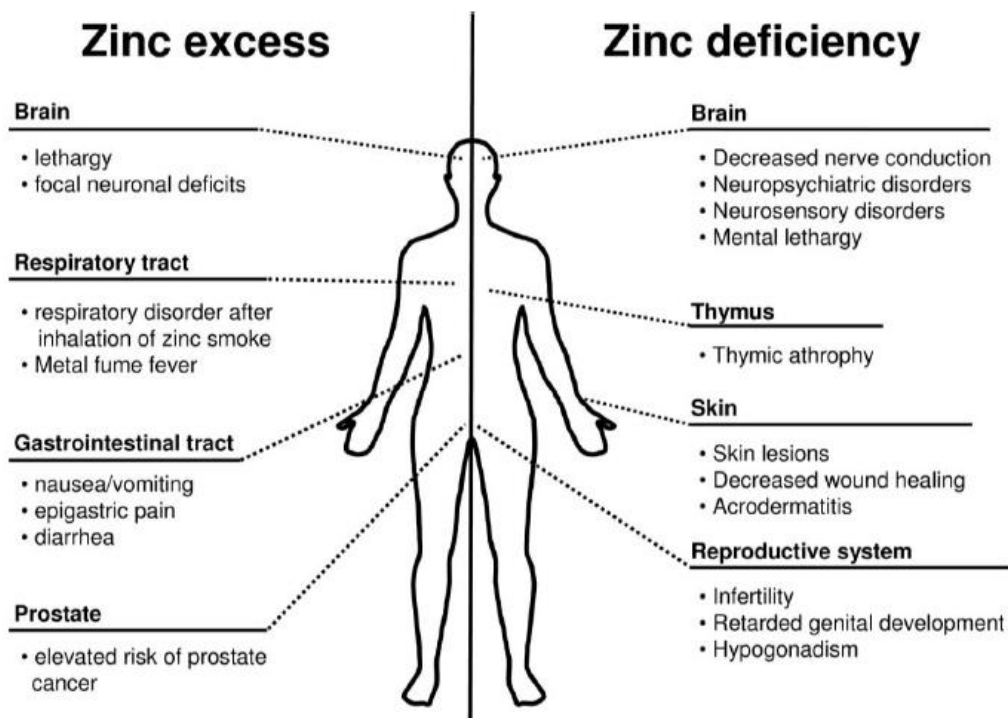


Figure 3: Comparison of the effects of zinc intoxication versus deficiency (Plum et al., 2010)

Manganese (Mn)

Manganese is an essential element necessary for physiological process that support development, growth and neuronal function (Kwakye et al., 2015). But with high exposure to manganese, it accumulates in the basal ganglia region of brain and may cause a syndrome like parkinsonian. The organs affected by manganese is nervous system and the clinical effects are central and peripheral neuropathies (Mahurpawar, 2015).

Some manganese deficiencies have been reported in human body with symptoms including dermatitis, slowed growth of hair and nails, decreased serum cholesterol levels, and decreased levels of clotting proteins. Its toxicity causes neurological effects associated to muscle weakness and limb tremor. The preferentially damaged human organ is the brain (Santamaria, 2008).

1.7.3. Source of heavy metals pollution

Excessive quantity of heavy metals in soil, air and water is due to natural and anthropogenic activities (Figure 4). Anthropogenic activities such as mining industries are the main source of heavy metals release (Aderinola et al.,2012).

In rock, they exist as their ores in different chemical forms, from which they are recovered as minerals. Heavy metals ores include sulfides such as iron, arsenic, lead, zinc, cobalt, gold, silver and nickel, oxides such as aluminum, manganese, gold, selenium and antimony. Some exist as sulfides, oxides or both sulfides and oxides ores such as iron, copper and cobalt. Ore minerals tend to occur in families whereby metals that exist naturally as sulfides would mostly occur together, likewise for oxides. Therefore, sulfides of lead, cadmium, arsenic and mercury would naturally be found occurring together with sulfides of iron (pyrite, FeS_2) and copper (Chalcopyrite, CuFeS_2), (Duruibe et al. 2007).

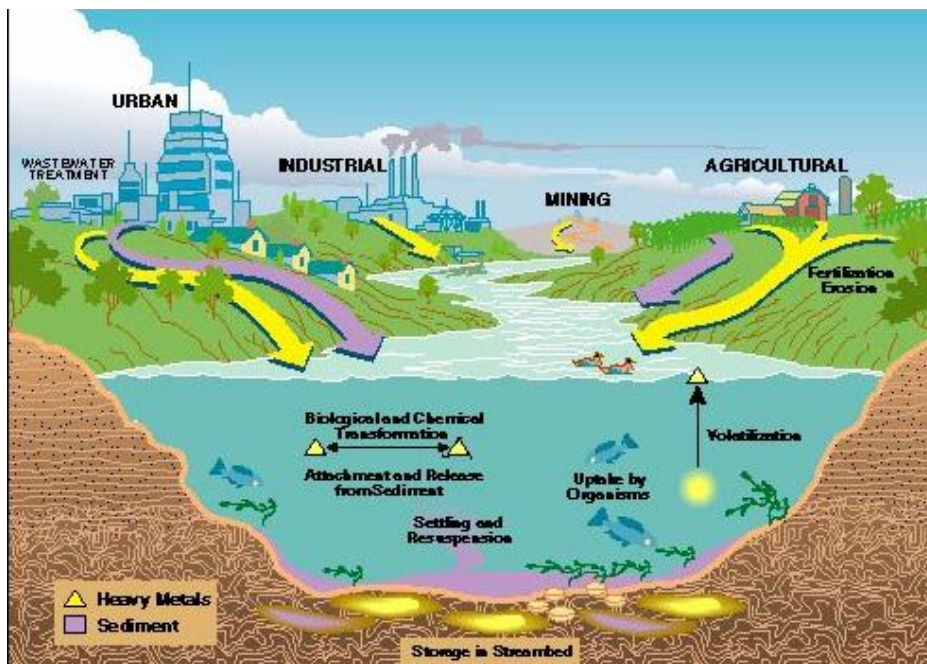


Figure 4 : Source of heavy metals pollution (Garbarino et al., 1995).

1.7.4. Fate of heavy metals as pollution

In some cases, even after mining activities have ceased, the emitted metals continue to persist in the environment. During mining processes, such as hydrometallurgical process or pyrometallurgical process, some heavy metals are left behind with tailings; some others are transported by wind and flood, creating various environmental problems. Mining activities

and other geochemical processes hence result in generation of acid mine drainage (AMD), a phenomenon commonly associated with mining activities. Through mining activities, water of rivers and streams is most emphatically polluted. Heavy metals are transported as either dissolved species in water or as an integral part of suspended sediments. Dissolved species in water have the greatest potential of causing the most deleterious effects (Duruibe et al., 2007).

Heavy metals are contained in four reservoirs in an aquatic environment, namely, the surface water, the pore water, the suspended sediment, and the bottom sediment. During transport, sediment bound metals are removed from the water column and stored in alluvial deposits for years before they are reintroduced into the aquatic environment (Pintilie et al., 2007).

Metals can either be transported with the water and suspended sediment or stored within the riverbed bottom sediments. Heavy metals are transported as (1) dissolved species in the water, (2) suspended insoluble chemical solids, or (3) components of the suspended natural sediments. Metals dissolved in the water can exist as hydrated metal ions or as aqueous metal complexes with other organic or inorganic constituents (Garbarino et al., 1995).

The behavior of heavy metals are governed by a range of different physical and chemical processes, which dictate their availability and mobility. In water phase, the chemical form of a metal determines the biological availability and chemical reactivity (sorption /desorption, precipitation/dissolution) towards other components of the system. Also the mobility and bioavailability of metals bound to sediments depend on multiple factors, with sediment characteristics and the physical-chemical form of the metal being the key factors (Pintilie et al., 2007).

1.7.4.1 Pollution of aquatic life

Pollution of the natural aquatic environment by heavy metals is a worldwide problem because of their toxicity, persistence, abiotic degradation in the environment, and bioaccumulation in food chain (Tang et al., 2016).

Human and aquatic life are often threatened by the transport of pollutants through riverine systems to coastal water (Kashefipour & Roshanfekar, 2012).

Heavy metals transported into the aquatic system are mainly incorporated into bottom sediment through adsorption, flocculation, and precipitation in the water column, and they may be toxic to aquatic organisms when threshold concentrations are reached. However, metals that settle out of the water column are more likely to be re-suspended and re-dissolved

into pore water, from where sediment-associated heavy metals can be released into the overlying water by diffusive fluxes. Diffusive fluxes not only result in a concentration gradient at the sediment-water interface, but also deteriorate the quality of water and potentially cause secondary contamination to the water environment (Tang et al., 2016).

When iron is among heavy metals which are dissolved in water, Acid Mine Drainage (AMD) could occur. The following section explains the feature of AMD.

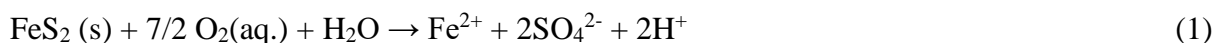
1.7.4.2. Acid mine drainage pollution

Acid mine drainage (AMD) is produced by the oxidation of sulfide minerals chiefly pyrite (FeS_2). This is a natural chemical reaction which can proceed when minerals are exposed at air and water. Acid mine drainage is found around the world both because of naturally occurring processes and activities associated with land disturbances, such as highway construction and mining where acid-forming minerals are exposed at the surface of the earth (Jennings et al., 2008). These acidic conditions can cause metals to dissolve, which can lead to pollution of water.

1.7.4.2.1. Chemistry of Acid Mine drainage

Chemical reaction of acid mine drainage appears straightforward, but becomes complicated quickly as geochemistry and physical characteristics can vary greatly from site to site (Costello, 2003).

Pyrite (FeS_2) is the main responsible for starting acid generation. When pyrite is exposed to oxygen and water, it will be oxidized, resulting in hydrogen ion release-acidity, sulfate ions, and soluble metal cations (see following equations), (Costello, 2003 & Jennings et al., 2008). During this oxidation process occurring at low rate, water can buffer the acid generated. The exposition of surface area of these sulfur-bearing allows excess acid generation beyond water's natural buffering capacities (Jennings et al., 2008).



Further oxidation of Fe^{2+} (ferrous iron) to Fe^{3+} (ferric iron) occurs when sufficient oxygen is dissolved in water or when water is exposed to sufficient atmospheric oxygen (Costello, 2003, & Jennings et al., 2008).



Ferric ions can either precipitate as ochre $\text{Fe}(\text{OH})_3$, the red-orange precipitate in water affected by acid mine drainage or it can react directly with pyrite to produce more ferrous iron and acidity (Costello, 2003).



Once waters are sufficiently acidic, acidophilic bacteria (bacteria that thrive in low pH), can play a significant role in accelerating the chemical reactions which are taking place. *Thiobacillus Ferroxidans*, bacteria, is commonly referenced in this case. These bacteria catalyze the oxidation of ferrous iron, further perpetuating equations 2 through 4. Another microbe belonging to the Archaea Kingdom, named *Ferroplasma Acidarmanus* (Costelo, 2003), has been discovered to also play a significant role in the production of acidity in mine waters.

1.7.4.2.2. Effects of Acid Mine Drainage on aquatic life

During acid mine drainage, metals are released into the surrounding environment, and become readily available to biological organisms. In water, for example, when fish are exposed directly to metals and H^+ ions through their gills, impaired respiration may result from chronic and acute toxicity. Fish are also exposed indirectly to metals through ingestion of contaminated sediment and food items. Iron hydroxides and oxyhydroxides formed during weathering of sulfide may physically coat the surface of stream sediments and stream beds, destroying habitat, diminishing the availability of clean gravels used for spawning, and reducing fish food items such as benthic macro invertebrates. Acid mine drainage, characterized by acidic metalliferous conditions in water, is responsible for physical, chemical and biological degradation of stream habitat (Jennings et al., 2008).

Obvious sign of highly polluted water is death of fishes (figure 5), (Solomon, 2008).



Figure 5: Dead fish by AMD effect (Solomon, 2008).

1.7.5. Heavy metals transport in water

Once introduced to environment, heavy metals may spread to various environmental components which may be caused by the interactions of the nature. Hence, heavy metals may chemically or physically interact with the natural compounds, which change their forms of existence in the environment. They may be bound or soared by particular natural substances, which may increase or decrease mobility (Dube et al., 2001).

The prediction of solute transport for aquifers or groundwater systems is based on the convective-dispersive (or advective-dispersive) solute transport theory, which is also applicable in other transport media, such as surface water. Basically, the convective-dispersive solute transport theory is based on Fick's first law which was established by the mid-19th century. The original Fick's first law was established for molecular diffusion in surface water. Later by the mid-20th century, Fick's first law was extended to solute transport in ground water by including the dispersion effect (Batu, 2006).

Contaminants solutes are transported by advection, diluted by diffusion and hydrodynamic dispersion, and undergo various chemical reactions. Under simplifying assumptions, also supported by experiments, the hydrodynamic dispersion is approximated as a Gaussian diffusion and summing up the molecular diffusion at the pore-scale, one arrives at a local scale to a diffusive model with diffusive flux governed by Fick's law (Suciu, 2014).

I.8. Case study

This dissertation intends to analyse the evolution of pollution generated by the contaminant plume originated from the leachate coming from a landfill coal ash. It is based on a real field situation in Medas area (figure 6), Municipality of Gondomar in Portugal, nearby Douro river.

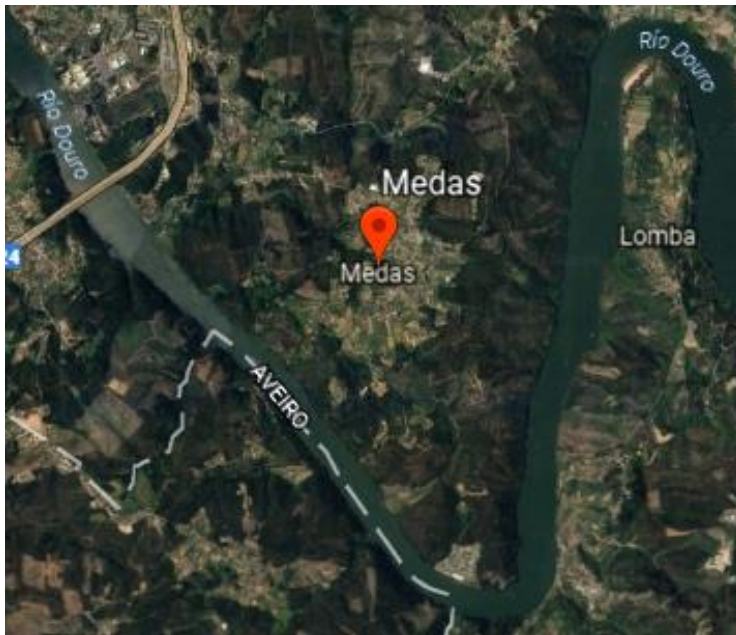


Figure 6: Map of the study area²

There was a thermo-electric power plant (TPP) which was used to burn coal from different coalfields, and stockpiled coal ash on land. The study area is presented as following:

² <https://earth.google.com/web> 09/07/2017

The coal ash was stockpiled on surface ground during approximately five decades, following the natural slope of relief. On the south side of the landfill, there are three systems of drains, the first one formed by a big tube ,called “Tubo Fibrocimento”, was used to drain leachate coming from the stockpile of coal ash , the second, small one, was used to drain mine water, the third is a system formed of two small channels called “Manilha 1 and Manilha 2 used to drain rain water (figure7).

At the other side of the stockpile, there is another water drain used to drain water from the coal park.

The collected water of those four drains forms a small stream which flows into Douro river at approximately 120 m.



Figure 7: Aspect of water collection system on the study area

I.8.1. Douro River

Douro River is one of the longest Rivers in the Iberian Peninsula sharing its 930km with Spain and Portugal, while the 98000km² of its watershed cover about 17% of the Iberian Peninsula. It flows into the Atlantic Ocean at 41° 08' N and 8° 42' W, near Portugal's second largest Porto city. Douro River and its tributaries are heavily damned for hydroelectric power generation and irrigation. In the Portuguese side of the watershed (20% of the total) the dams built in the last 40 years have a capacity of 1.1km³ of water, while on the Spanish side their capacity exceeds 7km³ of water. The mean annual discharge of the Douro River at the end of its course was 421 m³. s⁻¹ between 1985 and 1994. In Jun 1985, the last dam (Crestuma), located at 21.6 km from the mouth, started operating and the estuary was confined to its present length (Vieira & Bordalo, 2000).

The quick-paced industrial and urban development of the region within the estuary's watershed threatens water quality, recreational and aesthetic value of this natural resource that has been, historically, of great importance to northern Portugal (Vieira & Bordalo, 2000).

Chapter 2. DISSERTATION METHODOLOGY

In this case study, a unidimensional unsteady state transport model in water is applied, based on the development of the first Fick's law with time and distance variables including advection, dispersive-diffusion and degradation from the source, considering a first-order kinetics. The final equation is thus implemented using both Microsoft excel and Matlab. The simulation allows to estimate the final concentrations of the contaminant at the discharge point into Douro river. Those concentrations are compared to the threshold limits allowed to be discharged into wastewater by the government of Portugal.

The following sections explain the model application.

2.1. Transport model application from Fibrocimento tube to Douro river

Transport of heavy metals/chemicals from Fibrocimento tube to Douro river is generally described with advection-dispersion equation. This equation distinguishes two transport modes: advective transport as a result of passive movement with water and dispersive /diffusive transport to account for diffusion and small-scale variation in the flow velocity as well as any other process that contributes to solute spreading.

Solute spreading is generally considered to be a Fickian or Gaussian diffusion/dispersion process (Genuchten et al., 2013).

2.1.1. Advection/convective process

Advection or convective process is a process in which a particle dissolved by a fluid will move with the velocity of the fluid (Vested et al., 1993).

2.1.2. Dispersion process

Dispersion is defined as the combination of process responsible for spreading particles within a fluid. Those processes are generally recognized to be molecular diffusion, turbulent diffusion and non-homogeneous velocity distribution (Vested et al., 1993).

2.1.3. One-dimensional model within surface water

Heavy metals/chemicals transport from Fibrocimento tube to Douro river is considered as unidimensional model based on Fick's first law. Assuming a tubular reactor (figure 8) with a

length L traversed by a solution of heavy metals/chemicals in water whose diffusivity is D (m^2/s), velocity is $V(z, t)$ and a concentration $C(z, t)$ of solute that does not react during the transport, as there is concentration gradient of the compound, there is simultaneously diffusion transport of solute. Considered also an infinitesimal element of volume located at Z distance from the entrance of the contaminated water and dz , the thick, J represent the diffusive flux of the first law of Fick (equation 5).

$$J = -D \frac{\partial C}{\partial z} \quad (5)$$

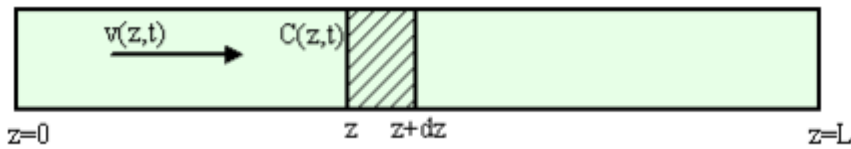


Figure 8: Tubular reactor

Developing the equation 5, the mass balance is given by the following components:

$$\text{Entry} = VSC + SJ \quad (6)$$

$$\text{Exit} = VSC + SJ + \frac{\partial(VSC + SJ)}{\partial z} dz \quad (7)$$

$$\text{Accumulation} = \frac{\partial(SCdz)}{\partial t} \quad (8)$$

Where V is the volume in [L^3], S is the section in [L^2], C is concentration [ML^{-3}]

$$\text{The result of the global balance is } \frac{\partial(SCdz)}{\partial t} = VSC + SJ - [VSC + SJ + \frac{\partial(VSC + SJ)}{\partial z} dz] \quad (9)$$

Dividing both sides by $S \cdot dz$, results:

$$\frac{\partial C}{\partial t} + \frac{\partial(VC + J)}{\partial z} = 0 \quad (10)$$

Substituting the value of diffusion flux used in Fick's law, the result model is:

$$\frac{\partial C}{\partial t} + \frac{\partial(VC)}{\partial z} = \frac{\partial}{\partial z} \left(D \frac{\partial C}{\partial z} \right) \quad (11)$$

Admitting that V and D are constants, we have an equation which describes the simultaneous transport considering both convection and diffusion.

$$\frac{\partial C}{\partial t} + V \frac{\partial C}{\partial z} = D \frac{\partial^2 C}{\partial z^2} \quad (12)$$

2.1.4. Solution of the one-dimensional model

As the equation 12 considers both a convective and diffusive transport model, this equation can be solved using Laplace transform provided that there is a change from previous variable (z, t) to (ξ, τ) using $\xi = z-vt$ relation and $\tau = t$.

If we assume that the initial conditions are represented by $C(z, 0) = C_0$, i. e before release, the contaminant concentration was zero, the system will be powered by a C_0 concentration of pollutant.

The solution of the equation 12 is as following:

$$C(z, t) = \frac{C_0}{2} \operatorname{erfc}\left(\frac{z-vt}{\sqrt{4Dt}}\right), z \geq vt \quad (13)$$

$$C(z, t) = \frac{C_0}{2} \left[1 + \operatorname{erf}\left(\frac{vt-z}{\sqrt{4Dt}}\right)\right], z < vt$$

2.1.5. Solution of the equation taking into account of degradation

As stated by equation (12):

$$D_1 \frac{\partial^2 C}{\partial z^2} - V \frac{\partial C}{\partial z} = \frac{\partial C}{\partial t} \quad (14)$$

Where: D_1 is the longitudinal coefficient of hydrodynamic dispersion, C the concentration of the solute, V the linear velocity of the groundwater, Z the transported distance and t , the time.

The hydrodynamic dispersion coefficient D is the result of two mechanisms, mechanical and molecular dispersion and can be expressed by:

$$D_1 = \alpha_1 V + D \quad (15)$$

Where α_1 is the longitudinal dispersivity in [L] and D is the molecular dispersion coefficient.

A relatively simple way to include compounds degradation in surface water is assuming that there are consumed in a chemical reaction with 1st order kinetics (degradation process). We now have a system with convective transport, dispersive and chemical reactions. If we introduce the 1st order kinetic constant λ , the equation which describes the process is as follow:

$$\frac{\partial C}{\partial t} = -V \frac{\partial C}{\partial z} - \lambda C + D_1 \frac{\partial^2 C}{\partial z^2} \quad (16)$$

Considering that in this case study, the source Fibrocimento is continuously delivering contaminated water to the stream, this is hence considered as a step disturbance and the answer of such system is given by :

$$C(z, t) = \frac{C_0}{2} \operatorname{erfc}\left(\frac{z-vt}{\sqrt{4Dt}}\right) e^{-\lambda t}, Z \geq Vt \quad (17)$$

$$C(z, t) = \frac{C_0}{2} \left[1 + \operatorname{erf}\left(\frac{Vt-Z}{\sqrt{4Dt}}\right)\right] e^{-\lambda t}, Z < Vt$$

These equations will be used as solutions of one dimensional model from Fibrocimento pipe to Douro River. The remaining task is the definition of some parameters as well as kinetic constant and diffusion coefficient.

As previously considered that all elimination procedures are expressed as having 1st order kinetics. The total elimination kinetic constant will be the sum of degradation, dissolution, volatilization and sedimentation:

$$\lambda = \lambda_{\text{deg}} + \lambda_v + \lambda_s \quad (18)$$

In this case study, dissolution, volatilization and sedimentation phenomena are not considered. The total constant elimination kinetic is then composed by the degradation kinetic λ_{deg} .

$$\lambda = \lambda_{\text{deg}} \quad (19)$$

The following step is the determination of the kinetic constant and diffusion coefficient.

2.1.5.1. Kinetic constant study

Considering the path way of polluted water from Fibrocimento pipe to Douro river, there should be a decrease of heavy metals or chemicals concentration in water as the polluted water passes on earth surface and through soil. This decrease is due to natural attenuation of heavy metals and other chemicals in water. The natural attenuation occurs mainly by degradation and adsorption under a pseudo-first-order kinetic constant.

The pseudo-first-order kinetic constant of adsorption of heavy metals or chemicals by soil depends mainly on the mineralogical and organic matter composition of the soil. Soil composition is playing a key role in natural attenuation as a filter. Clay is the most efficient soil for heavy metals or other chemicals attenuation because clay minerals have a great potentiality to adsorb them due to their large specific surface area, chemical and mechanical stability, layered structure, and high cationic exchanger capacity (Sdiri et al., 2011).

Organic compounds and other natural compounds are also efficient in heavy metals and other chemicals removal such as fly ash, silica gel, zeolite, lignin, seaweed, wool wastes, agricultural wastes and chitosan (Badawi et al., 2017).

All those materials playing a key role in natural attenuation of heavy metals and other chemicals, are assumed to be occurring in the area.

2.1.5.1.1. Adsorption kinetic constant determination

The adsorption kinetic and rate determining steps of the metal ions adsorption processes onto the adsorbents can be determined and explained from the adsorption kinetics models. The most known and applicable kinetic models of heavy metals or other chemicals adsorption on the adsorbents are two : pseudo-first-order and pseudo-second-order kinetic models (Badawi et al., 2017 & Carvalho et al., 2008).

The pseudo-first-order kinetic model suggests that the rate of sorption is proportionally dependant to the number of adsorption active sites of the adsorbents. The pseudo-first-order kinetic model is expressed as (Badawi et al., 2017, Maleki & Karimi-jashni, 2017):

$$\text{Log} (q_e - q_t) = \log q_e - \frac{K_1}{2.303} t \quad (20)$$

Where : q_e and q_t are the amount of metal ions adsorbed on sorbent material (here are clays and chitosan) in mg/g at equilibrium and at time t , respectively, and k_1 is the rate constant of pseudo-first-order kinetic constant (min^{-1}). K_1 is hence determined using adsorption isotherm models which determine the efficiency of adsorption process. There are several known adsorption isotherm models such as Lanmuir, Frenlich, Temkin and Dubinum-Radushkevich adsorption models applicable for the adsorption of metal ions from solutions (Badawi et al., 2017 & Sdiri et al., 2011).

The pseudo-second-order kinetic model (if applicable) predicts the rate determining step of adsorption process and the bonds nature between the adsorbents and the metal ions. The equation of state of the intraparticle diffusion kinetic model (pseudo-second-order kinetic model) is expressed as follows:

$$q_t = K_{\text{int}}^{1/2} \quad (21)$$

Where q_t is the amount of metal ions adsorbed by the sorbents in mg/g after t time and K_{int} is the rate constant of intraparticle diffusion step in $\text{mg/g min}^{1/2}$ (Badawi et al., 2017).

As the pseudo-first order kinetic model uses numerical method which necessitates validation of solution obtained typically via experimental results and the pseudo-second-order kinetic model uses analytical method with simplifications, assumptions (Islam, 2006), the values of pseudo-first-order kinetic model are considered as realistic.

2.1.5.1.2. Natural clays for heavy metals adsorption

Recently, clays or clay materials have gained much attention as the adsorbent. Clay minerals, which are important constituents of soil for immobilization of contaminants, play the role of

taking up various pollutants as water flows over the soil or penetrates into the ground. The immobilization of contaminants takes place through either ion exchange or adsorption processes, or a combination of both. The high adsorption properties, non toxicity, abundant availability, high specific surface area, mechanical stability, layered structure, and high cation exchange capacity, make clays and clay materials to be attractive adsorbents for the removal of different pollutants (Maleki & Karimi-jashni, 2017).

Using the pseudo-first-order kinetic model, Carvalho et al., (2008) , Sdiri et al., (2011), Maleki & Karimi-jashni, (2017), Kim & Kwak, (2017) determined the kinetic constant of some heavy metals removal by adsorption on clays as given in the table 2.

2.1.5.1.3.Chitosan as natural occurring for Aluminum adsorption

Chitosan is a natural, biodegradable extremely abundant and non toxic polymer. It has been proposed as a potentially attractive material for various uses, mainly in engineering, biotechnology and medicine, the generic formula is expressed by $(C_6H_{11}O_4N)_n$.

Chitosan is considered as the most suitable and attractive sorbent in the adsorption of organic and inorganic pollutants because chitin is the second biopolymer in the presence after cellulose. Chitosan is effective in the heavy metals or other chemicals uptake due to the higher content of terminal amino groups which acts as a coordination sites (Assis & Silva, 2003).

The choice of natural chitosan as material for aluminum removal is because aluminum can not be removed by clay materials. It needs organic materials to be adsorbed, and according to the composition of the chitosan, it is possible to assume that it is occurring as an organic matter in the nature, here in the study area.

The pseudo-kinetic adsorption constant of aluminum on chitosan determined by Badawi et al., (2017) with the laboratory experiment is given in table 2.

Table 2: First order kinetic constant of heavy metals/chemicals removal in water

Element	Kinetic constant (1/sec)
Al	1.49×10^{-4} (f)
Fe	7×10^{-5} (d)
Pb	4.98×10^{-4} (c)
Mn	1×10^{-4} (d)
Cu	1.34×10^{-4} (c)
Zn	1.40×10^{-4} (c)
As	2×10^{-4} (d)
Ni	5×10^{-5} (e)

(c) (Kim & Kwak, 2017)

(d) (Dousova et al., 2011)

(e) (Maleki & Karimi-jashni, 2017)

(f) (Badawi et al., 2017)

2.1.5.2. Estimating Diffusion Coefficients in Aqueous Systems

One of the most commonly used approaches for estimating diffusion coefficients for nonionic species in liquids at dilute concentration is that of (Wilke and Chang 1955, in Thibodeaux & Mackay, 2011). This method incorporates the dependence on temperature and viscosity, the theoretical derivation obtained with a solvent association parameter and explicit dependence on the molar volume of the diffusing species (Thibodeaux & Mackay, 2010 & Gulliver, 2007).

$$D = \frac{7.4 * 10^{-8} (\Phi M)^{1/2} T}{\tilde{v}^{0.6} \eta} \quad (22)$$

Where D = the diffusivity of a heavy metals or chemicals in water (m^2s^{-1})

Φ = the association constant for water, 2.26, dimensionless;

M = the molecular weight of water, 18.0gmol^{-1} ;

T = the system temperature (K);

\tilde{v} = the molar volume of heavy metals or chemicals at its boiling point (1atm) in m^{-3}

mol⁻¹;

η = the viscosity of water in cP ($1\text{kgm}^{-1}\text{s}^{-1} = 1\text{Pas} = 1000\text{ cP}$).

The relationship described above is not dimensionally consistent; therefore, accurate estimates of aqueous diffusivity will only be obtained if the values of the parameters used have specific units. This correlation provides estimates with average errors of $\approx 10\%$.

Another semi empirical correlation for estimating diffusivities is developed based on the Wilke-Chang equation by (Othmer & Thakar 1953, in Thibodeaux & Mackay, 2011) with further modification by (Hayduk & Laudie 1974, in Thibodeaux & Mackay, 2011) for nonionic compounds in water:

$$D = \frac{13.26 * 10^{-5}}{\bar{v}^{0.589} \eta^{1.14}} \quad (23)$$

Where all terms are the same (and have the same units) as those in Wilke-Chang equation. Slight changes were made to the parameter values (Φ takes the value 2.6 instead of 2.26 indicated above) and the power-law dependencies on molar volume and viscosity (Thibodeaux & Mackay, 2010 & Gulliver, 2007).

The advantage of the Hayduk-Laudie method over that of Wilke-Chang is that it was specifically developed for estimating diffusivities in water. The average error anticipated for this correlation is $<6\%$ (Thibodeaux & Mackay, 2010). The molar volume estimation for molecules is given in table 11 in annex and the following table 3 gives the calculated diffusivity coefficients according to Wilke-Chang (D_1) and according to Hayduk-Laudie (D_2).

Table 3 : Diffusivity coefficient estimation

Chemicals	D_1 (m ² s ⁻¹)	D_2 (m ² s ⁻¹)
Al	0.4419	0.1171
Cu	0.5416	0.1429
Fe	0.5416	0.1433
Mn	0.5313	0.1403
Zn	0.4657	0.1232
As	0.3761	0.0999
Ni	0.5675	0.1497
Pb	0.3077	0.0820

D_1 is according to Wilke-Chang

D_2 is according to Hayduk-Laudie

Comparing the deviation error in calculating the first diffusivity $\approx 10\%$ according to Walke-chang and for the second $<6\%$ according to Hayduk-Laudie and considering that Hayduk-Laudie formula is developed for estimating diffusivities in water, this one (D_2) is considered as realistic (table 3).

2.2.Transport model implementation

The following sections explain the implementation methodologies of the final equation (17) of the transport model using Microsoft excel and Matlab.

2.2.1.Microsoft excel implementation protocol

Distance variable is applied to 6 different distances, which allows to get 6 curves for each chemical. The 5 first curves of the model are plotted using an interval of time of 1 hour and the last curve is plotted with 10.5 hours interval of time. This time is calculated (chap 3.2) assuming that the concentration arriving into Douro river is maximal, without degradation.

Each model is discretized using 1m distance-step until 120 m , distance between the source Fibrocimento and Douro river.

The choice of the interval time and the distance-step model discretization has the aim of smoothing the curves and fitting the model respectively.

Time variable is applied for 5 different times, which allows to get 5 curves . Four curves are plotted using an interval of distance of 20 m and one curve (4th) is plotted using an interval of distance of 40 m. The model is thus discretized using 0.1h (6 min) time-step until 10.5 hours. This time will allow to determine graphically the residence time considering the degradation of first order.

For both distance and time variables, the single curve is selected with time equal to 10.5 hours and distance equal to 120m respectively in order to determine graphically the predicted residence time of each heavy metal or chemical and the simulated concentration discharged into Douro river.

The predicted residence time is graphically determined using time variable and the simulated concentration of heavy metals in water discharged into Douro river is determined graphically using distance variable.

This concentration entering into Douro river is hence compared to the Limit Value of Emission (LVE) of residues discharged into water given by the Decree-Law n° 236/98 of the Ministry of Environment of Portugal.

2.2.2. Matlab implementation protocol

As for Microsoft excel, the interval of time of 0.1h (360sec) and the distance-step of 1m are used to smooth and feet the curve and the model respectively, in matlab also, they are used likewise but for time variable, the time is discretized until a value greater than 10.5h because the simulated residence time is sometimes greater than that value. The protocols for both time variable and distance variabl are given below.

2.2.2.1. Transport model-Time variable implementation protocol

```
% Transport model time evolution for each heavy metal/chemical;
% t is time in seconds;
% d is the distance in m;
% V is the velocity of water in m/sec;
% D is the diffusivity of each heavy metal/chemical in m2/sec;
% λ is the kinetic constant in 1/sec;
% Co is the initial concentration of each heavy metal/chemical in µg/l;
% C is the predicted concentration of heavy metal/chemical in µg/l;
clear
t=0:360:150000;
d=120;
D= value of diffisivity corresponding to each heavy metal/chemical;
V=0.003156;
λ= value of the kinetic constant corresponding to each heavy metal/chemical;
%A=sqrt(4×D×t);
%B=exp(-λ×t);
Co= initial value corresponding to each heavy metal/chemical;
if(d>(V×t)) ;
C=(Co/2)×erf((d-(t×V))/sqrt(4×D×t))×exp(-λ×t);
else
C=(Co/2)×(1+erf((t×V)-d)/sqrt(4×D×t))×exp(-λ×t);
end
plot(t,C)
```

2.2.2. 2.Transport model-Distance variable implementation protocol

```

% Transport model distance evolution for each heavy metal/chemical ;
% t is time in seconds;
% d is the distance in m,
% V is the velocity of water in m/sec;
% D is the diffusivity of each heavy metal/chemical in m2/sec;
% λ is the kinetic constant in 1/sec;
% Co is the initial concentration in µg/l;
% C is the predicted concentration of each heavy metal/chemical;
clear;
t=38013.27;
d=0:1:120;
D= value of diffusivity corresponding to each heavy metal/chemical;
V=0.003156;
λ= value kinetic constant corresponding to each heavy metal/chemical;
%A=sqrt(4×D×t);
%B=exp(-λ×t);
Co= initial value corresponding to each heavy metal/chemical;
if(d>(V×t)) ;
C=(Co/2)×erf((d-(t×V))/sqrt(4×D×t))×exp(-λ×t);
else
C=(Co/2)×(1+erf((t×V)-d)/sqrt(4×D×t))×exp(-λ×t);
end
plot(d,C)

```

2.3. Available data

2.3.1 Data from monitoring field

This method uses data from monitoring field made from 2007 until 2015. The following data (table 4) are pH of water and concentration of heavy metals, other chemicals and sulfide at different date. The data have been collected at the source of pollution (Fibrocimento tube), in Douro river surface water and at 2.5 m deep.

Table 4: Concentration and pH of heavy metals and sulfide at Fibrocimento source, in Douro surface water and at 2.5m deep in water.

	Date	pH	SO4 mg/L	Al (µg/L)	Cu (µg/L)	Fe (µg/L)	Mn (µg/L)	Zn (µg/L)	As (µg/L)	Ni(µg/L)	Pb (µg/L)
Source	27-08-2007	3.4	-	-	-	-	-	-	[17 - 19]	[1.170 - 1.190]	[4 - 5]
	18-12-2008	3.1	-	-	-	-	-	-	[20 - 22]	[1.400 - 1.420]	[4 - 6]
	24-08-2009	3.1	-	-	-	-	-	-	[3 - 4]	[800 - 1000]	[4 - 5]
	17-08-2010	3.2	-	-	-	-	-	-	[41 - 43]	[1.220 - 1.240]	[3 - 4]
	18-10-2010	3.1	[1800 - 2000]	-	[60 - 70]	[30500 - 30700]	[150000 - 160000]	[1400 - 1500]	[50 - 70]	[1.170 - 1.190]	[3 - 4]
	01-09-2011	3.2	[2100 - 2300]	[21000 - 23000]	[70 - 90]	-	-	[1600 - 1800]	-	[1300 - 1400]	-
	11-01-2012	3.2	[1700 - 1900]	[22000 - 24000]	[60- 70]	[44000 - 46000]	[200000 - 220000]	[1600 - 1800]	[50 - 70]	[1100 - 1300]	-
	28-08-2012	2.9	[1500 - 1700]	[20000 - 22000]	[80 - 90]	[31000 - 33000]	[2600 - 2800]	[1400 - 1600]	[11 - 13]	[1100 - 1200]	-
	19-02-2013	3.8	[2100 - 2300]	[20000 - 22000]	[90 - 100]	[112000 - 114000]	[150000 - 170000]	[1500 - 1700]	[90 - 100]	[1200 - 1300]	-
	27-08-2013	3.3	[1400 - 1600]	[22000 - 24000]	[50 - 70]	[16000 - 18000]	[130000 - 150000]	[1300 - 1500]	[30 - 40]	[1100 - 1200]	-
	11-03-2014	5.4	[1800 - 2000]	[1000 - 1200]	[0.010 - 0.020]	[90000 - 110000]	[130000 - 150000]	[1.1 - 1.3]	[2 - 4]	[900 - 1100]	[2 - 4]
	08-08-2014	3.8	[9 - 11]	[4600 - 4800]	[0.05 - 0.07]	[1400- 1600]	[6800 - 7000]	[1.8 - 2.0]	[2 - 4]	[200 - 300]	[0.002 - 0.003]
	20-02-2015	4.7	[2000 - 2200]	[2400 - 2600]	[70- 90]	[3200 - 3400]	[6900 - 7100]	[1400 - 1600]	[900 - 100]	[1200 - 1300]	[0.002 - 0.003]
Douro surface water	18-102010	7.5	[14 - 15]	[11 - 13]	[4 - 5]	-	-	[10 - 12]	[2 - 3]	[3 - 4]	[3 - 4]
	11-01-2012	6.6	[23 - 25]	[8 - 10]	[4-6]	[44000 - 46000]	[200000 - 220000]	[9 - 11]	[3 - 5]	[3 - 5]	-
	28-08-2013	7.7	[36 - 38]	[10 - 12]	[3 - 4]	[91000 - 93000]	[2600 - 2800]	[12 - 14]	[3 - 5]	[3 - 5]	-
	19/02/2013	7.6	[15 - 17]	[11 - 13]	[3 - 5]	[112000 - 114000]	[150000 - 170000]	[12 - 14]	[2 - 4]	[3 - 5]	-
	27/08/2013	8	[38 - 40]	[12 - 14]	[3 - 5]	[16000 -18000]	[130000 - 150000]	[14 - 16]	[3 - 5]	[3 - 5]	-
	11/03/2014	8	[22 - 23]	[7 - 9]	[0.003 - 0.005]	[90000 -110000]	[130000 - 150000]	[0.014 - 0.016]	[2 - 4]	[3 - 5]	[3-5]
	08/08/2014	7.4	[37-39]	[29 - 31]	[0.001 - 0.002]	[1400 - 1600]	[6800 - 7000]	[0.04 - 0.06]	[3 - 5]	[0.004 - 0.006]	[0.002 - 0.004]
	20/02/2014	6.9	[21 - 23]	[120 -140]	[0.001 - 0.01]	[3200 - 3400]	[6900 -7100]	[0.04 - 0.05]	[0.002 - 0.003]	[0.004 - 0.005]	[0.002 - 0.003]
Douro water 2.5m deep	18/10/2010	7.4	[14 - 15]	[13 - 15]	[4- 6]	[9 - 11]	[17 - 19]	[10 - 12]	[3 - 5]	[3 - 4]	[3 - 4]
	11/03/2014	8	[21 - 22]	[6 - 8]	[0.003- 0.005]	[45 - 47]	[12 - 14]	[0.014 - 0.016]	[2 - 4]	[3 - 5]	[3 - 5]
	08/082014	7.5	[31 - 33]	[20 - 40]	[0.003- 0.005]	[49 - 51]	[0.014 - 0.016]	[0.04 - 0.06]	[2 - 4]	[0.004 - 0.006]	[0.002 - 0.004]
	20/02/2015	7	[14 - 16]	[120 - 140]	[0.001- 0.01]	[91 - 92]	[36 - 38]	[0.04 - 0.05]	[0.002-0.003]	[0.004 - 0.005]	[0.002 - 0.003]

2.3.2. Calculated and converted dimensions

The table 5 shows existing dimensions, calculated and converted dimensions (table 10 in annexe) such as:

Section S (m^2) of the pipe calculated using the measured diameter (0.55m) of the pipe;

Velocity V (m/s) of contaminated water exiting from the pipe, calculated using the following formula: $V = \frac{Q}{S}$ (24)

The dimension converted data is (table 5):

Flow rate of contaminated water Q (l/s) converted from measured flow rate Q (l/min) exiting from the pipe.

Table 5: Characteristic of the tube

Existing dimensions	
Q exit the pipe (l/sec)	0.075
Diameter of Pipe (m)	0.550
Calculated dimensions	
Section of Pipe (m^2)	0.237
Velocity (m/s)	0.003

Chapter 3. RESULT AND DISCUSSION

3.1. Data analysis

When analyzing the given data from field monitorings made from 2007 to 2015, some remarks appear:

The pH at the source of pollution, Fibrocimento tube is in the range of 2.9-5.4 and the pH in Douro river is in the range of 6.6-8.0.

Some hypothetical assertions can be emitted:

The pH at the source of pollution, Fibrocimento, in the range of 2.9-5.4 is due to Acid Mine Drainage (AMD) generation. But the river water has a pH in the buffer range of 6.6-8.0. There should be occurred a natural attenuation of Acid Mine drainage.

There is an imminent risk of toxic pollution of heavy metals in Douro river.

Based on these hypothesis, this chapter is going to discuss the result and deliver a general and realistic overview on the landfill coal ash pollution.

3.2. Results

Results depend on the assumed maximal time. The maximal time is the time calculated assuming that the concentration of heavy metals or chemicals getting into Douro river is maximal, without degradation or adsorption. This time is considered as maximal because it is determined using the maximal distance of 120m.

With this assumption, in the equation 17; $z = vt$ (25)

where z is the distance between Fibrocimento source of pollutants and Douro river, $z = 120$ m; and v is the velocity of water (m/sec), t is the time (sec).

$$t = \frac{z}{v} \quad (26)$$

As $v = 3.15 \times 10^{-3}$ m/sec, $t = \frac{120}{0.00315} = 38013.27$ sec, like 10.55 hours.

This time is applied in the model in order to get the predicted concentration of heavy metals or chemicals discharged into Douro river considering degradation and adsorption.

The results for both excel and matlab implementation are presented with graphics of transport model-time evolution and transport model-distance evolution (figures 9 to 56) and with table 6 and 7.

The result for matlab are presented to validate the result from Microsoft excel. For each heavy metal or chemical, the graphic with one curve is plotted using time of 38013.27 sec (10.5 h) for distance variable and 120m for time variable. From the transport model-time variable, the simulated time residence is determined and from the transport model-distance variable, the predicted concentration discharged into Douro river is determined like in excel implementation.

3.2.1. Results from Microsoft excel implementation

3.2.1.1. Results from Microsoft excel for transport model-time evolution with degradation from the source

One graphic with 5 curves and an other graphic with 1 curve explain the transport model-time evolution for each heavy metal or chemical. In the graphic with 5 curves, the first curve C-20m($\mu\text{g/l}$) is plotted using a distance of 20 m from the source, the second curve C-40m($\mu\text{g/l}$) is plotted using 40 m from the source, the third curve C-60m($\mu\text{g/l}$) is plotted using 60 m from the source, the fourth curve C-100m($\mu\text{g/l}$) is plotted using 100 m from the source and the fifth curve C-120m($\mu\text{g/l}$) is plotted using 120 m from the source (distance between the source and Douro river).

The choice of the number of plotted curves has the aim of smoothing and fitting the graphics. It is not a determined and dependant number.

The fifth curve is hence extracted and constitute the second graphic with 1 curve. This graphic allows to determine the residence time of every heavy metal or chemical in the area.

The following graphics explain the chemical's behaviors from aluminum to lead.

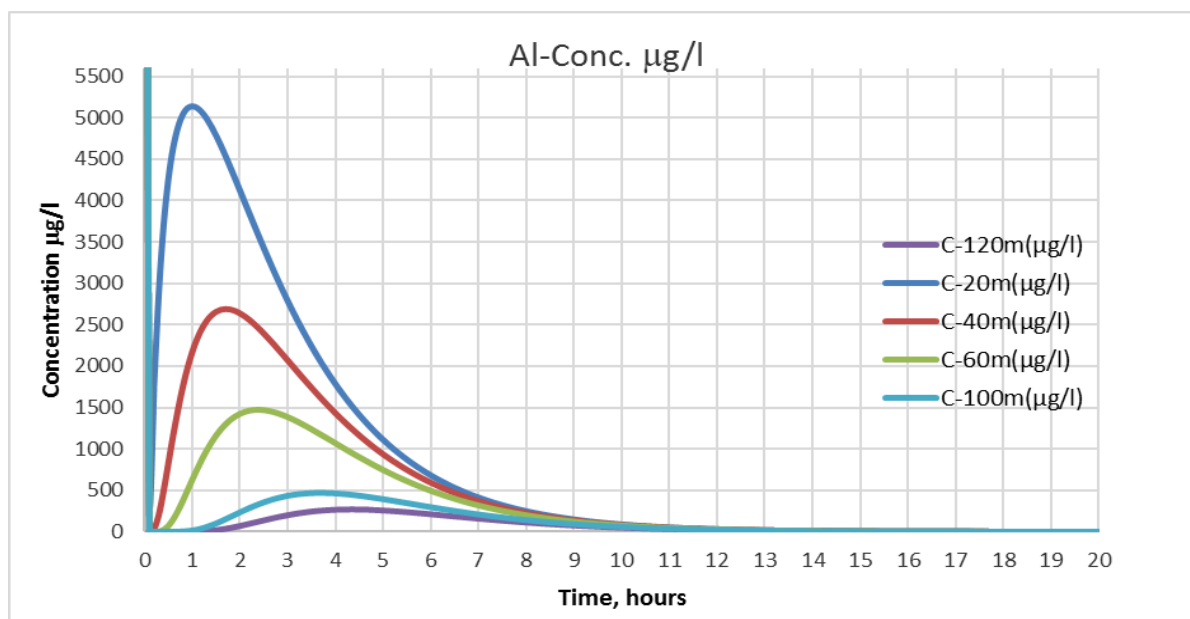


Figure 9:Graphic of aluminum transport model- time evolution

This graphic (figure 9) describes the behavior of aluminum with the spread concentration at the source of 23000 µg/l. The curve C-20m(µg/l) plotted with a distance of 20 m from the source shows that the pick of maximal concentration occurs after 1 hour. The aluminum maximal concentration is 5121.07 µg/l. This pick shows that even though there is a decrease of concentration due to natural attenuation, there is an accumulation. From this pick, the accumulation stops and starts the decreasing of accumulated chemical until a low concentration of 0.00012 µg/l, after 35hours (smulated residence time). The second curve C-40m(µg/l) plotted with a distance of 40 m from the source shows that the pick of maximal concentration of 2638.73 µg/l occurs after 2 hours. The low concentration of 0.00012 µg/l occurs at a simulated residence time of 35.2 hours. The third curve C-60m(µg/l) plotted with a distance of 60 m from the source shows that the pick of maximal concentration of 1446.88 µg/l occurs after 2.7 hours. The low concentration of 0.00010 µg/l occurs at 35.6hours, simulated residence time. The fourth curve C-100m(µg/l) plotted with 100m from the source shows that the pick of maximal concentration of 463.25 µg/l occurs after 4 hours. The low concentration of 0.00011 µg/l occurs at a simulated residence time of 35.4 hours. The fifth curve C-120m(µg/l) is plotted with 120 m , distance from the source Fibrocimento to Douro river (figure 10)

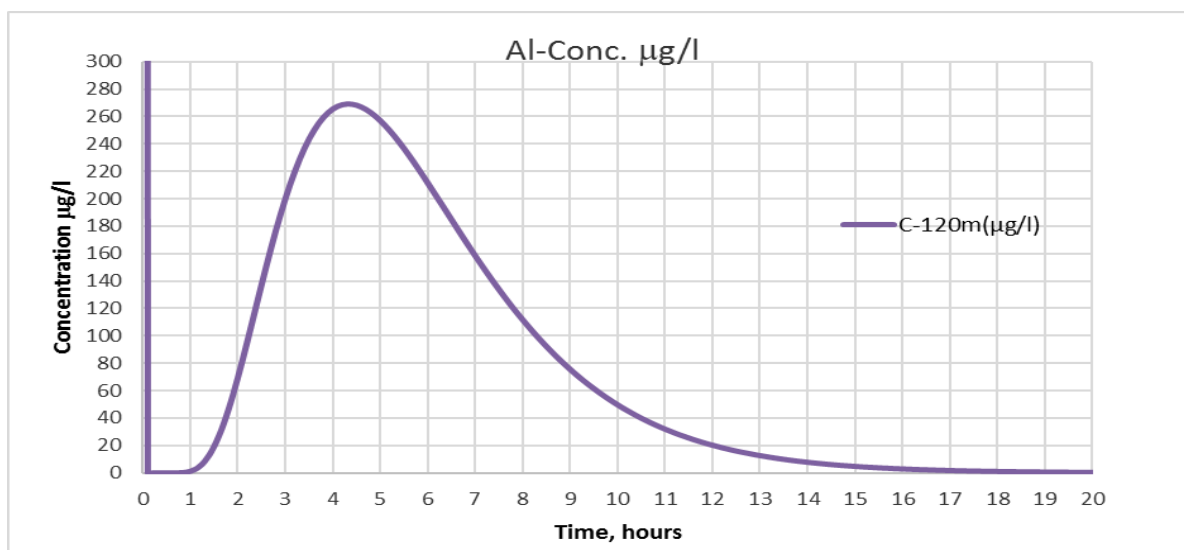


Figure 10: Graphic of the fifth curve of the aluminum transport model-time evolution

The graphic (figure 10) shows that the maximal concentration of 267.00 $\mu\text{g/l}$ occurs after 4.6 hours. The low concentration of 0.00010 $\mu\text{g/l}$ occurs at 35.6 hours, simulated residence time of aluminum in the area.

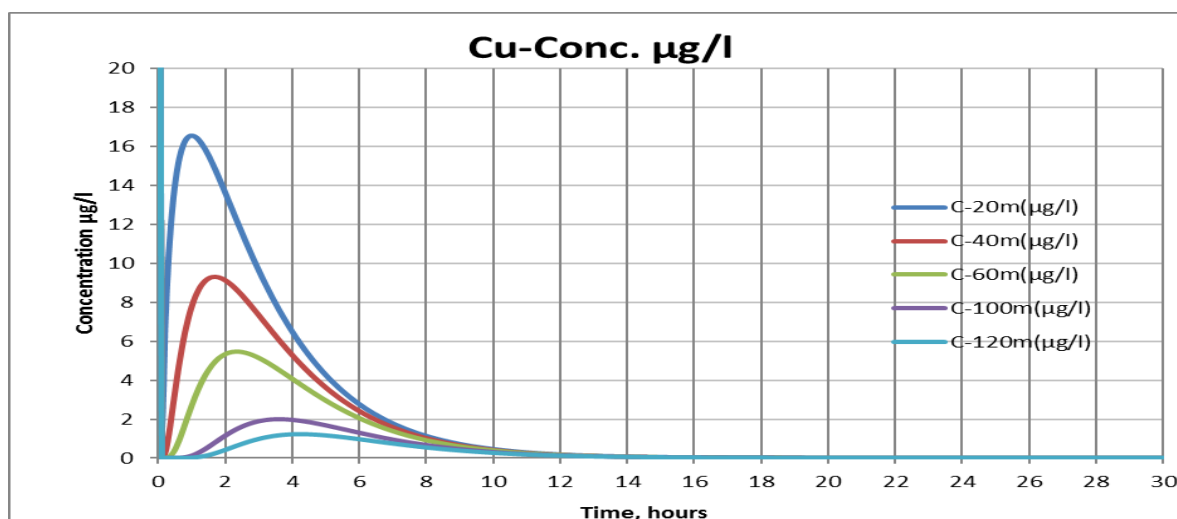


Figure11: Graphic of copper transport model-time evolution

The graphic (figure 11) describes the behavior of copper with the spread concentration at the source of 68 $\mu\text{g/l}$. The curve C-20m($\mu\text{g/l}$) plotted with a distance of 20 m from the source shows that the pick of maximal concentration of 16.32 $\mu\text{g/l}$ occurs after 1.2 hours. This pick shows that even though there is a decrease of concentration due to natural attenuation, there is an accumulation. From this pick, the accumulation stops and starts the decreasing of accumulated chemical until a low concentration of 0.00010 $\mu\text{g/l}$, after 27.6 hours (smulated residence time). The second curve C-40m($\mu\text{g/l}$) plotted with a distance of 40 m from the

source shows that the pick of maximal concentration of $9.11 \mu\text{g/l}$ occurs after 2 hours. The low concentration of $0.00010 \mu\text{g/l}$ occurs at a simulated residence time of 27.6 hours. The third curve C-60m($\mu\text{g/l}$) plotted with a distance of 60 m from the source shows that the pick of maximal concentration of $5.39 \mu\text{g/l}$ occurs after 2.6 hours. The low concentration of $0.00010 \mu\text{g/l}$ occurs at 27.6 hours which is the simulated residence time. The fourth curve C-100m($\mu\text{g/l}$) plotted with 100 m from the source shows that the pick of maximal concentration of $1.98 \mu\text{g/l}$ occurs after 3.7 hours. The low concentration of $0.00010 (\mu\text{g/l})$ occurs at a simulated residence time of 27.6 hours. The fifth curve C-120m($\mu\text{g/l}$) is plotted with 120 m , distance from the source Fibrocimento to Douro river (figure 12).

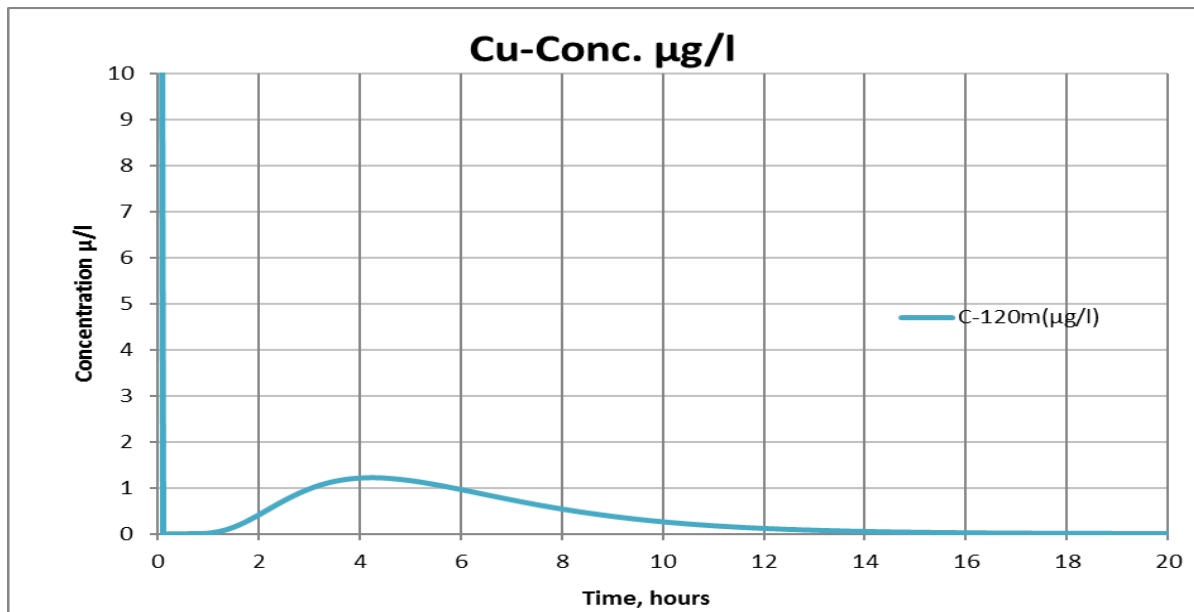


Figure12: Graphic of the fith curve of copper transport model-time evolution

This graphic (figure 12) shows that the maximal concentration of $1.21 \mu\text{g/l}$ occurs after 4.3 hours. The low concentration of $0.00010 \mu\text{g/l}$ occurs at 27.5 hours, simulated residence time of copper in the area.

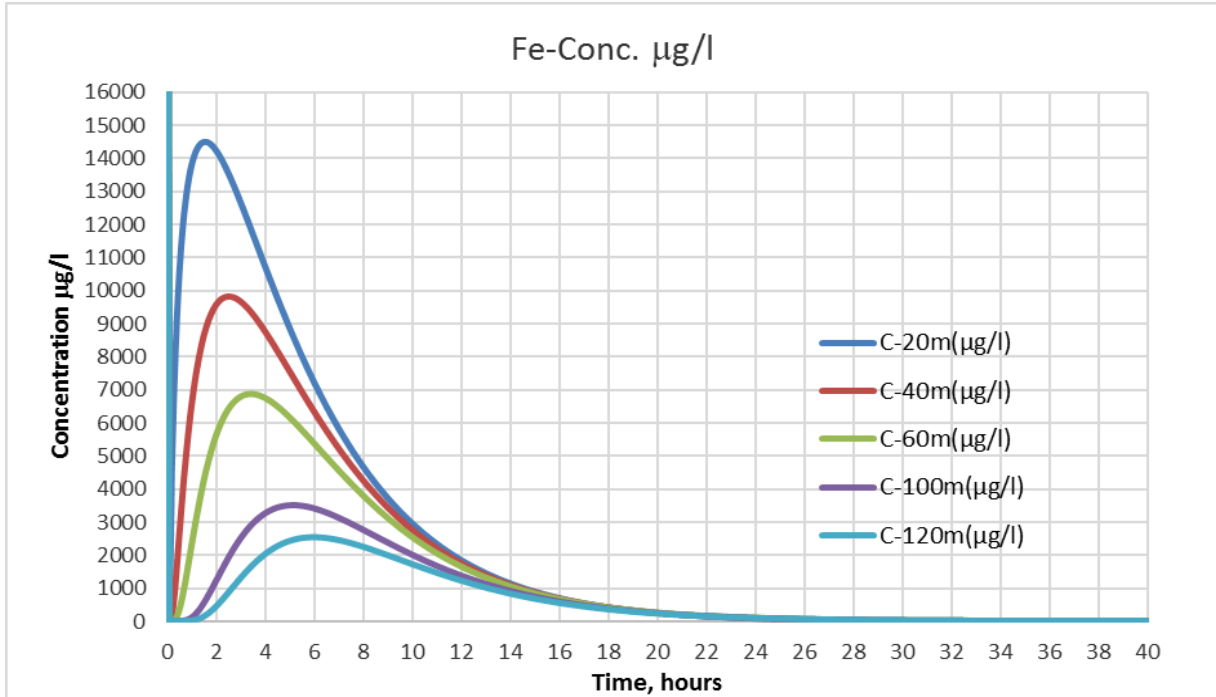


Figure 13: Graphic of iron transport model-time evolution

The graphic (figure 13) describes the behavior of iron with the spread concentration at the source of $45000 \mu\text{g/l}$. The curve C-20m($\mu\text{g/l}$) plotted with a distance of 20 m from the source shows that the pick of maximal concentration of $14243.45 \mu\text{g/l}$ occurs after 2 hours. This pick shows that even though there is a decrease of concentration due to natural attenuation, there is an accumulation. From this pick, the accumulation stops and starts the decreasing of accumulated chemical until a low concentration of $0.00010 \mu\text{g/l}$, after 79 hours (smulated residence time). The second curve C-40m($\mu\text{g/l}$) plotted with a distance of 40 m from the source shows that the pick of maximal concentration of $9671.59 \mu\text{g/l}$ occurs after 3 hours. The low concentration of $0.00010 \mu\text{g/l}$ occurs at 79 hours. The third curve C-60m($\mu\text{g/l}$) plotted with a distance of 60 m from the source shows that the pick of maximal concentration of $6699.71 \mu\text{g/l}$ occurs after 4.1 hours. The low concentration of $0.00010 \mu\text{g/l}$ occurs at 79 hours. The fourth curve C-100m($\mu\text{g/l}$) plotted with 100 m from the source shows that the pick of maximal concentration of $3357.96 \mu\text{g/l}$ occurs after 6.2 hours. The low concentration of $0.00010 \mu\text{g/l}$ occurs at 79 hours. The fifth curve C-120m($\mu\text{g/l}$) is plotted with 120 m , distance from the source Fibrocimento to Douro river (figure 14).

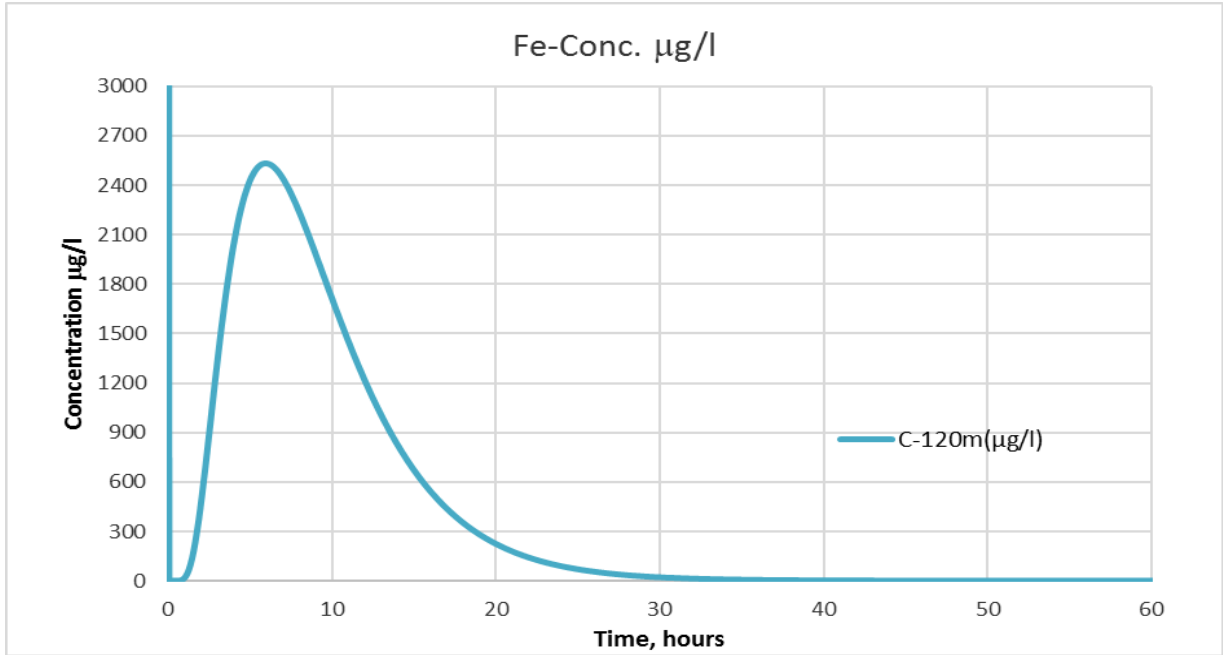


Figure 14: Graphic of the fith curve of iron transport model-time evolution

This graphic (figure 14) shows that the maximal concentration of 2473.84 $\mu\text{g/l}$ occurs after 6.8 hours. The low concentration of 0.00010 $\mu\text{g/l}$ occurs at 79 hours, simulated residence time of iron in the area.

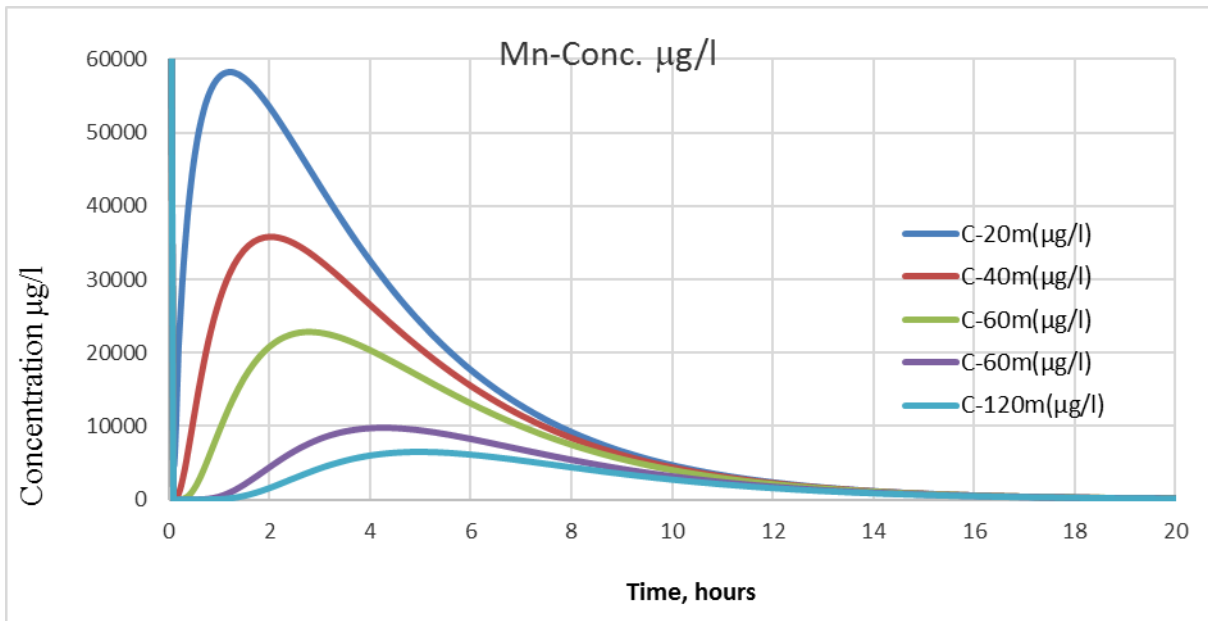


Figure 15: Graphic of manganese transport model-time evolution

The graphic (figure 15) describes the behavior of manganese with the spread concentration at the source of 210000 $\mu\text{g/l}$. The curve C-20m($\mu\text{g/l}$) plotted with a distance of 20 m from the

source shows that the pick of maximal concentration of 58216.83 $\mu\text{g/l}$ occurs after 1.3 hours. This pick shows that even though there is a decrease of concentration due to natural attenuation, there is an accumulation. From this pick, the accumulation stops and starts the decreasing of accumulated chemical until a low concentration of 0.00010 $\mu\text{g/l}$, after 59.5 hours (simulated residence time). The second curve C-40m($\mu\text{g/l}$) plotted with a distance of 40 m from the source shows that the pick of maximal concentration of 35799.38 $\mu\text{g/l}$ occurs after 2.1 hours. The low concentration of 0.00010 $\mu\text{g/l}$ occurs at 59.5 hours. The third curve C-60m($\mu\text{g/l}$) plotted with a distance of 60 m from the source shows that the pick of maximal concentration of 22634.80 $\mu\text{g/l}$ occurs after 3.1 hours. The low concentration of 0.00010 $\mu\text{g/l}$ occurs at 59.5 hours. The fourth curve C-100m($\mu\text{g/l}$) plotted with 100 m from the source shows that the pick of maximal concentration of 9699.67 $\mu\text{g/l}$ occurs after 4.6 hours. The low concentration of 0.00010 $\mu\text{g/l}$ occurs at 59.5 hours. The fifth curve C-120m($\mu\text{g/l}$) is plotted with 120 m, distance from the source Fibrocimento to Douro river (figure 16).

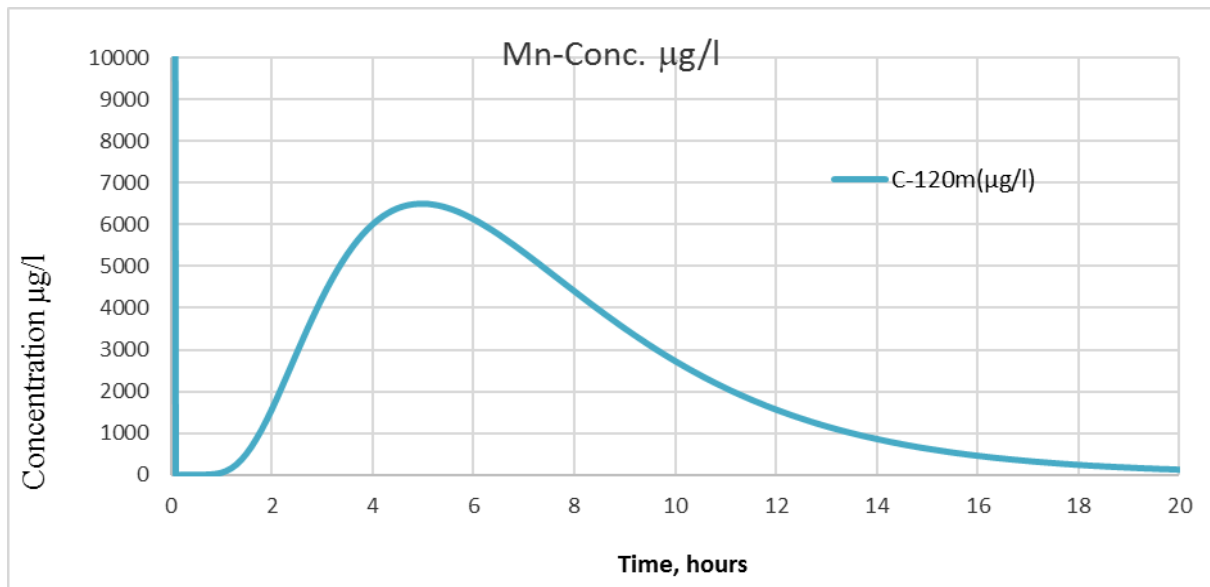


Figure 16: Graphic of the fifth curve of manganese transport model-time evolution

This graphic (figure 16) shows that the maximal concentration of 6422.03 $\mu\text{g/l}$ occurs after 5.4 hours. The low concentration of 0.00010 $\mu\text{g/l}$ occurs at 59.5 hours, simulated residence time of manganese in the area.

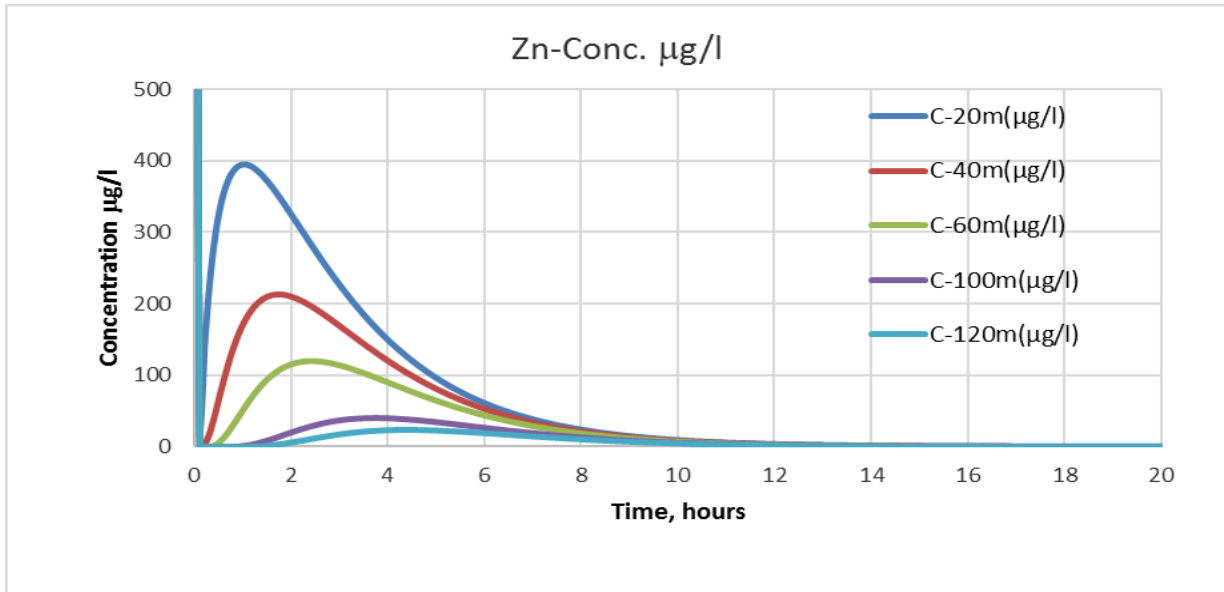


Figure 17: Graphic of zinc transport model-time evolution

The graphic (figure 17) describes the behavior of zinc with the spread concentration at the source of 1700 µg/l. The curve C-20m (µg/l) plotted with a distance of 20 m from the source shows that the pick of maximal concentration of 391.08 µg/l occurs after 1.2 hours. This pick shows that even though there is a decrease of concentration due to natural attenuation, there is an accumulation. From this pick, the accumulation stops and starts the decreasing of accumulated chemical until a low concentration of 0.00010 µg/l, after 32.7 hours (smulated residence time). The second curve C-40m(µg/l) plotted with a distance of 40 m from the source shows that the pick of maximal concentration of 210.26 µg/l occurs after 2 hours. The low concentration of 0.00010 µg/l occurs at 32.7 hours. The third curve C-60m(µg/l) plotted with a distance of 60 m from the source shows that the pick of maximal concentration of 118.77 µg/l occurs after 2.7 hours. The low concentration of 0.00010 µg/l occurs at 32.7 hours. The fourth curve C-100m(µg/l) plotted with 100 m from the source shows that the pick of maximal concentration of 40.27 µg/l occurs after 4 hours. The low concentration of 0.00010 µg/l occurs at 32.7 hours. The fifth curve C-120m(µg/l) is plotted with 120 m , distance from the source Fibrocimento to Douro river (figure 18).

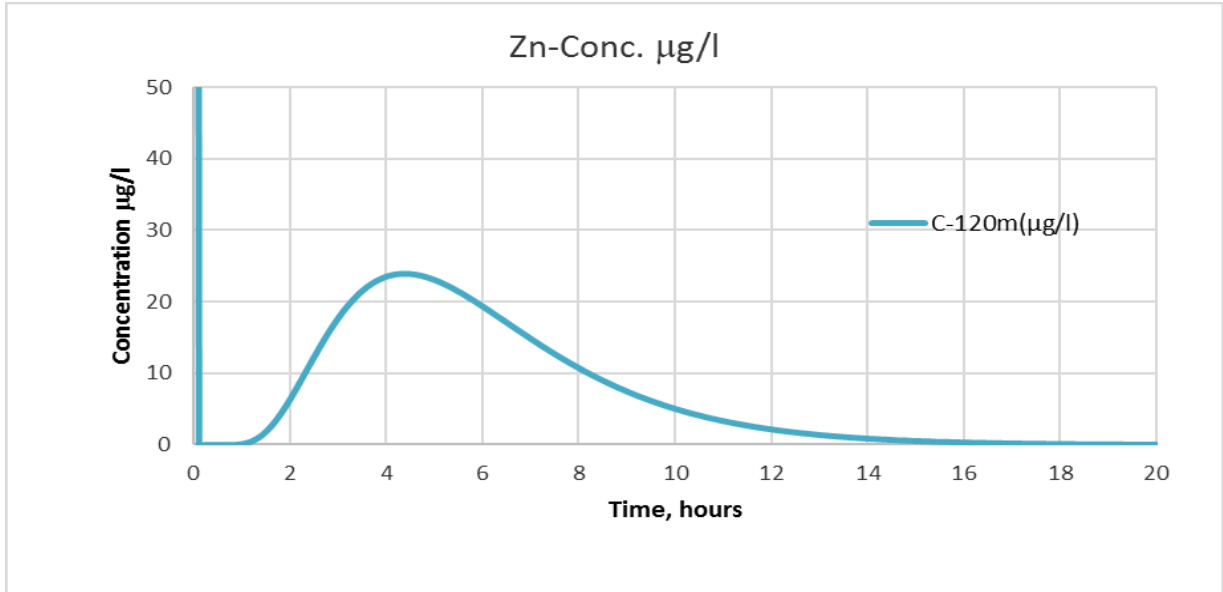


Figure 18: Graphic of the fifth curve of zinc transport model-time evolution

This graphic (figure 18) shows that the maximal concentration of $23.73 \mu\text{g/l}$ occurs after 4.7 hours. The low concentration of $0.00010 \mu\text{g/l}$ occurs at 32.6 hours, simulated residence time of zinc in the area.

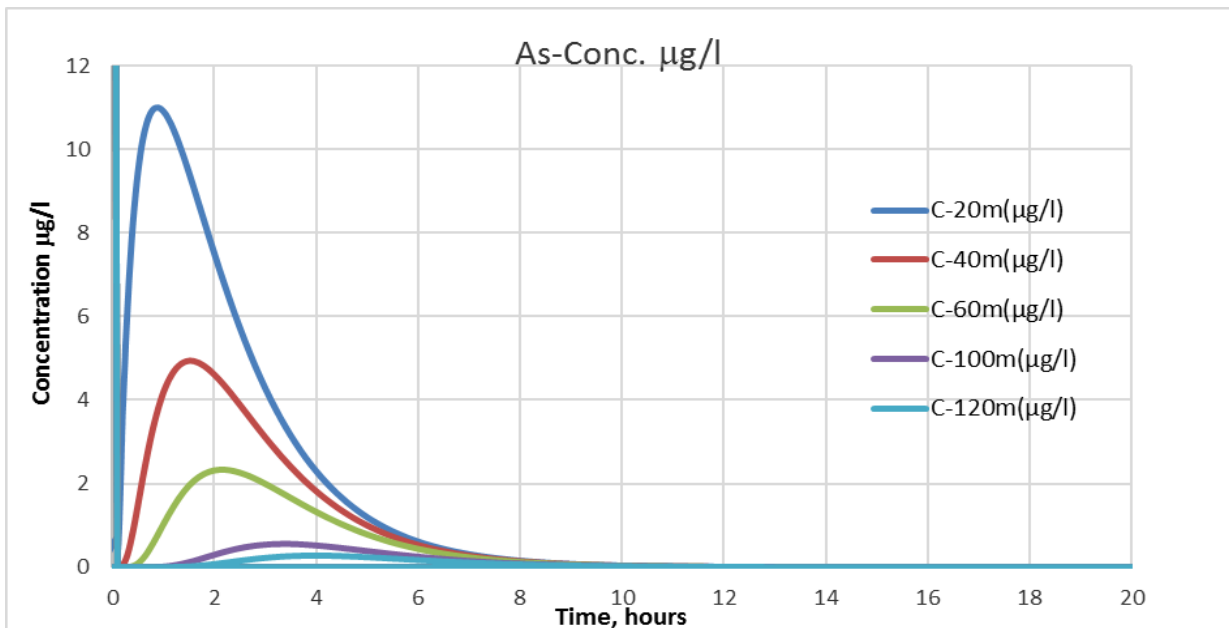


Figure 19: Graphic of arsenic transport model-time evolution

The graphic (figure 19) describes the behavior of arsenic with the spread concentration at the source of $60 \mu\text{g/l}$. The curve C-20m ($\mu\text{g/l}$) plotted with a distance of 20 m from the source shows that the pick of maximal concentration of $10.91 \mu\text{g/l}$ occurs after 1 hour. This pick

shows that even though there is a decrease of concentration due to natural attenuation, there is an accumulation. From this pick, the accumulation stops and starts the decreasing of accumulated chemical until a low concentration of $0.00010 \mu\text{g/l}$, after 18.4 hours (smulated residence time). The second curve C-40m($\mu\text{g/l}$) plotted with a distance of 40 m from the source shows that the pick of maximal concentration of $4.88 \mu\text{g/l}$ occurs after 1.7 hours. The low concentration of $0.00010 \mu\text{g/l}$ occurs at 18.3 hours. The third curve C-60m($\mu\text{g/l}$) plotted with a distance of 60 m from the source shows that the pick of maximal concentration of $2.29 \mu\text{g/l}$ occurs after 2.4 hours. The low concentration of $0.00010 \mu\text{g/l}$ occurs at 18.3 hours. The fourth curve C-100m($\mu\text{g/l}$) plotted with 100 m from the source shows that the pick of maximal concentration of $0.55 \mu\text{g/l}$ occurs after 3.5 hours. The low concentration of $0.00010 \mu\text{g/l}$ occurs at 18.2 hours. The fifth curve C-120m($\mu\text{g/l}$) is plotted with 120 m , distance from the source Fibrocimento to Douro river (figure 20).

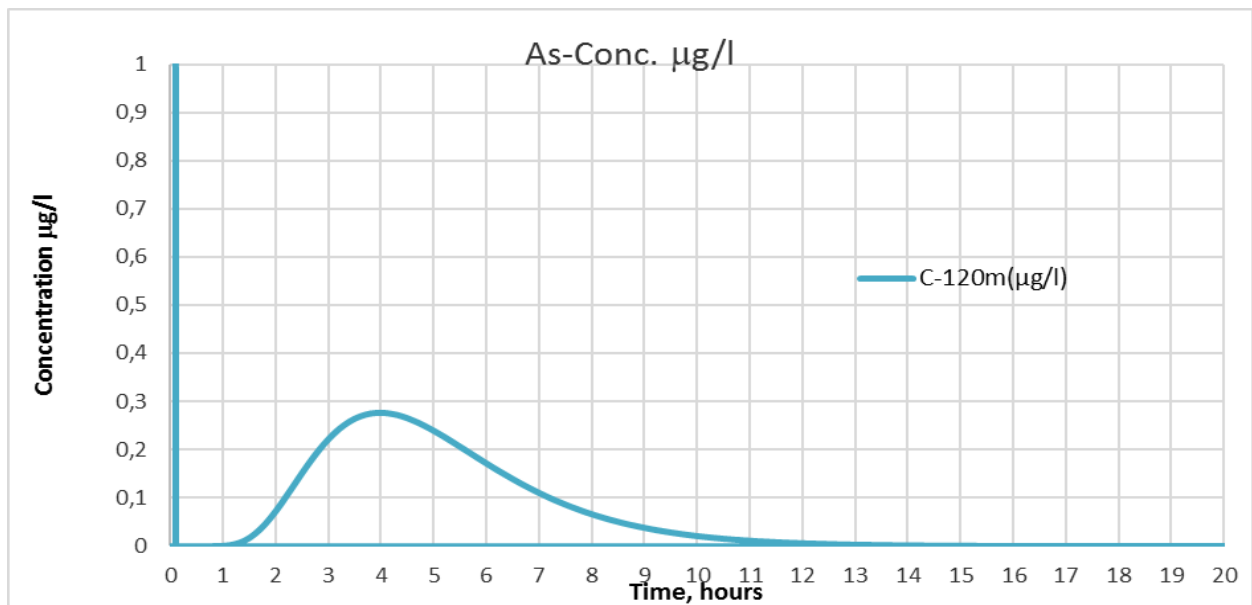


Figure 20: Graphic of the fith curve of arsenic transport model-time evolution

This graphic (figure 20) shows that the maximal concentration of $0.27 (\mu\text{g/l})$ occurs after 4.3 hours. The low concentration of $0.00010 \mu\text{g/l}$ occurs at 18.1 hours, simulated residence time of arsenic in the area.

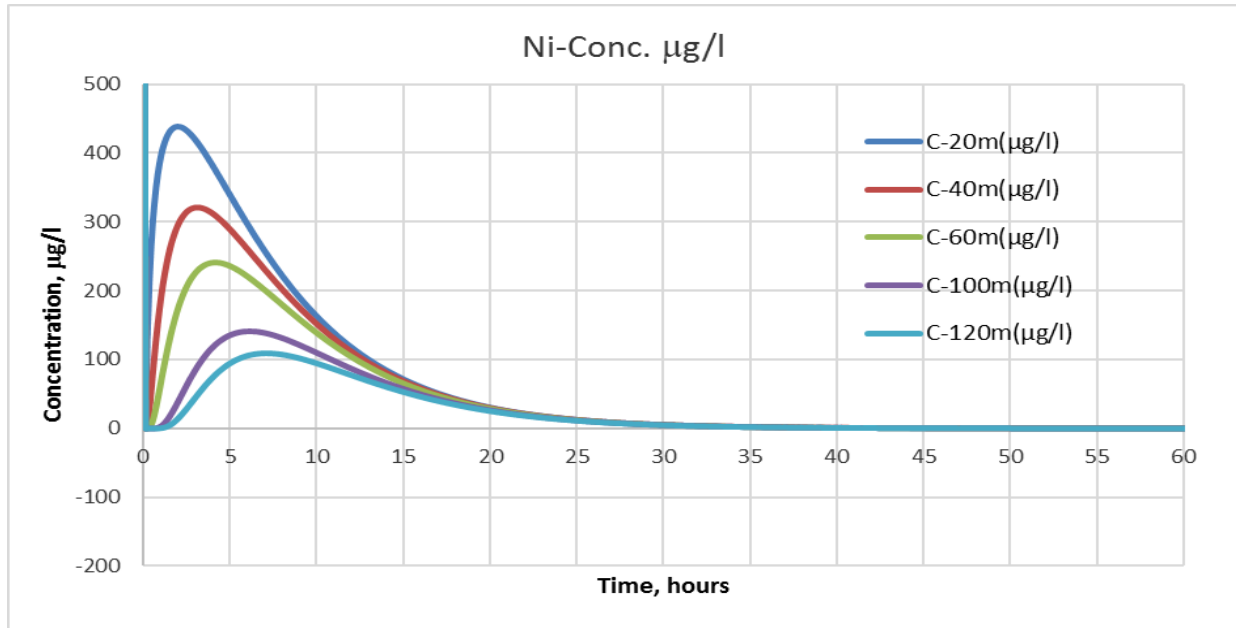


Figure 21: Graphic of nickel transport model-time evolution

The graphic (figure 21) describes the behavior of nickel with the spread concentration at the source of 1200 µg/l. The curve C-20m(µg/l) plotted with a distance of 20 m from the source shows that the pick of maximal concentration of 433.82 µg/l occurs after 2.4 hours. This pick shows that even though there is a decrease of concentration due to natural attenuation, there is an accumulation. From this pick, the accumulation stops and starts the decreasing of accumulated chemical until a low concentration of 0.00010 µg/l, after 90.5 hours (smulated residence time). The second curve C-40m(µg/l) plotted with a distance of 40 m from the source shows that the pick of maximal concentration of 319.52 µg/l occurs after 3.4 hours. The low concentration of 0.00010 µg/l occurs at 90.4 hours. The third curve C-60m(µg/l) plotted with a distance of 60 m from the source shows that the pick of maximal concentration of 239.25 µg/l occurs after 4.6 hours. The low concentration of 0.00010 µg/l occurs at 90.4 hours. The fourth curve C-100m(µg/l) plotted with 100 m from the source shows that the pick of maximal concentration of 140.27 µg/l occurs after 6.6 hours. The low concentration of 0.00010 µg/l occurs at 90.4 hours. The fifth curve C-120m(µg/l) is plotted with 120 m , distance from the source Fibrocimento to Douro river (figure 22).

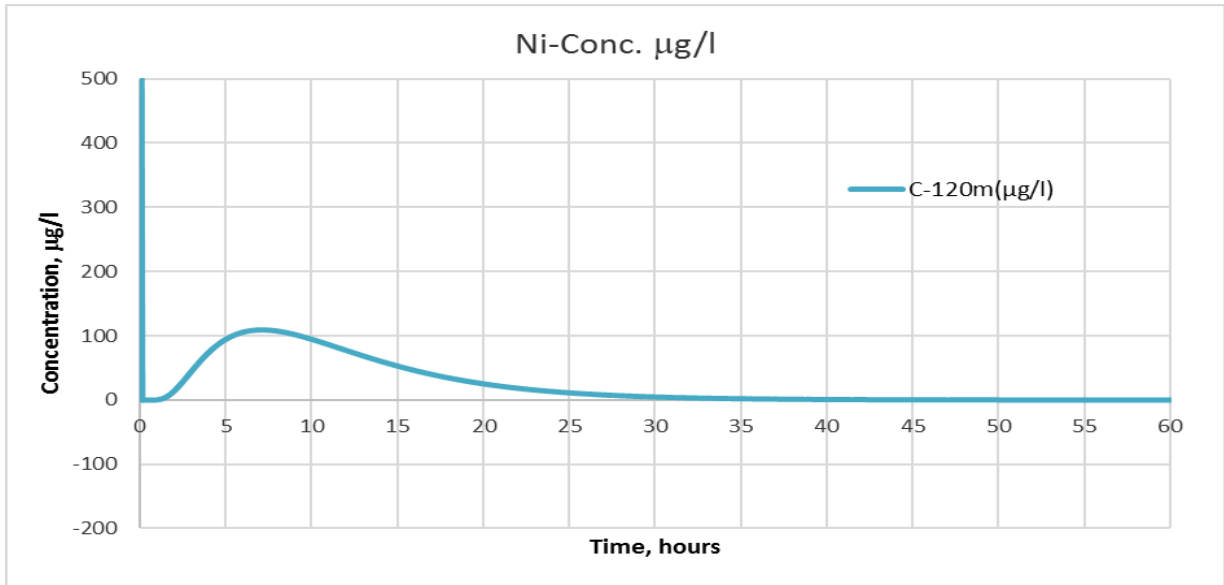


Figure 22 : Graphic of the fith curve of nickel transport model-time evolution

This graphic (figure 22) shows that the maximal concentration of 107 $\mu\text{g/l}$ occurs after 4.3 hours. The low concentration of 0.00010 $\mu\text{g/l}$ occurs at 90.4 hours, simulated residence time of nickel in the area.

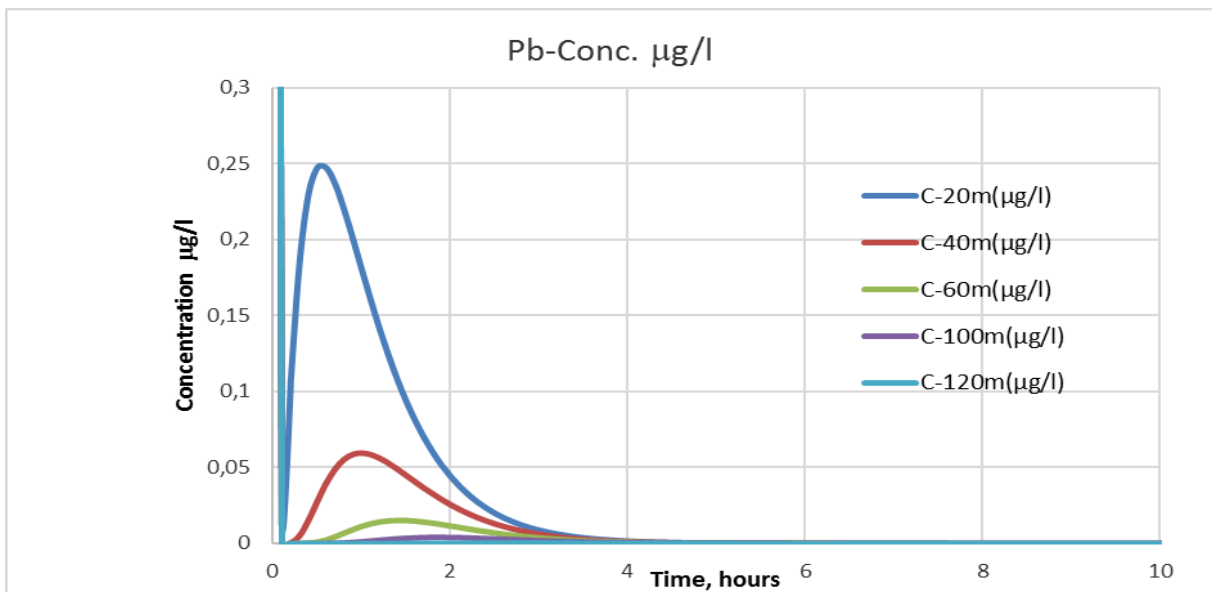


Figure 23: Graphic of lead transport model-time evolution

The graphic (figure 23) describes the behavior of lead with the spread concentration at the source of 3 $\mu\text{g/l}$. The curve C-20m($\mu\text{g/l}$) plotted with a distance of 20 m from the source shows that the pick of maximal concentration of 0.24 $\mu\text{g/l}$ occurs after 0.6 hour. This pick shows that even though there is a decrease of concentration due to natural attenuation, there is

an accumulation. From this pick, the accumulation stops and starts the decreasing of accumulated chemical until a low concentration of $0.00010 \mu\text{g/l}$, after 5.6 hours (smulated residence time). The second curve C-40m($\mu\text{g/l}$) plotted with a distance of 40 m from the source shows that the pick of maximal concentration of $0.058 \mu\text{g/l}$ occurs after 1.1 hours. The low concentration of $0.00010 \mu\text{g/l}$ occurs at 5.5 hours. The third curve C-60m($\mu\text{g/l}$) plotted with a distance of 60 m from the source shows that the pick of maximal concentration of $0.015 \mu\text{g/l}$ occurs after 1.5 hours. The low concentration of $0.00010 \mu\text{g/l}$ occurs at 5.3 hours. The fourth curve C-100m($\mu\text{g/l}$) plotted with 100 m from the source shows that the pick of maximal concentration of $0.004 \mu\text{g/l}$ occurs after 1.9 hours. The low concentration of $0.00010 \mu\text{g/l}$ occurs at 5.1 hours. The fifth curve C-120m($\mu\text{g/l}$) is plotted with 120 m , distance from the source Fibrocimento to Douro river (figure 24).

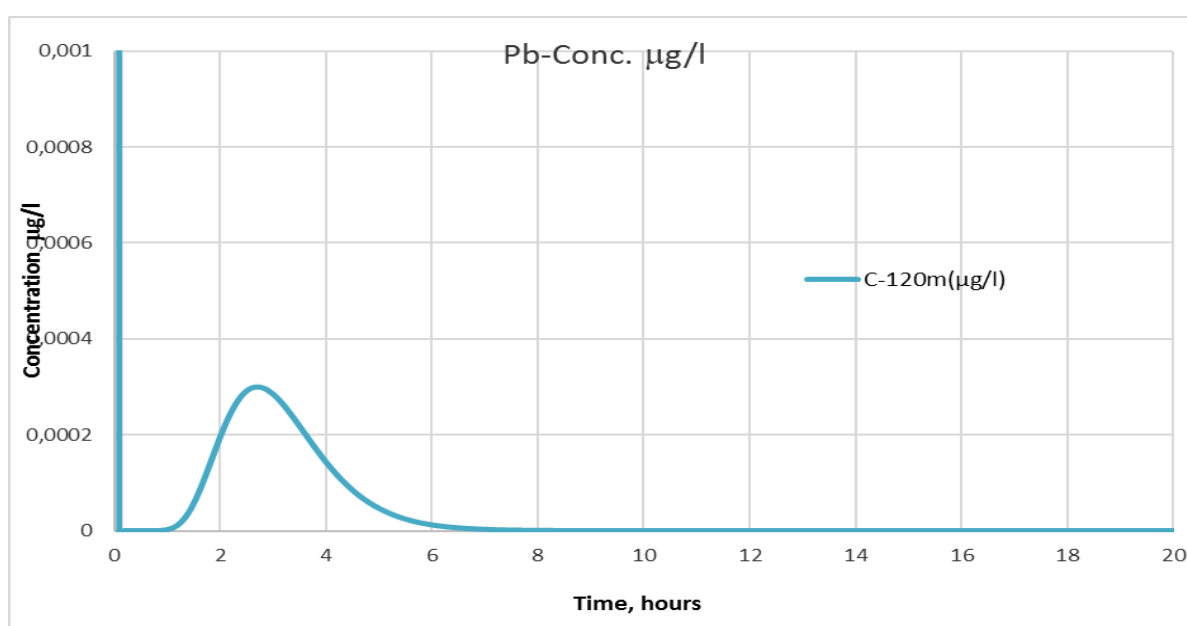


Figure 24: Graphic of the fifth curve of lead transport model-time evolution

This graphic (figure 24) shows that the maximal concentration of $0.00029 \mu\text{g/l}$ occurs after 2.8 hours. The low concentration of $0.00010 \mu\text{g/l}$ occurs at 4.3 hours, simulated residence time of lead in the area.

3.2.1.2. Results from Microsoft excel for transport model- distance evolution with degradation from the source

Like in the transport model-time evolution, two type of graphics explain the transport model. One graphic has one curve and another one has six curves, the first curve C-1h($\mu\text{g/l}$) is plotted with time from the start equal to 1 hour (3600sec), the second curve C-2h($\mu\text{g/l}$) is plotted with the time from the start equal to 2 hours (7200sec), the third curve C-3h($\mu\text{g/l}$) is

plotted with the time from the start equal to 3 hours (10800 sec), the fourth curve C-4h($\mu\text{g/l}$) is plotted with the time from the start equal to 4 hours (14400 sec), the fifth curve C-5h($\mu\text{g/l}$) is plotted with the time from the start equal to 5 hours (18000 Sec), the sixth curve C-10.5h($\mu\text{g/l}$) is plotted with the time from the start equal to 10.5 hours (38013.27 sec).

Also in this case, the choice of the number of plotted curves has the aim of smoothing and fitting the graphics, it is not a determined and dependant number.

The sixth curve is selected and constitute the second type of graphic with one curve. This graphic allows to determine the simulated concentration discharged into Douro river.

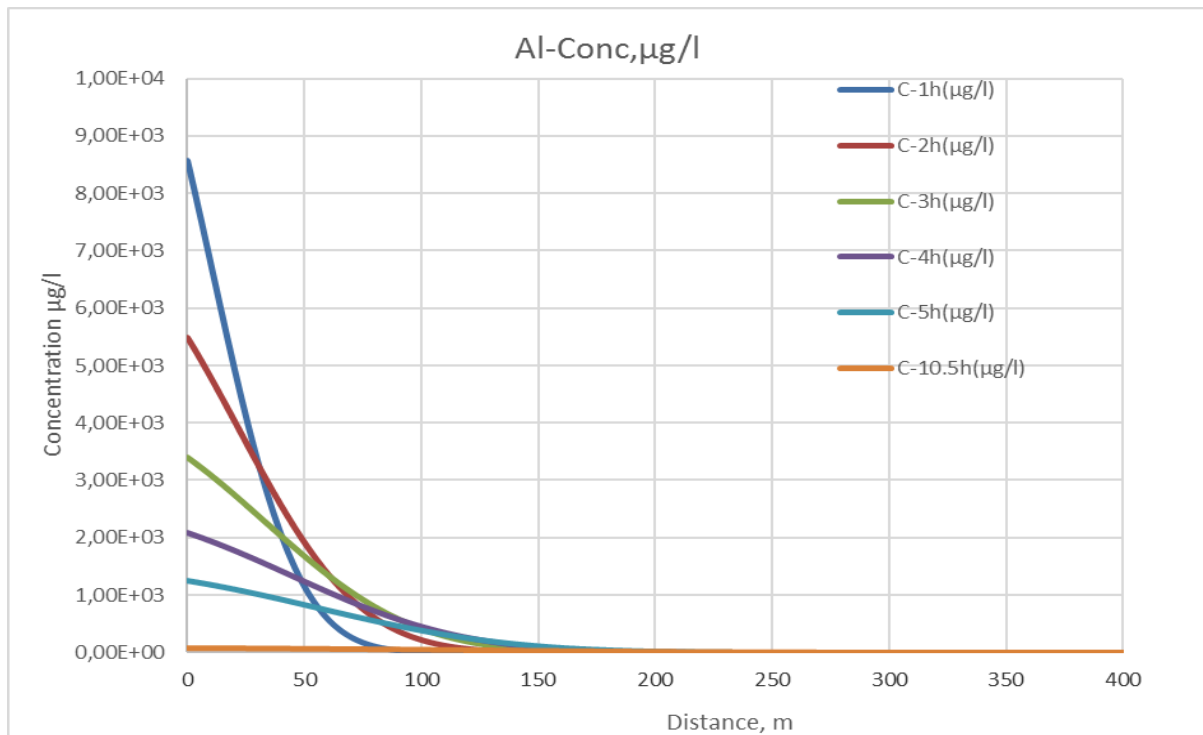


Figure 25: Graphic of aluminum transport model-distance evolution

The graphic (figure 25) describes the behavior of aluminum in the transport model-distance evolution with the spread concentration of $23000 \mu\text{g/l}$ at the source. The curve C-1h($\mu\text{g/l}$) plotted with a time of 1 hour from the start shows that the concentration of aluminum in water discharged into Douro river after 1 hour is equal to $1.07 \mu\text{g/l}$. The second curve C-2h($\mu\text{g/l}$) plotted with a time of 2 hours from the start shows that the concentration of aluminum in water discharged into Douro river is $6.54 \cdot 10^1 \mu\text{g/l}$. The third curve C-3h($\mu\text{g/l}$) plotted with a time of 3 hours from the start shows that the concentration of aluminum in water is $1.92 \cdot 10^2 \mu\text{g/l}$. The fourth curve C-4h($\mu\text{g/l}$) plotted with time of 4 hours from the start shows that the concentration of aluminum in water is $2.58 \cdot 10^2 \mu\text{g/l}$. The fifth curve C-

5h($\mu\text{g/l}$) plotted with a time of 5 hours from the start shows that the concentration of aluminum in water is $2.51 \cdot 10^2 \mu\text{g/l}$. With the sixth curve, the predicted concentration of aluminum in water discharged into Douro river is determined by figure 26.

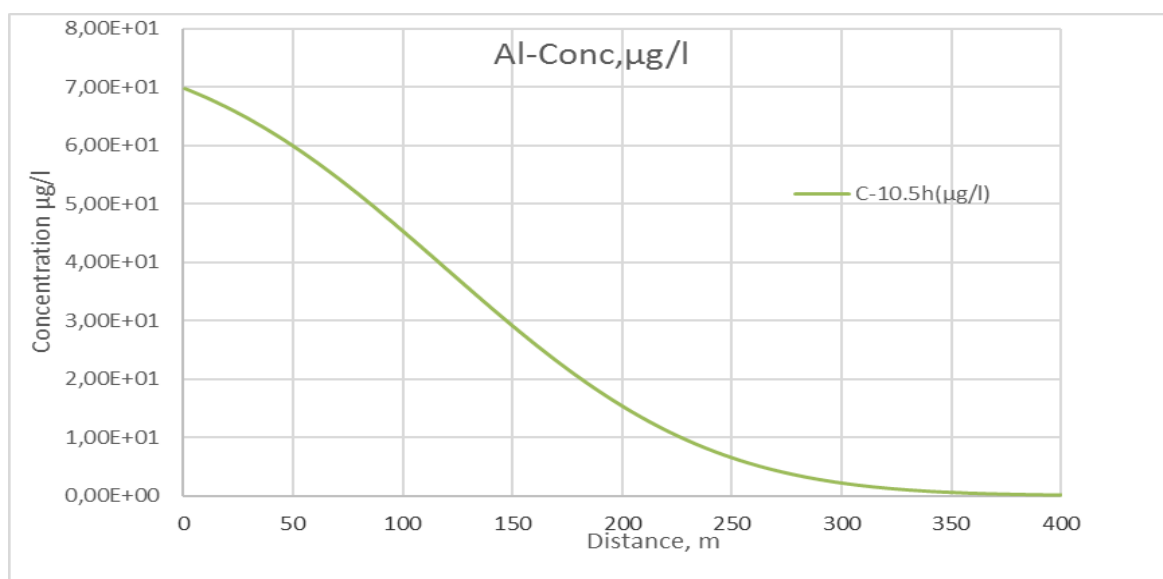


Figure 26: Graphic of the sixth curve of aluminum transport model-distance evolution

This graphic (figure 26) determines that the predicted concentration of aluminum in water discharged into Douro river is $3.89 \cdot 10^1 \mu\text{g/l}$.

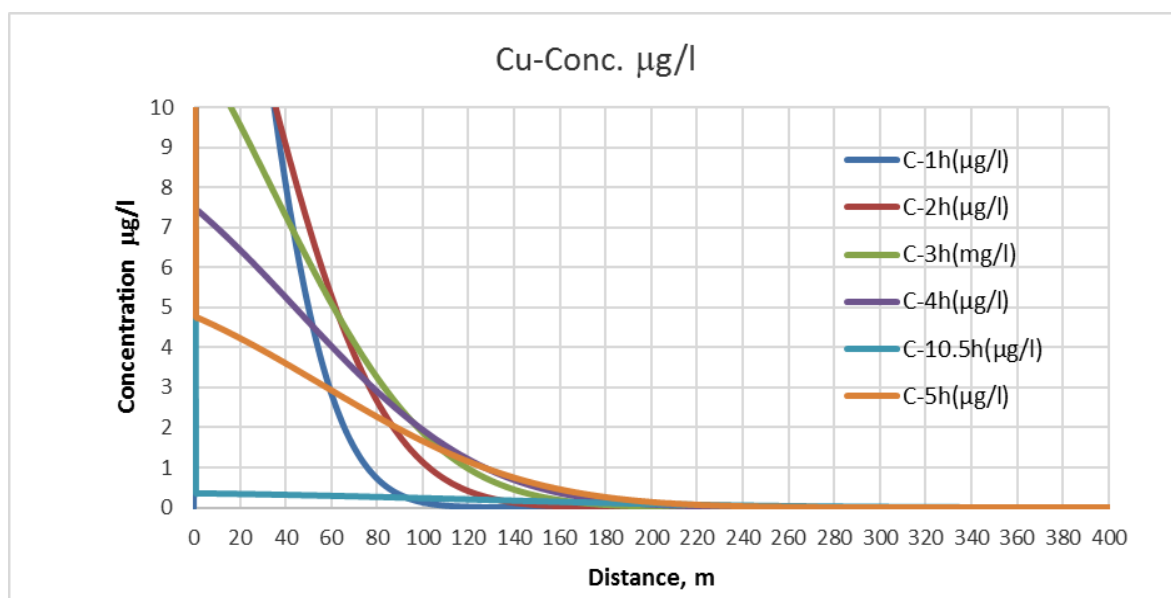


Figure 27: Graphic of copper transport model- distance evolution

The graphic (figure 27) describes the behavior of copper in the transport model-distance evolution with the spread concentration of $68 \mu\text{g/l}$ at the source. The curve C-1h($\mu\text{g/l}$) plotted

with a time of 1 hour from the start shows that the concentration of copper in water discharged into Douro river after 1 hour is equal to $1.49 \cdot 10^{-2} \mu\text{g/l}$. The second curve C-2h($\mu\text{g/l}$) plotted with a time of 2 hours from the start shows that the concentration of copper in water is $4.15 \cdot 10^{-1} \mu\text{g/l}$. The third curve C-3h($\mu\text{g/l}$) plotted with a time of 3 hours from the start shows that the concentration of copper in water is $9.77 \cdot 10^{-1} \mu\text{g/l}$. The fourth curve C-4h($\mu\text{g/l}$) plotted with a time of 4 hours from the start shows that the concentration of copper in water is $1.18 \mu\text{g/l}$. The fifth curve C-5h($\mu\text{g/l}$) plotted with a time of 5 hours from the start shows that the concentration of copper in water is $2.05 \cdot 10^{-1} \mu\text{g/l}$. With the sixth curve, the predicted concentration of copper in water discharged into Douro river is determined by the figure 28.

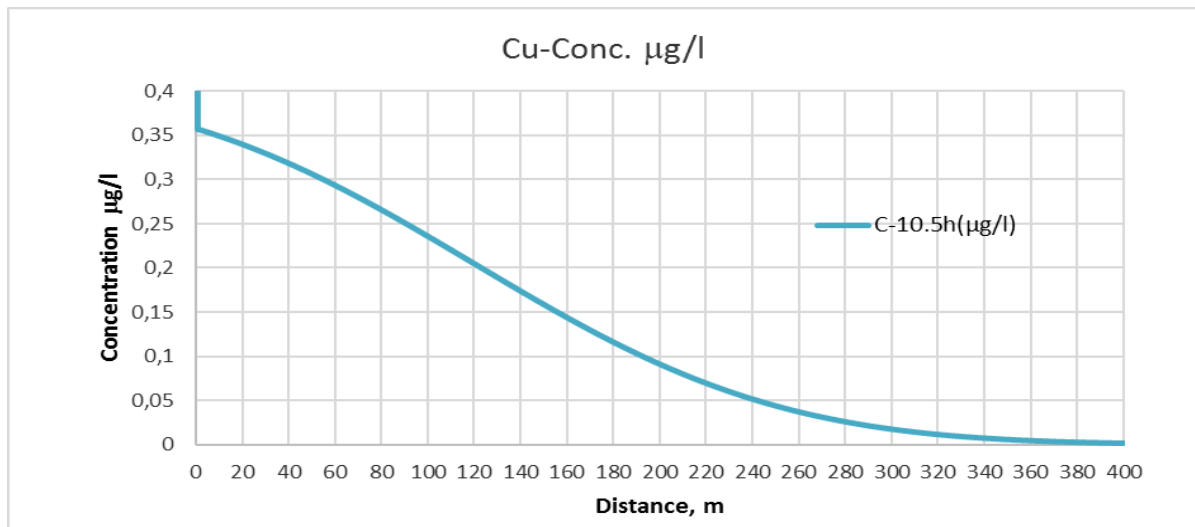


Figure 28: Graphic of the sixth curve of copper transport model-distance evolution

This graphic (figure 28) determines that the predicted concentration of copper in water discharged into Douro river is $2.05 \cdot 10^{-1} \mu\text{g/l}$.

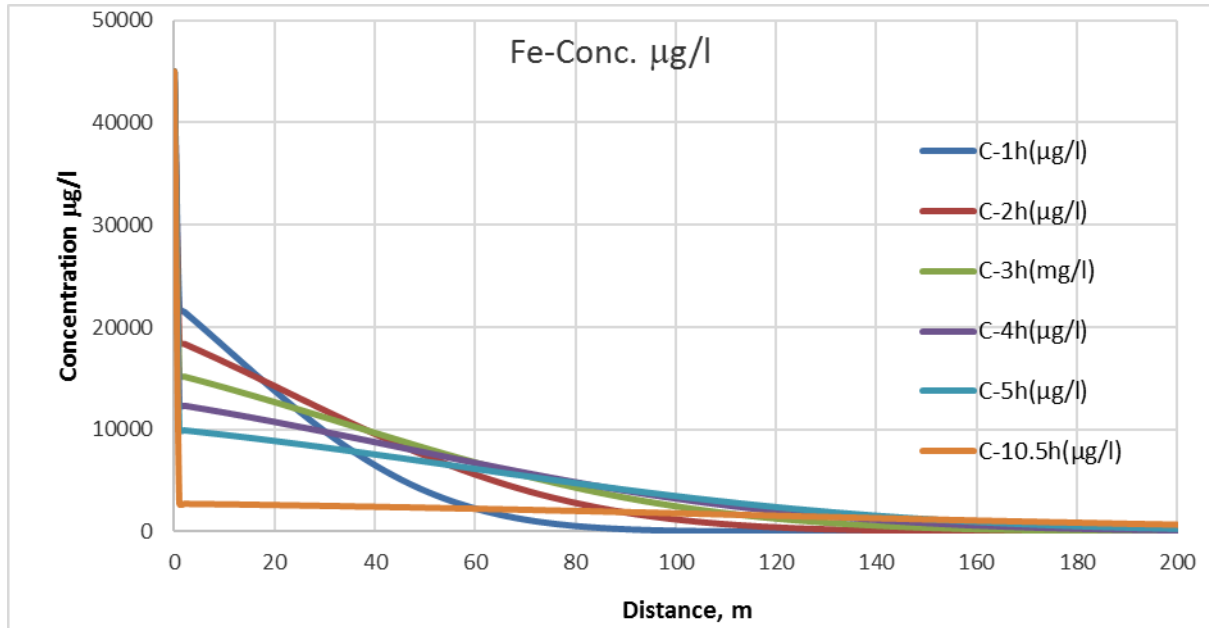


Figure 29: Graphic of iron transport model-distance evolution

The graphic (figure 29) describes the behavior of iron in the transport model- distance evolution with the spread concentration of 45000 µg/l at the source. The curve C-1h(µg/l) plotted with a time of 1 hour from the start shows that the concentration of iron in water discharged into Douro river after 1 hour is equal to $1.26 \cdot 10^1$ µg/l . The second curve C-2h(µg/l) plotted with a time of 2 hours from the start shows that the concentration of iron in water is $4.15 \cdot 10^2$ µg/l. The third curve C-3h(µg/l) plotted with a time of 3 hours from the start shows that the concentration of iron in water is $1.30 \cdot 10^3$ µg/l. The fourth curve C-4h(µg/l) plotted with a time of 4 hours from the start shows that the concentration of iron in water is $1.97 \cdot 10^3$ µg/l. The fifth curve C-5h(µg/l) plotted with a time of 5 hours from the start shows that the concentration of iron in water is $2.42 \cdot 10^3$ µg/l. With the sixth curve, the predicted concentration of iron in water discharged into Douro river is determined by the figure 30.

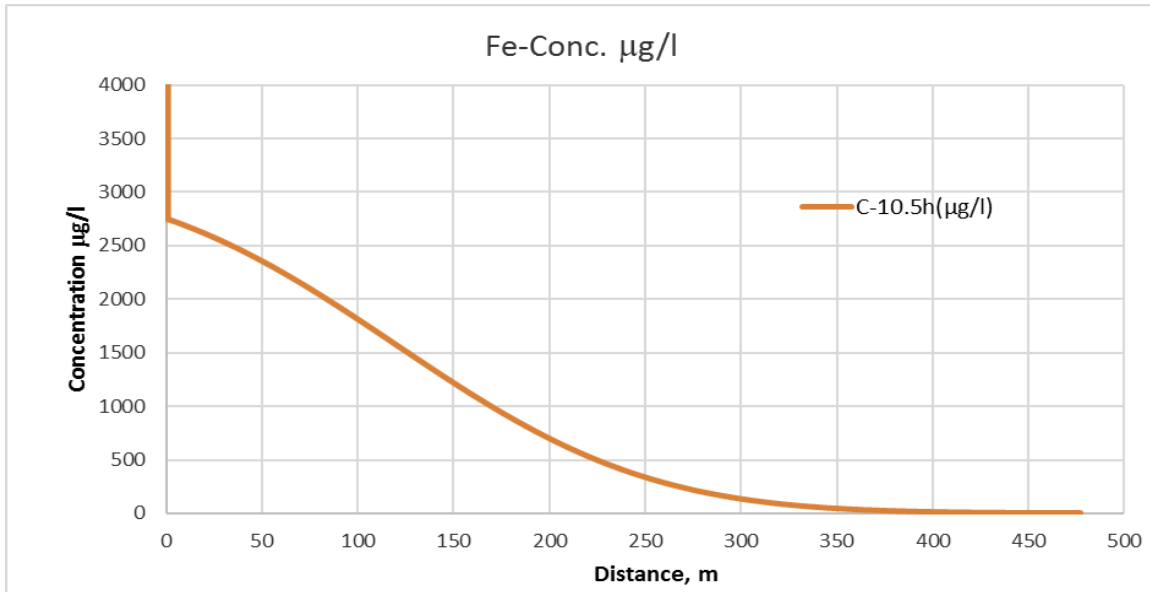


Figure 30: Graphic of the sixth curve of iron transport model-distance evolution

This graphic (figure 30) determines that the predicted concentration of iron in water discharged into Douro river is $1.57 \cdot 10^3 \mu\text{g/l}$.

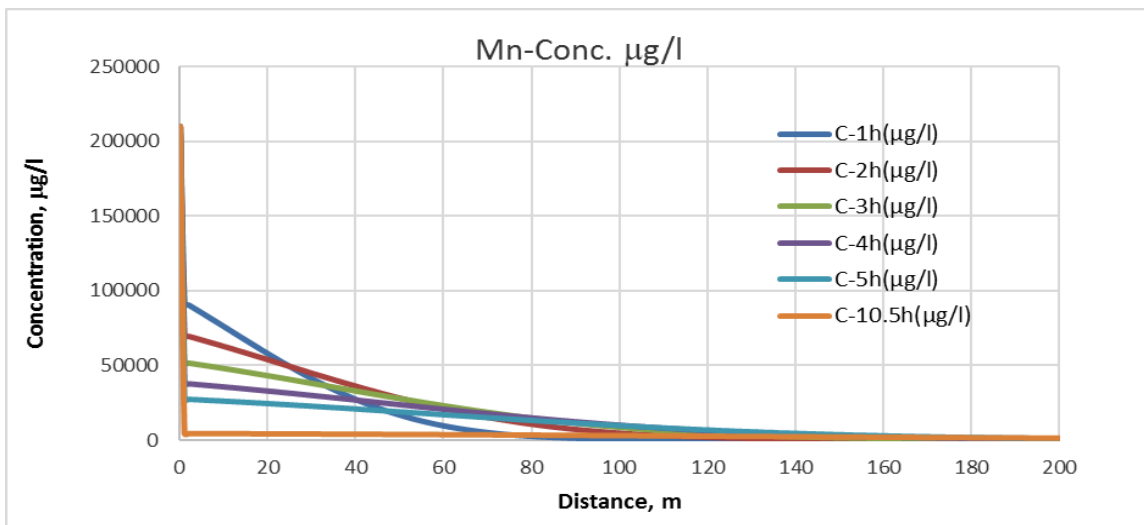


Figure 31: Graphic of manganese transport model-distance evolution

The graphic (figure 31) describes the behavior of manganese in the transport model- distance evolution with the spread concentration of $210000 \mu\text{g/l}$ at the source. The curve C-1h($\mu\text{g/l}$) plotted with a time of 1 hour from the start shows that the concentration of manganese in water discharged into Douro river after 1 hour is equal to $4.63 \cdot 10^4 \mu\text{g/l}$. The second curve C-2h($\mu\text{g/l}$) plotted with a time of 2 hours from the start shows that the concentration of manganese in water is $1.56 \cdot 10^3 \mu\text{g/l}$. The third curve C-3h($\mu\text{g/l}$) plotted with a time of 3 hours from the start shows that the concentration of manganese in water is $4.23 \cdot 10^3 \mu\text{g/l}$.

The fourth curve C-4h($\mu\text{g/l}$) plotted with time of 4 hours from the start shows that the concentration of manganese in water is $5.84 \cdot 10^3 \mu\text{g/l}$. The fifth curve C-5h($\mu\text{g/l}$) plotted with a time of 5 hours from the start shows that the concentration of manganese in water is $6.49 \cdot 10^3 \mu\text{g/l}$. With the sixth curve, the predicted concentration of manganese in water discharged into Douro river is determined by the figure 32.

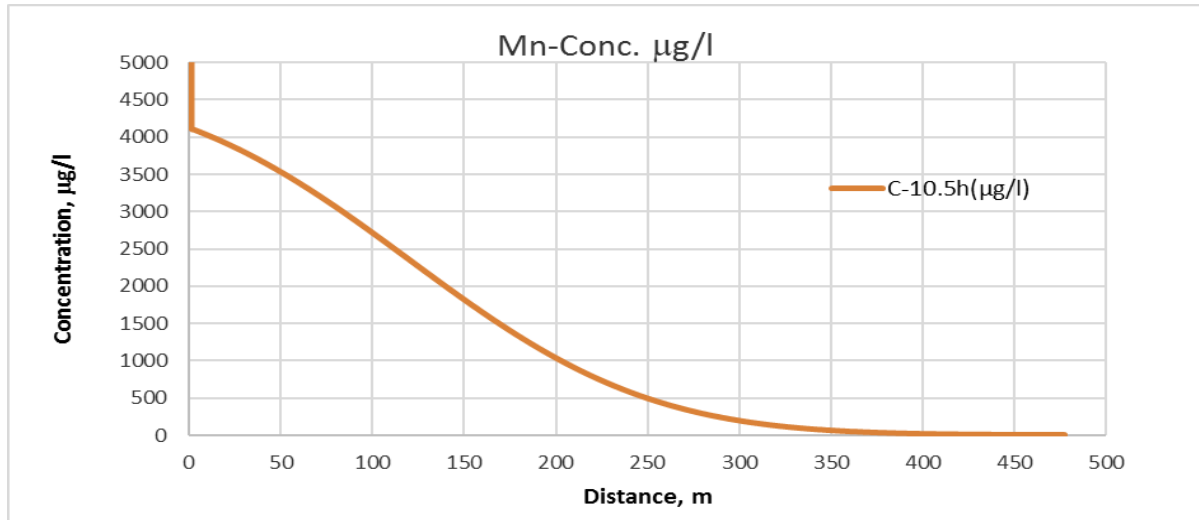


Figure 32: Graphic of the sixth curve of manganese transport model-distance evolution

This graphic (figure 32) determines that the predicted concentration of manganese in water discharged into Douro river is $2.35 \cdot 10^3 \mu\text{g/l}$.

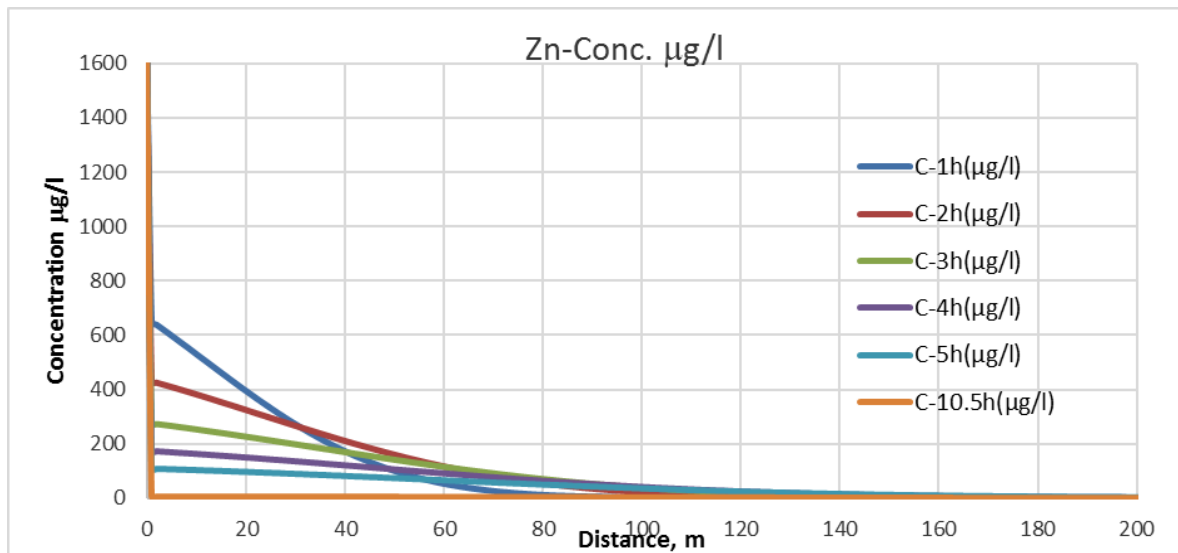


Figure 33: Graphic of zinc transport model-Distance evolution

The graphic (figure 33) describes the behavior of zinc in the transport model- distance evolution with the spread concentration of $1700 \mu\text{g/l}$ at the source. The curve C-1h($\mu\text{g/l}$) plotted with a time of 1 hour from the start shows that the concentration of zinc in water discharged into Douro river after 1 hour is equal to $1.36 \cdot 10^1 \mu\text{g/l}$. The second curve C-2h($\mu\text{g/l}$) plotted with a time of 2 hours from the start shows that the concentration of zinc in water is $6.47 \mu\text{g/l}$. The third curve C-3h($\mu\text{g/l}$) plotted with a time of 3 hours from the start shows that the concentration of zinc in water is $1.78 \cdot 10^1 \mu\text{g/l}$. The fourth curve C-4h($\mu\text{g/l}$) plotted with a time of 4 hours from the start shows that the concentration of zinc in water is $2.29 \cdot 10^1 \mu\text{g/l}$. The fifth curve C-5h($\mu\text{g/l}$) plotted with a time of 5 hours from the start shows that the concentration of zinc in water is $3.31 \cdot 10^1 \mu\text{g/l}$. With the sixth curve, the predicted concentration of zinc in water discharged into Douro river is determined by the figure 34.

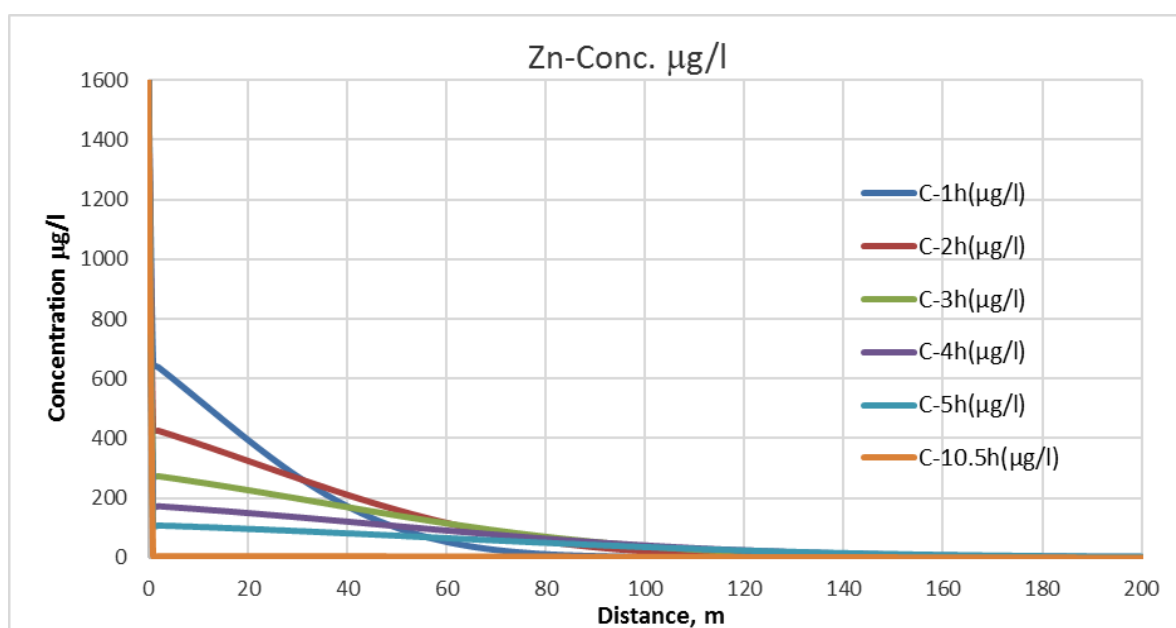


Figure 34: Graphic of the sixth curve of zinc transport model-distance evolution

This graphic (figure 34) determines that the predicted concentration of zinc in water discharged into Douro river is $4.02 \mu\text{g/l}$.

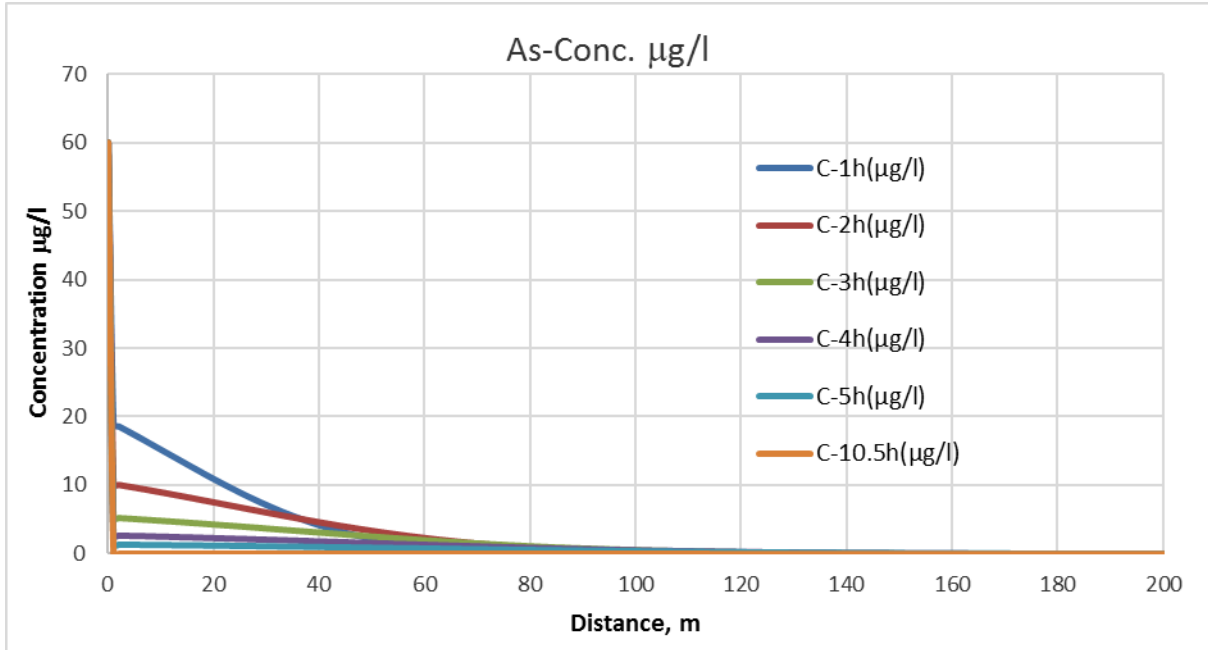


Figure 35: Graphic of arsenic transport model-Distance evolution

The graphic (figure 35) describes the behavior of arsenic in the transport model-distance evolution with the spread concentration of $60 \mu\text{g/l}$ at the source. The curve C-1h($\mu\text{g/l}$) plotted with a time of 1 hour from the start shows that the concentration of arsenic in water discharged into Douro river after 1 hour is equal to $6.39 \cdot 10^{-4} \mu\text{g/l}$. The second curve C-2h($\mu\text{g/l}$) plotted with a time of 2 hours from the start shows that the concentration of arsenic in water is $6.82 \cdot 10^{-2} \mu\text{g/l}$. The third curve C-3h($\mu\text{g/l}$) plotted with a time of 3 hours from the start shows that the concentration of arsenic in water is $2.13 \cdot 10^{-1} \mu\text{g/l}$. The fourth curve C-4h($\mu\text{g/l}$) plotted with time of 4 hours from the start shows that the concentration of arsenic in water is $2.68 \cdot 10^{-1} \mu\text{g/l}$. The fifth curve C-5h($\mu\text{g/l}$) plotted with a time of 5 hours from the start shows that the concentration of arsenic in water is $2.33 \cdot 10^{-1} \mu\text{g/l}$. With the sixth curve, the predicted concentration of arsenic in water discharged into Douro river is determined by the figure 36.

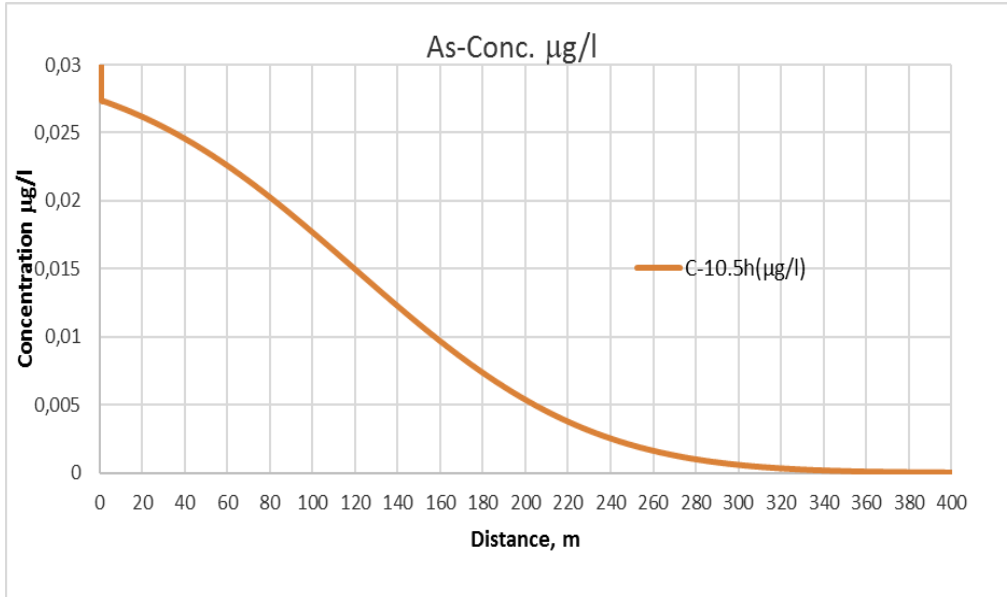


Figure 36: Graphic of the sixth curve of arsenic transport model-distance evolution

This graphic (figure 36) determines that the predicted concentration of arsenic in water discharged into Douro river is $1.50 \cdot 10^{-2} \mu\text{g/l}$.

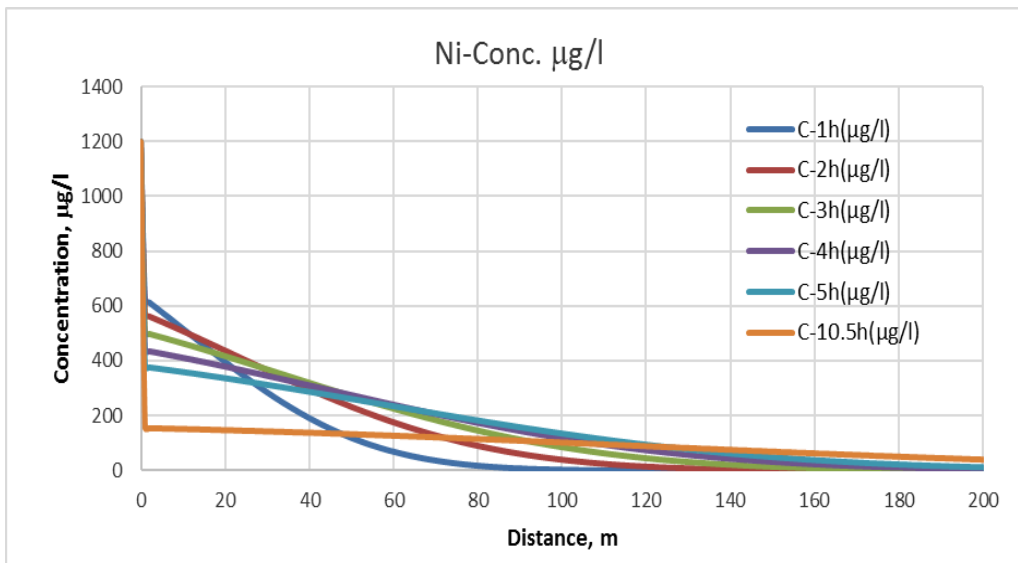


Figure 37: Graphic of nickel transport model-distance evolution

The graphic (figure 37) describes the behavior of nickel in the transport model-distance evolution with the spread concentration of $1200 \mu\text{g/l}$ at the source. The curve C-1h(µg/l) plotted with a time of 1 hour from the start shows that the concentration of nickel in water discharged into Douro river after 1 hour is equal to $4.69 \cdot 10^{-1} \mu\text{g/l}$. The second curve C-2h(µg/l) plotted with a time of 2 hours from the start shows that the concentration of nickel

in water is $1.51 \cdot 10^1 \mu\text{g/l}$. The third curve C-3h($\mu\text{g/l}$) plotted with a time of 3 hours from the start shows that the concentration of nickel in water is $4.58 \cdot 10^1 \mu\text{g/l}$. The fourth curve C-4h($\mu\text{g/l}$) plotted with time of 4 hours from the start shows that the concentration of nickel in water is $7.30 \cdot 10^1 \mu\text{g/l}$. The fifth curve C-5h($\mu\text{g/l}$) plotted with a time of 5 hours from the start shows that the concentration of nickel in water is $9.50 \cdot 10^1 \mu\text{g/l}$. With the sixth curve, the predicted concentration of nickel in water discharged into Douro river is determined by the figure 38.

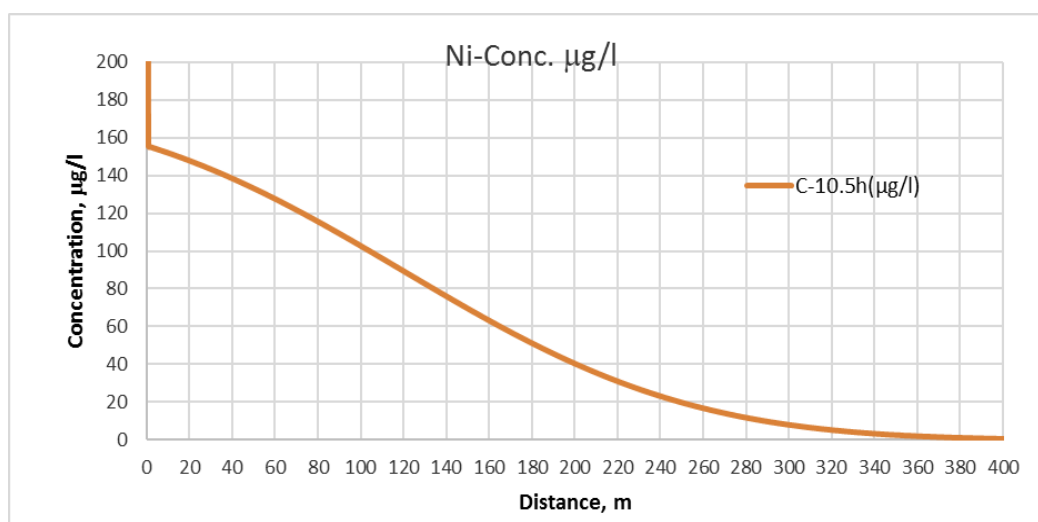


Figure 38: Graphic of the sixth curve of nickel transport model-distance evolution

This graphic (figure 38) determines that the predicted concentration of nickel in water discharged into Douro river is $8.97 \cdot 10^1 \mu\text{g/l}$.

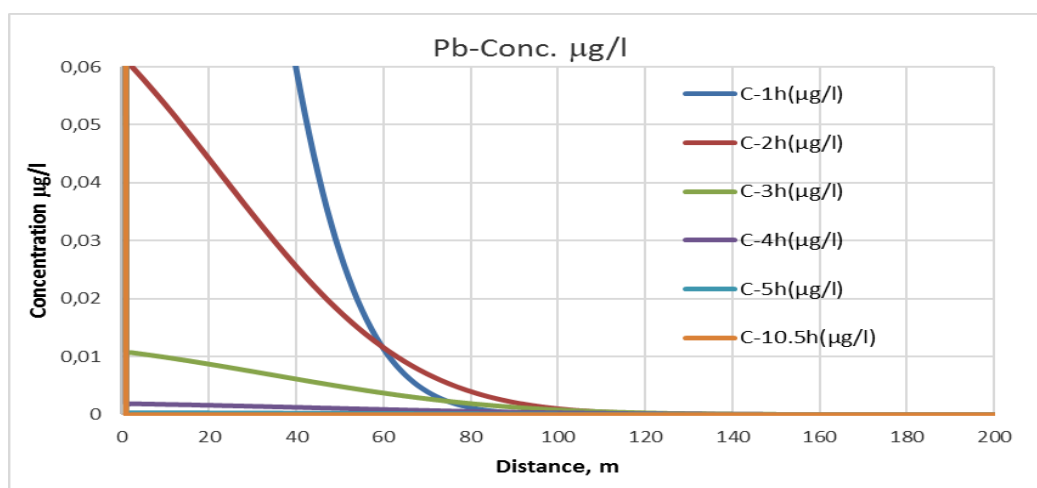


Figure 39: Graphic of lead transport model-distance evolution

The graphic (figure 39) describes the behavior of lead in the transport model-distance evolution with the spread concentration of $3 \mu\text{g/l}$ at the source. The curve C-1h($\mu\text{g/l}$) plotted

with a time of 1 hour from the start shows that the concentration of lead in water discharged into Douro river after 1 hour is equal to $1.97 \cdot 10^{-6} \mu\text{g/l}$. The second curve C-2h($\mu\text{g/l}$) plotted with a time of 2 hours from the start shows that the concentration of lead in water is $1.94 \cdot 10^{-4} \mu\text{g/l}$. The third curve C-3h($\mu\text{g/l}$) plotted with a time of 3 hours from the start shows that the concentration of lead in water is $2.85 \cdot 10^{-4} \mu\text{g/l}$. The fourth curve C-4h($\mu\text{g/l}$) plotted with a time of 4 hours from the start shows that the concentration of lead in water is $1.44 \cdot 10^{-4} \mu\text{g/l}$. The fifth curve C-5h($\mu\text{g/l}$) plotted with a time of 5 hours from the start shows that the concentration of lead in water is $4.68 \cdot 10^{-5} \mu\text{g/l}$. With the sixth curve, the predicted concentration of lead in water discharged into Douro river is determined by the figure 40.

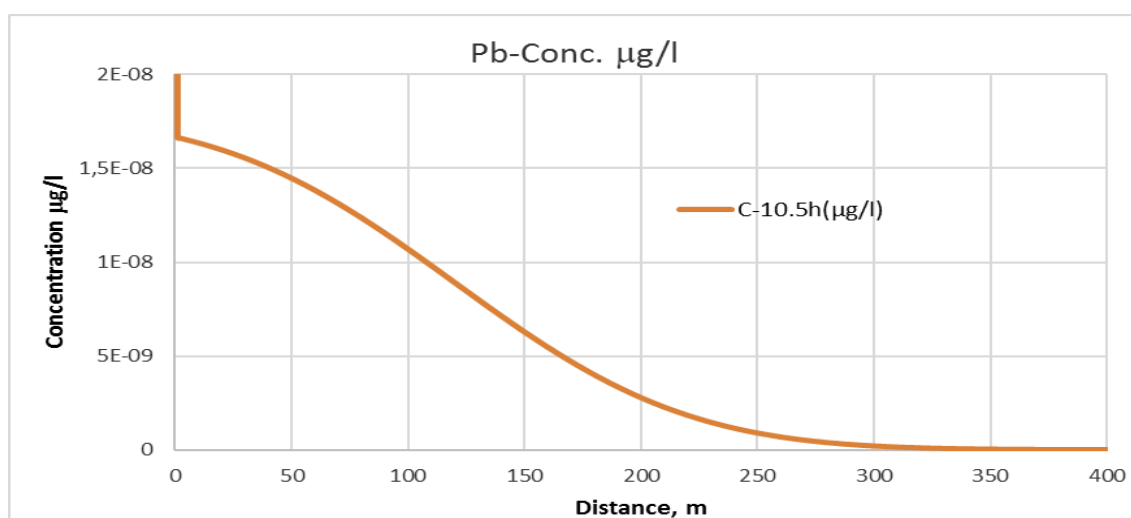


Figure 40: Graphic of the sixth curve of lead transport model-Distance evolution

This graphic (figure 40) determines that the predicted concentration of lead in water discharged into Douro river is $8.89 \cdot 10^{-9} \mu\text{g/l}$.

The following table 6 shows the simulated residence time of each chemical in the area and the predicted concentration discharged into Douro river from Microsoft excel implementation.

Table 6: Simulated residence time and predicted values of concentration from excel implementation of each chemical getting into Douro river

Element	Simulated residence time (hours)	Predicted values of concentration discharged into Douro river ($\mu\text{g/l}$)	Predicted values of concentration discharged into Douro river (mg/l)
Al	35.6	3.8×10^1	3.8×10^{-2}
Cu	27.5	2.0×10^{-1}	2.0×10^{-4}
Fe	79	1.5×10^3	1.5
Mn	59.5	2.3×10^3	2.3
Zn	32.6	4.0	4.0×10^{-3}
As	18.1	1.5×10^{-2}	1.5×10^{-5}
Ni	90.4	8.9×10^1	8.9×10^{-2}
Pb	4.3	8.8×10^{-9}	8.8×10^{-12}

3.2.2. Results from matlab implementation

In this section the graphics of one curve are presented with the corresponding variables as defined in the protocol implementation methodology (section 2.2.2.) to determine the simulated residence time and the predicted concentration of heavy metals or other chemicals discharged into Douro river.

3.2.2.1. Matlab results for a transport model- time evolution with degradation from the source

The following graphics are plotted for all heavy metals and other chemicals.

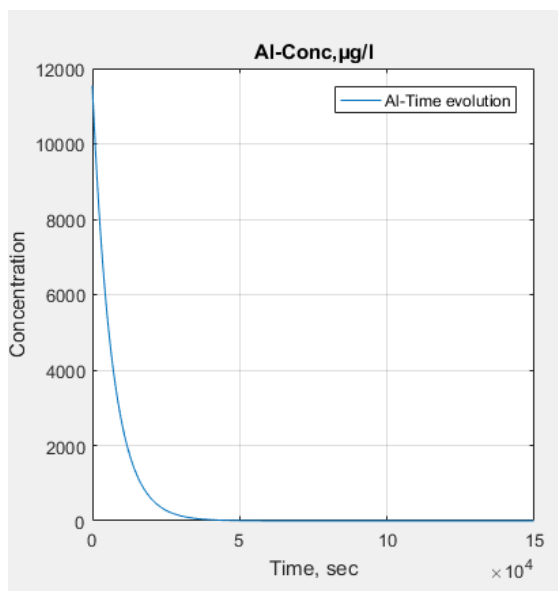


Figure 41: Aluminum transport model-time evolution graphic from matlab

Aluminum low concentration of 0.00010 µg/l occurs at 124560 sec (34.6 h), simulated residence time.

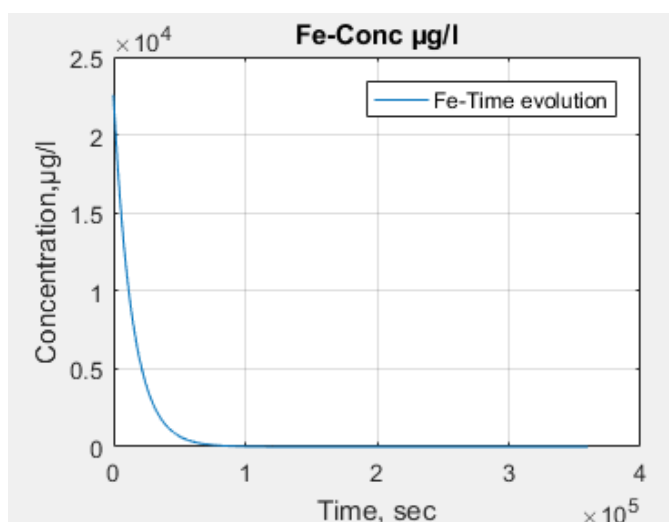


Figure 42: Iron transport model-time evolution graphic from matlab

Iron low concentration of 0.00010 µg/l occurs at 274680 sec (76.3 h), simulated residence time.

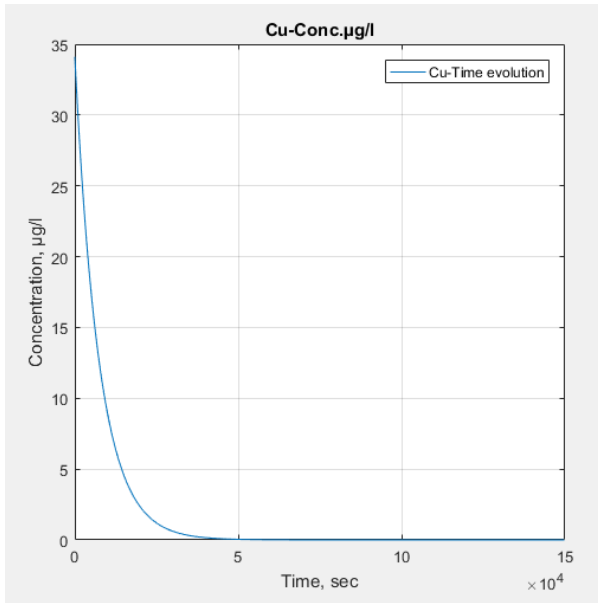


Figure 43: Copper transport model-time evolution graphic from matlab

Copper low concentration of $0.00010 \mu\text{g/l}$ occurs at 95040 sec (26.4 h), simulated residence time.

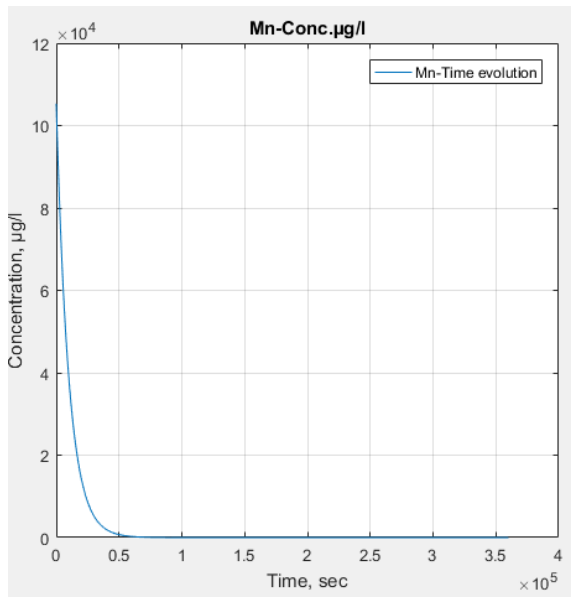


Figure 44: Manganese transport model-time evolution graphic from matlab

Manganese low concentration of $0.00010 \mu\text{g/l}$ occurs at 207720 sec (57.7h), simulated residence time.

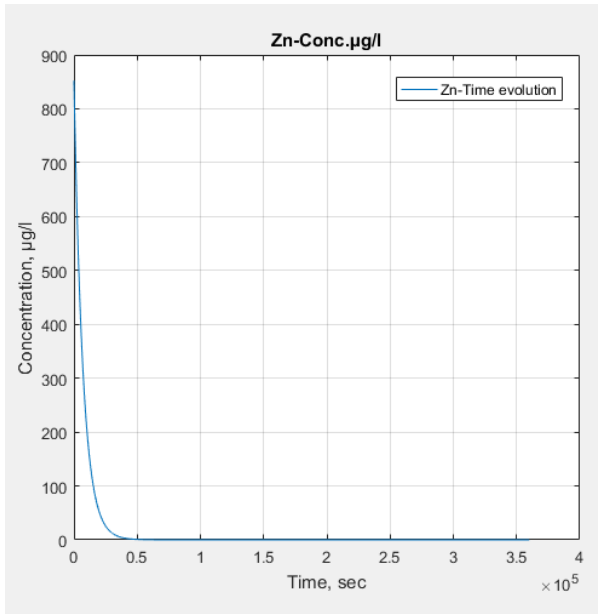


Figure 45: Zinc transport model-time evolution graphic from matlab

Zinc low concentration of 0.00010 µg/l occurs at 113760 sec (31.6 h), simulated residence time.

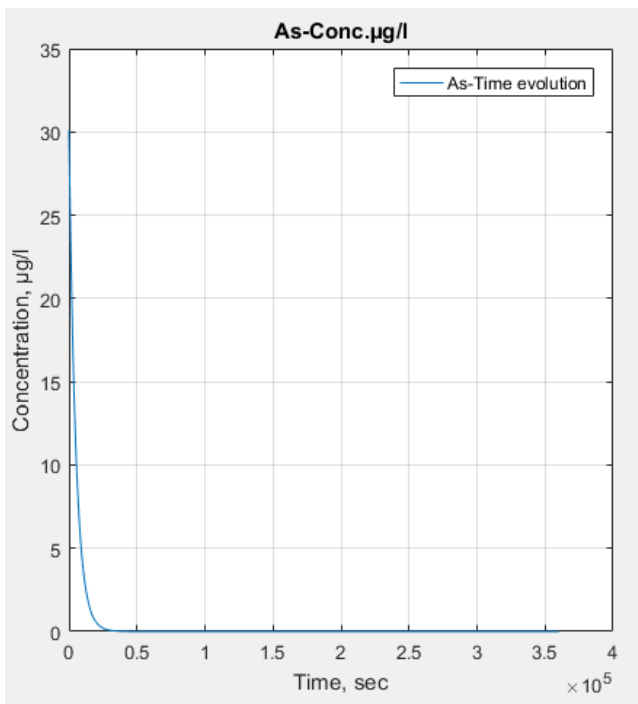


Figure 46: Arsenic transport model-time evolution graphic from matlab

Arsenic low concentration of 0.00010 µg/l occurs at 63000sec (17.5 h), simulated residence time.

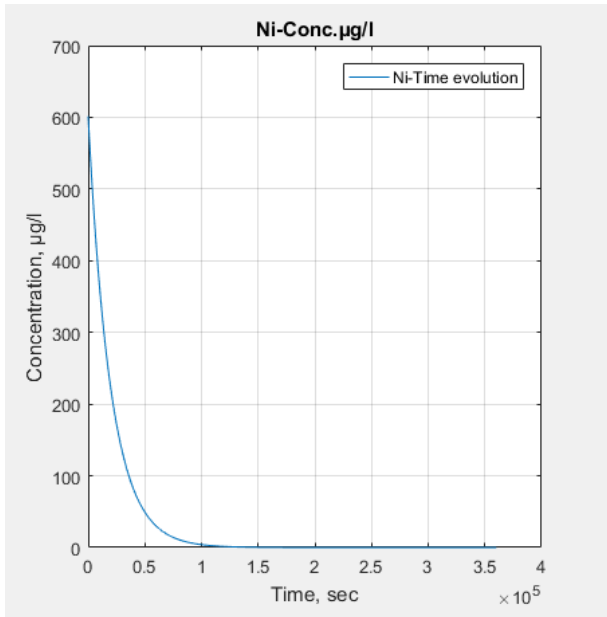


Figure 47: Nickel transport model-time evolution graphic from matlab

Nickel low concentration of 0.00010 µg/l occurs at 312120 sec (86.7 h), simulated residence time.

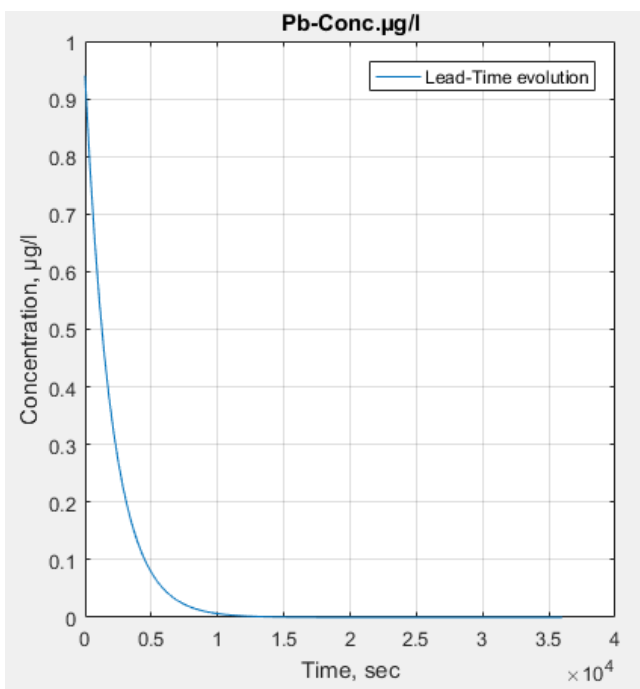


Figure 48: Lead transport model-time evolution graphic from matlab

Lead low concentration of 0.00010 µg/l occurs at 18360 sec (5.1 h), simulated residence time.

3.2.2.2 Matlab results for a transport model-distance evolution with degradation from the source

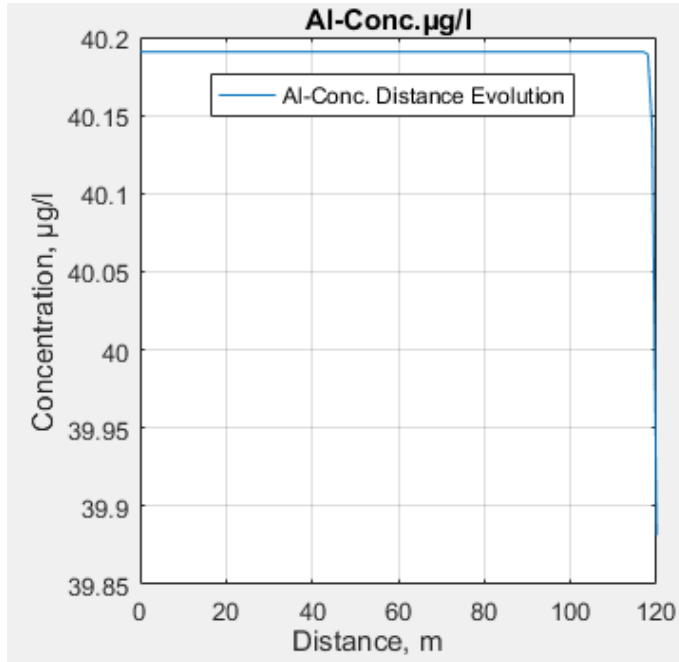


Figure 49: Aluminum transport model- distance evolution graphic from matlab

The concentration of aluminum discharged into Douro river is $39.8 \mu\text{g/l}$ ($3.9 \times 10^{-2} \text{ mg/l}$).

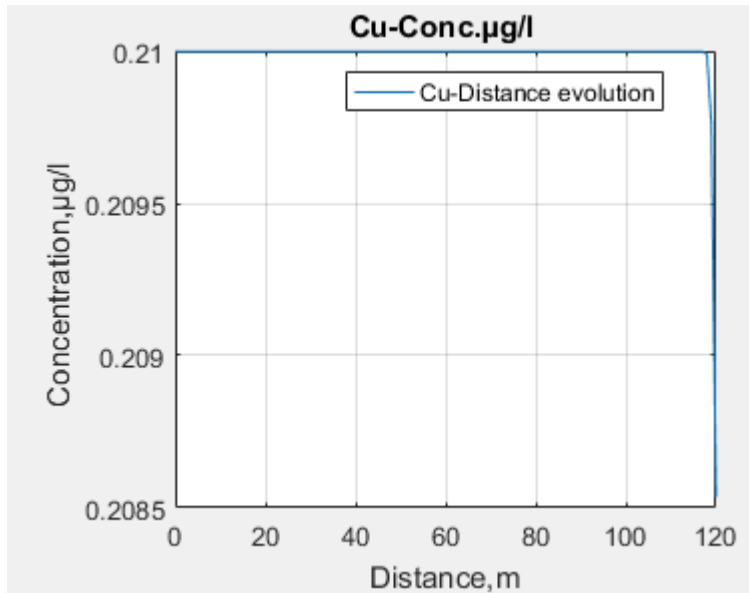


Figure 50: Copper transport model- distance evolution graphic from matlab

The concentration of copper discharged into Douro river is $0.208 \mu\text{g/l}$ ($2.08 \times 10^{-2} \text{ mg/l}$).

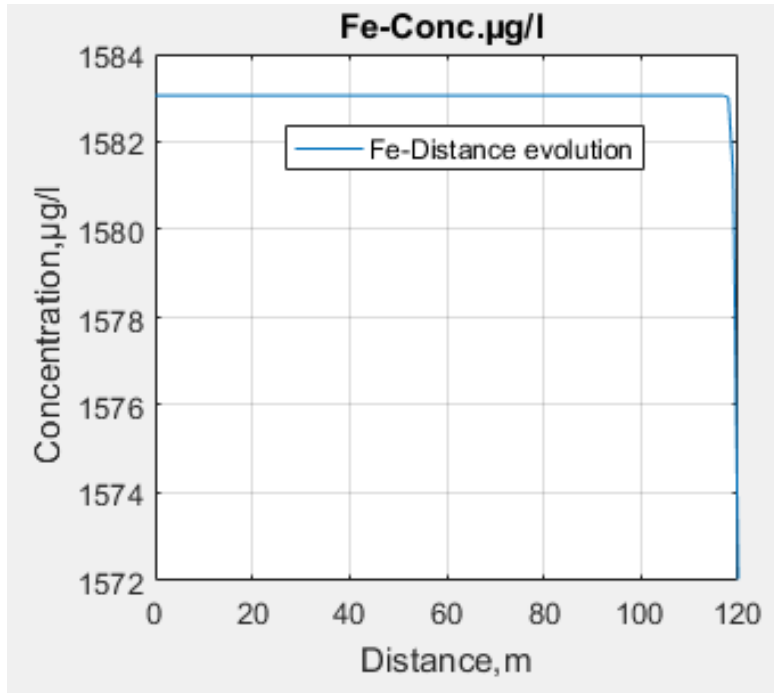


Figure 51: Iron transport model- distance evolution graphic from matlab

The concentration of iron discharged into Douro river is 1.57×10^3 µg/l (1.57 mg/l).

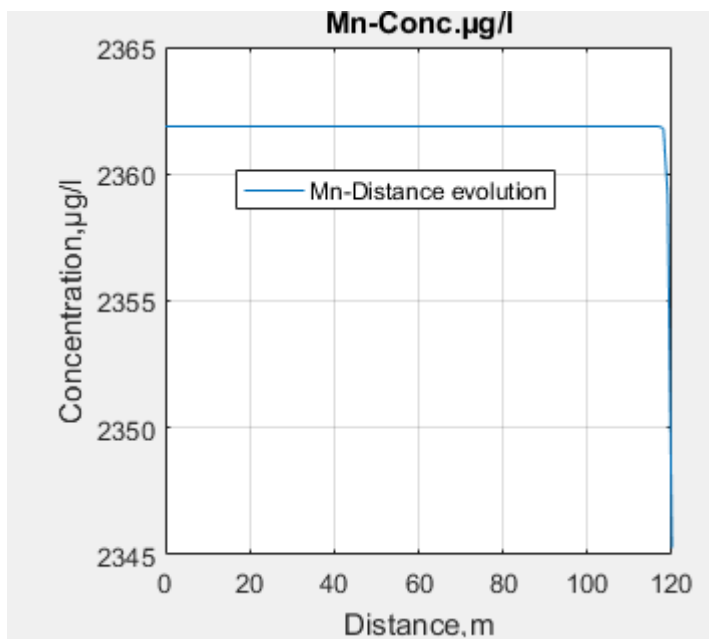


Figure 52: Manganese transport model- distance evolution graphic from matlab

The concentration of manganese discharged into Douro river is 2.34×10^3 µg/l (2.34 mg/l).

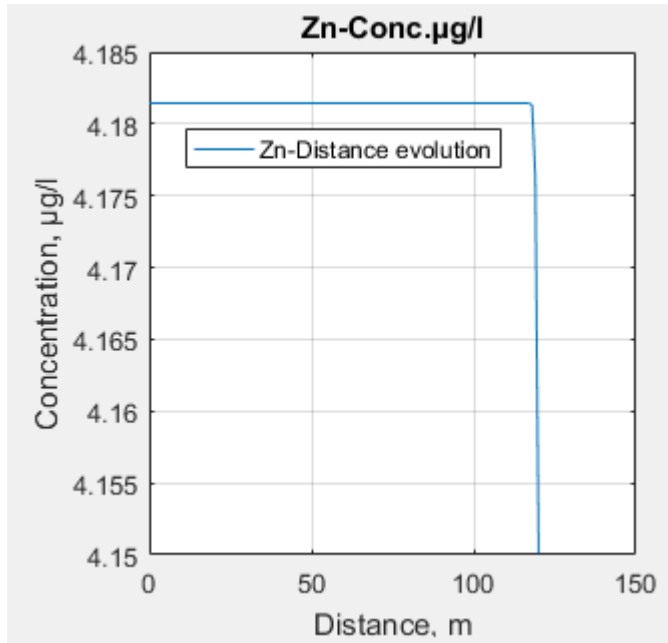


Figure 53: Zinc transport model- distance evolution graphic from matlab

The concentration of zinc discharged into Douro river is $4.15 \mu\text{g/l}$ ($4.15 \times 10^{-3} \text{ mg/l}$).

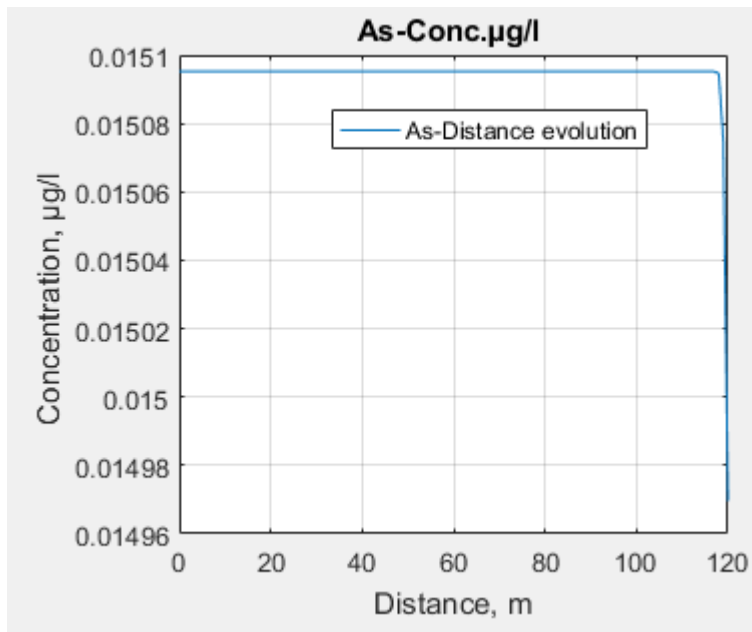


Figure 54: Arsenic transport model- distance evolution graphic from matlab

The concentration of arsenic discharged into Douro river is $1.51 \times 10^{-2} \mu\text{g/l}$ ($1.51 \times 10^{-5} \text{ mg/l}$).

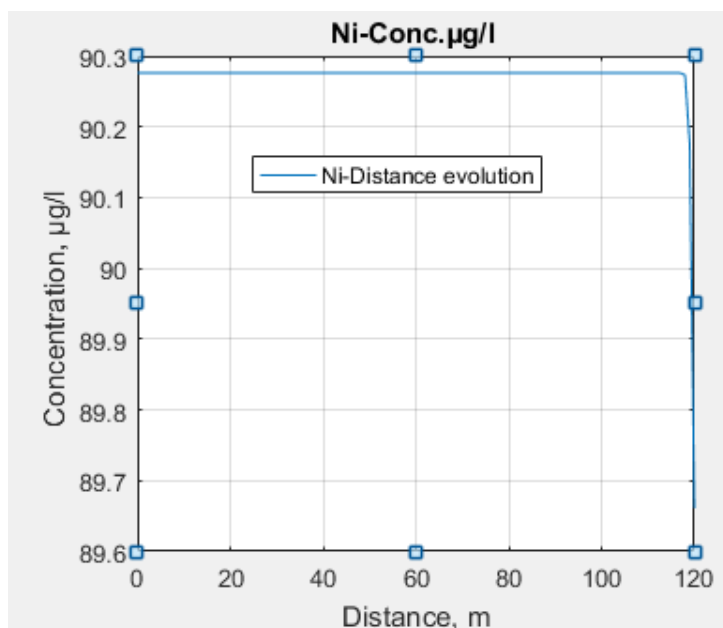


Figure 55: Nickel transport model- distance evolution graphic from matlab

The concentration of nickel discharged into Douro river is $89.6 \mu\text{g/l}$ ($8.9 \times 10^{-2} \text{ mg/l}$).

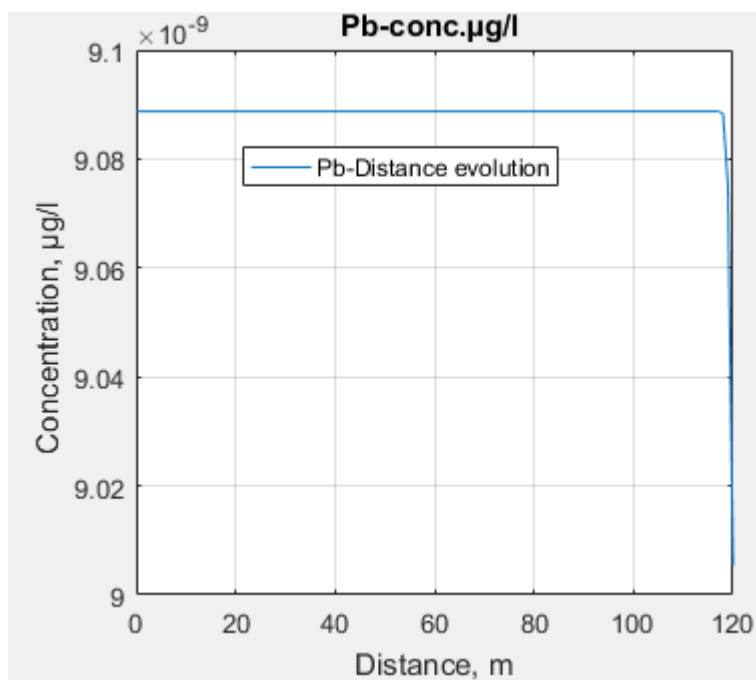


Figure 56: Lead transport model- distance evolution graphic from matlab

The concentration of lead discharged into Douro river is $9.00 \times 10^{-9} \mu\text{g/l}$ ($9.00 \times 10^{-12} \text{ mg/l}$).

The following table7, presents the results from matlab of predicted concentration discharged into Douro and the simulated residence time of each heavy metal or other chemical.

Table 7: Simulated residence time and predicted values of concentration of heavy metals and other chemicals discharged into Douro river from matlab implementation

Element	Simulated residence time from Matlab (hours)	Predicted values of concentration discharged into Douro river from Matlab (mg/l)
Al	34.6	3.9×10^{-2}
Cu	26.4	2.0×10^{-2}
Fe	76.3	1.5
Mn	57.7	2.3
Zn	31.6	4.1
As	17.5	1.5×10^{-5}
Ni	86.7	8.9×10^{-2}
Pb	5.1	9.0×10^{-12}

3.3. Microsoft-Excel and matlab cross validation

In this section a cross validation is made by comparison of values from excel and matlab (table 8). The comparison shows that there is not a very great variation in values, the low difference between some values could be due to instrumental error. Every one could consider to use the result from Matlab or from Microsoft-excel, there is no change concerning the conclusion.

In the following sections, the values from Microsoft-excel are used in the comparison with the threshold limit values.

Table 8: Excel and Matlab cross validation values

Element	Simulated residence time from Excel (hours)	Predicted values of concentration discharged into Douro river from Excel (mg/l)	Simulated residence time from Matlab (hours)	Predicted values of concentration discharged into Douro river from Matlab (mg/l)
Al	35.6	3.8×10^{-2}	34.6	3.9×10^{-2}
Cu	27.5	2.0×10^{-4}	26.4	2.0×10^{-2}
Fe	79	1.5	76.3	1.5
Mn	59.5	2.3	57.7	2.3
Zn	32.6	4.0×10^{-3}	31.6	4.1
As	18.1	1.5×10^{-5}	17.5	1.5×10^{-5}
Ni	90.4	8.9×10^{-2}	86.7	8.9×10^{-2}
Pb	4.3	8.8×10^{-12}	5.1	9.0×10^{-12}

3.4. Discussion

Based on the two hypotheses formulated previously in section 3.1., this section discusses how is the evolution of the pollution of water from the landfill coal ash to Douro river. This pollution could occur in two possible ways:

1. Toxicity caused by the concentration of heavy metals or other chemicals in water discharged into Douro river;
2. Acidity of water caused by the AMD of water discharged into Douro river.

3.4.1. Toxicity caused by the concentration of heavy metals in water

The analyse of the evolution of the concentration of heavy metals or other chemicals in water from the landfill coal ash to Douro river and the comparison (Table 9) of the concentration of heavy metals or other chemicals in water discharged into Douro river to the threshold limit value of emission of residues in water, shows that only manganese exceeds the threshold limit value according to data collected in the monitoring field on 11th January, 2012 . During

the previous and followed monitoring field, the concentration measured at the source was lower, which means manganese is not an acute environmental threat. The concentrations of other heavy metals or chemicals do not exceed the threshold limit value. All of them are degraded in the pathway to Douro river.

This shows that heavy metals or chemicals are removed from polluted water when it is flowing through soils from the source Fibrocimento to Douro river. This is a natural attenuation, the way how it occurs is explained in the section 3.4.3.

Table 9: Comparison of predicted values of concentration discharged into Douro river to the threshold limit values

Heavy metal element	Predicted values of concentration discharged into Douro river (mg/l)	Threshold limit values (mg/l)
Al	3.8×10^{-2}	10
Cu	2.0×10^{-4}	1.0
Fe	1.5	2.0
Mn	2.3	2.0
Zn	4.0×10^{-3}	0.5
AS	1.5×10^{-5}	1.0
Ni	8.9×10^{-2}	2.0
Pb	8.8×10^{-12}	1.0

3.4.2. Acidity of water caused by the AMD

The analyse of pH of water at the source in the range of 2.9-5.4 reveals that AMD is occurred. But the pH 6.6-8.0 of water in Douro river is in the buffer range. This shows that a natural attenuation of AMD and pH buffering occurred during the path way from the source to Douro river. This natural attenuation of AMD and pH buffering is explained in the section 3.4.4.

3.4.3. Natural attenuation of heavy metals

From Fibrocimento pipe to Douro river, polluted water is flowing on surface ground and through soils. There is an interaction between soil and water and soil composition is playing a key role in natural attenuation as a filter. Clay minerals have a great potentiality to adsorb heavy metals due to their large specific surface area, chemical and mechanical stability, layered structure, and high cationic exchanger capacity (Sdiri et al., 2011). Natural organic compounds in the soil plays also a key role of heavy metals and other chemicals attenuation by adsorption (Badawi et al., 2017, Assis & Valmir, 2003). Those materials playing a role of natural attenuation are assumed to be occurring in the study area.

3.4.4. Natural attenuation of AMD and pH buffering

Natural attenuation of acidity and pH buffering turn out to be a critical control on the environmental behavior.

As acidity is released to solution during pyrite weathering, the pH drops. There are other minerals however, that can consume acidity as they dissolve, thereby producing natural attenuation of acidity produced by pyrite weathering, helping to buffer the pH (Younger et al., 2002).

The natural attenuation of AMD occurs in two phases, by primary minerals weathering and by authigenic secondary minerals formation.

The first phase implies primary minerals of rock fragments, and as this case study deals with surface water flowing on surface ground, this phase is not applicable.

The second phase is applicable as it implies solutions and dissolved minerals. This phenomenon is explained in the following section.

3.4.4. 1. Authigenic secondary minerals formation

Secondary minerals are formed through precipitation from contaminated solutions. They are within sediments and occur as a coating on surfaces of mineralized clasts where they partially or completely replace them (Carbone et al., 2013).

The characteristic of secondary minerals formed during AMD depend on variation in chemical conditions of the receiving environment (particularly variation in pH, Eh, and temperature).

From a genetic point of view, three main settings for secondary mineral formation can be distinguished:

1. Unconsolidated precipitates, flocs, and loose suspensions;
2. Consolidated crusts and hardpans precipitating from seepage drainage of contaminated solutions within waste-rock dumps and tailings;
3. Efflorescent salts formed mainly on the surface waste rock deposits, tailing, and mine soils due to evaporation of mine waters in dry periods or as a consequence of the heat produced by exothermic reactions active during sulphide oxidation (Carbone et al., 2013).

As this case study deals with polluted water, the first setting formation of secondary minerals has a realistic meaningful explanation.

Even the mineralogy of the formed secondary minerals is quite variable, the main minerals can be grouped into three broad groups:

Fe-oxides, oxyhydroxides, and oxyhydroxysulphates (such as ferrihydrites 2), goethite, hematite, schwertmanite and jarosite, and other low crystalline Fe phases;

Hydrous Ca, Fe, Al, and other metal sulphates (such as gypsum, melanterite, copiapite, halotrichite, chalcantite, and episomite);

Other metal rich phases, usually with low crystalline, are basaluminite like Al minerals, woodwardite like Cu minerals and hydrozincite.

All these minerals have specific fields of stability within the wide range of pH and Eh conditions that typically occur in AMD environment (Carbone et al., 2013).

Chapter 4 : CONCLUSION AND RECOMMENDATIONS

4.1. Conclusion

This work “Water contamination in the area of a landfill coal ash” conducted by implementing the transport model of heavy chemicals in water contaminated by the leachate coming from the landfill coal ash in the area of Medas, Municipality of Gondomar, nearby Douro river reveals that the landfill coal ash is not a very big problematic pollution of Douro river.

Based on the transport model development using the Fickian first law and the implementation of the model using Microsoft excel and matlab, the results show that the concentration of only 1 chemical, Manganese in water discharged into Douro river exceeds the threshold limit value allowed by the Ministry of Environment of Portugal. This is not an imminent pollution threat as the applied concentration in the model was measured during the monitoring field made on 11/01/2012. This high value occurred once time. During the previous and followed monitoring fields, the measured concentration had low values than the used one.

The decrease of concentration of heavy metals during the pathway from Fibrocimento to Douro river is due to natural attenuation by adsorption of natural clay minerals and sorption into organic matter of the soil in the area.

Based on the analysis of AMD, causes and manifestations, there is also a natural attenuation occurring due to authigenic secondary minerals occurring during AMD itself.

4.2. Recommendations for future works

For future works, I recommend to environmental researchers to:

- Make a field sample of soil along the water path in order to analyze the soil density ρ ; soil-water partition coefficient K_s ; organic-carbon partition coefficient K_{co} ; organic material fraction f_{co} and octanol-water partition coefficient K_{wo} . All those parameters can help to calculate the retardation coefficient which can hence end up to getting the biodegradation kinetic constant;
- Undertake experimental studies concerning how a natural attenuation of heavy metals occurs by using natural minerals along the fibrocimento-Douro river pathway;
- Undertake experimental studies concerning how natural attenuation of AMD and pH buffering happens along the fibrocimeto-Douro river pathway.

References

- Acreman, M. (2004). *Water and Ecology. Series on Water and Ethics* (World Comm, Vol. 8). Paris: UNESCO.
- Aderinola, O. J., Clarke, E. O., Olarinmoye, O. M., Kusemiju, V., & Anatekhai, M. A. (2012). Heavy Metals in Surface Water, Sediments, Fish and Perwinkles of Lagos Lagoon. *Journal Of Agricultural & Environmental Sciences*, 5(5), 609–617.
- Assis, O. B. G., & Valmir, L. da S. (2003). Caracterização estrutural e da capacidade de absorção de água em filmes finos de quitosana processados em diversas concentrações. *Polímeros*, 13(4), 223–228.
<http://doi.org/10.1590/S0104-14282003000400006>
- Authman, M. M. N., Zaki, M. S., Khallaf, E. A., & Abbas, H. H. (2015). Use of Fish as Bio-indicator of the Effects of Heavy Metals Pollution. *Aquaculture Research & Development*, 6(4). <http://doi.org/10.4172/2155-9546.1000328>
- Badawi, M. A., Negm, N. A., Abou Kana, M. T. H., Hefni, H. H., & Abdel Moneem, M. M. (2017). Adsorption of aluminum and lead from wastewater by chitosan-tannic acid modified biopolymers: Isotherms, kinetics, thermodynamics and process mechanism. *International Journal of Biological Macromolecules*, 99, 465–476.
<http://doi.org/10.1016/j.ijbiomac.2017.03.003>
- Badiye, A., Kapoor, N., & Khajuria, H. (2013). Copper Toxicity : A Comprehensive Study. *Research Journal of Recent Sciences*, 2, 58–67.
 Retrieved from www.isca.in
- Batu, V. (2006). *Applied flow and solute transport modeling in aquifers: fundamental principals and analytical and numerical methods*. (Taylor & Francis, Eds.)*Textbook* (CRC Press). U. S.A. Retrieved from

<http://www.crcpress.com>

- Carbone, C., Dinelli, E., Marescotti, P., Gasparotto, G., & Lucchetti, G. (2013). The role of AMD secondary minerals in controlling environmental pollution: Indications from bulk leaching tests. *Journal of Geochemical Exploration*, 132, 188–200. <http://doi.org/10.1016/j.gexplo.2013.07.001>
- Carolin, C. F., Kumar, P. S., Saravanan, A., Joshiba, G. J., & Naushad, M. (2017). Efficient techniques for the removal of toxic heavy metals from aquatic environment: A review. *Journal of Environmental Chemical Engineering*, 5(3), 2782–2799. <http://doi.org/10.1016/j.jece.2017.05.029>
- Carvalho, W. A., Vignado, C., & Fontana, J. (2008). Ni (II) removal from aqueous effluents by silylated clays, 153, 1240–1247. <http://doi.org/10.1016/j.jhazmat.2007.09.083>
- Chapman, D. (1996). *Water Quality Assessments - A Guide to Use of Biota , Sediments and Water in Environmental Monitoring - Second Edition* Edited by, (UNESCO/WHO).
- Chapman, P. M. (2007). Determining when contamination is pollution — Weight of evidence determinations for sediments and effluents, 33, 492–501. <http://doi.org/10.1016/j.envint.2006.09.001>
- Costello, C. (2003). *Acid Mine Drainage : Innovative Treatment Technologies* Prepared by Technology Innovation Office, (Washington, DC). Retrieved from www.clu-in.org
- Das, K. K., Das, S. . N., & Dhundasi, S. A. (2008). Nickel, its adverse health effects & oxidative stress. *The Indian Journal of Medical Research*, 128(4), 412–425.
- Dipak, P. (2017). Research on heavy metal pollution of river Ganga: A review. *Annals of Agrarian Science*, 15(Science Direct), 278–286.

<http://doi.org/10.1016/j.aasci.2017.04.001>

- Directive 2006/118/EC of the European Parliament and of the council of 12 December 2006 on the protection of groundwater against pollution and deterioration. (2006). The europ. *Official Journal of the Eurpean Union*, 2006(1463).
- DL 236/98. (1998). *Diario da Republica*, 3676–3722.
- Dousova, B., Lhotka, M., Grygar, T., Machovic, V., & Herzogova, L. (2011). In situ co-adsorption of arsenic and iron / manganese ions on raw clays. *Elsvier*, 54, 166–171. <http://doi.org/10.1016/j.clay.2011.08.004>
- Dube, A., Zbytniewski, R., Kowalkowski, T., Cukrowska, E., & Buszewski, B. (2001). Adsorption and Migration of Heavy Metals in Soil. *Polish Journal of Environmental Studies*, 10(1), 1–10.
- Duruibe, J. O., Ogwuegbu, M. O. C., & Egwurugwu, J. N. (2007). Heavy metal pollution and human biotoxic effects. *International Journal of Physical Sciences*, 2(5), 112–118. <http://doi.org/10.1016/j.proenv.2011.09.146>
- Garbarino, J. R., Hayes, H. C., Roth, D. A., Antweiler, R. C., Brinton, T. I., & Taylor, H. E. (1995). Contaminants in the Mississippi River--Heavy Metals in the Mississippi River.
- Genuchten, T. V. M., Leij, F. J., Skaggs, T. H., Toride, N., Bradford, S. A., & Pontedeiro, E. M. (2013). Exact analytical solutions for contaminant transport in rivers 1. The equilibrium advection-dispersion equation. *Journal of Hydrology and Hydromechanics*, 61(2), 146–160. <http://doi.org/10.2478/johh-2013-0020>
- Groffman, P. M., Baron, J. S., Blett, T., Gold, A. J., Goodman, I., Gunderson, L. H., ... Wiens, J. (2006). Ecological Thresholds : The Key to Successful Environmental Management or an Important Concept with No Practical

Application ? *Ecosystems*, 9(1), 1–13. <http://doi.org/10.1007/s10021-003-0142-z>

Gulliver, J. S. (2007). *Introduction to chemical transport in the environment* (Cambridge). Cambridge. Retrieved from www.cambridge.org/9780521858502

Helmer, R., & Hespanhol, I. (1997). *Water Pollution Control - A Guide to the Use of Water Quality Management Principles*.

Hou, S., Yuan, L., Jin, P., Ding, B., Qin, N., Li, L., ... Deng, Y. (2013). A clinical study of the effects of lead poisoning on the intelligence and neurobehavioral abilities of children. *Theoretical Biology and Medical Modelling*, 10(BioMed Central), 13. <http://doi.org/10.1186/1742-4682-10-13>

Ibrahim, D., Froberg, B., Wolf, A., & Rusyniak, D. E. (2006). Heavy metal poisoning: Clinical presentations and pathophysiology. *Clinics in Laboratory Medicine*, 26(1), 67–97. <http://doi.org/10.1016/j.cll.2006.02.003>

Islam, M. A. (2006). a Comparison Between Analytical and Numerical Solution of the Krogh ' S Tissue Cylinder Model for. *Chemical Engineering, ChE* 24(1), 1–6.

Jaishankar, M., Tseten, T., Anbalagan, N., Mathew, B. B., & Beeregowda, K. N. (2014). Toxicity, mechanism and health effects of some heavy metals. *Interdisciplinary Toxicology*. <http://doi.org/10.2478/intox-2014-0009>

Jamie, B., & Ballance, R. (1996). *Water Quality Monitoring-A practical Guide to the Disign and Implementation of Fleshwater Quality studies and Monitoring Programe*, (UNESCO/WHO).

Jan, A. T., Azam, M., Siddiqui, K., Ali, A., Choi, I., & Haq, Q. M. R. (2015).

- Heavy metals and human health: Mechanistic insight into toxicity and counter defense system of antioxidants. *International Journal of Molecular Sciences*, 16(12), 29592–29630. <http://doi.org/10.3390/ijms161226183>
- Jeffrey, S. F. (2000). Iron poisoning. *Current Problems in Pediatrics*, 30(3), 71–90. <http://doi.org/10.1067/mps.2000.104055>
- Jennings, S. R., Neuman, D. R., & Blicher, P. S. (2008). Acid Mine Drainage and Effects on Fish Health and Ecology : A Review, (June).
- Kashefipour, S. M., & Roshanfekar, A. (2012). Numerical Modelling of Heavy Metals Transport Processes in Riverine Basins. *Numerical Modelling*, 91–114. <http://doi.org/10.5772/2292>
- Kim, H. S., Kim, Y. J., & Seo, Y. R. (2015). An Overview of Carcinogenic Heavy Metal: Molecular Toxicity Mechanism and Prevention. *Journal of Cancer Prevention*, 20(4), 232–40. <http://doi.org/10.15430/JCP.2015.20.4.232>
- Kim, J., & Kwak, S. (2017). Efficient and selective removal of heavy metals using microporous layered silicate AMH-3 as sorbent. *Chemical Engineering Journal*, 313, 975–982. <http://doi.org/10.1016/j.cej.2016.10.143>
- King, S. W., Savory, J., & Wills, M. R. (1981). Aluminum Toxicity in Relation to Kidney Disorders. *Annals of Clinical and Laboratory Science*, 11, 337–342.
- Krantzberg, P. G., Tamik, A., Simao, J. A. do C., Indarto, A., & Ekda, A. (2010). Advances in Water Quality Control. *Scientific Research Publishing, USA*, (USA). Retrieved from <http://www.scirp.org>
- Kwakye, G. F., Paoliello, M. M. B., Mukhopadhyay, S., Bowman, A. B., & Aschner, M. (2015). Manganese-induced parkinsonism and Parkinson's

disease: Shared and distinguishable features. *International Journal of Environmental Research and Public Health*, 12(7), 7519–7540.

<http://doi.org/10.3390/ijerph120707519>

Loague, K., & Corwin, D. L. (2016). Point and NonPoint Source Pollution, (April 2006). <http://doi.org/10.1002/0470848944.hsa097>

Mahurpawar, M. (2015). Effects of heavy metals on human health.

International Journal of Reseach-Granthaalayah, 2350(530), 2394–3629.

Maleki, S., & Karimi-jashni, A. (2017). Applied Clay Science Effect of ball milling process on the structure of local clay and its adsorption performance for Ni (II) removal. *Applied Clay Science*, 137, 213–224.

<http://doi.org/10.1016/j.clay.2016.12.008>

Mehdi, A., & Agency, U. S. E. P. (2008). *Environmental Engineering*

Dictionary. U. S.A.: Babylon. Retrieved from

<http://www.ecologydictionary.org/Acclimation>

Muysen, B. T. A., & Janssen, C. R. (2001). Zinc acclimation and its effect on the zinc tolerance of *Raphidocelis subcapitata* and *Chlorella vulgaris* in laboratory experiments. *Chemosphere*, 45(4–5), 507–514.

[http://doi.org/10.1016/S0045-6535\(01\)00047-9](http://doi.org/10.1016/S0045-6535(01)00047-9)

Pintilie, S., , Loredana Brânză, C. B., Pavel, L. V., Ungureanu, F., &

Gavrilescu, M. (2007). Modelling and Simulation of Heavy Metals

Transport in Water and Sediments, (February). Retrieved from

https://www.researchgate.net/profile/Maria_Gavrilescu/publication/233754784_MODELLING_AND_SIMULATION_OF_HEAVY_METALS_TRANSPORT_IN_WATER_AND_SEDIMENTS/links/0912f51497bd887f46000000.pdf

Plum, L. M., Rink, L., & Hajo, H. (2010). The essential toxin: Impact of zinc on

- human health. *International Journal of Environmental Research and Public Health*, 7(4), 1342–1365. <http://doi.org/10.3390/ijerph7041342>
- Rico, M. C., Hernández, L. M., & González, M. J. (1989). Water contamination by heavy metals (Hg, Cd, Pb, Cu and Zn) in Doñana National Park (Spain). *Bulletin of Environmental Contamination and Toxicology*, 42(4), 582–588. <http://doi.org/10.1007/BF01700241>
- Saha, J. C. J., Dikshit, A. K. A., Bandyopadhyay, M., & Saha, K. C. (1999). A Review of Arsenic Poisoning and its Effects on Human Health. *Critical Reviews in Environmental Science and Technology*, 29(3), Saha, J. C. J., Dikshit, A. K. A., Bandyopadhyay, M. [http://doi.org/1064-3389/99/\\$.50](http://doi.org/1064-3389/99/$.50)
- Santamaria, A. B. (2008). Manganese exposure, essentiality & toxicity. *Indian Journal of Medical Research*, 128(4), 484–500. <http://doi.org/10.5897/AJEST12.196>
- Sdiri, A., Higashi, T., Hatta, T., Jamoussi, F., & Tase, N. (2011). Evaluating the adsorptive capacity of montmorillonitic and calcareous clays on the removal of several heavy metals in aqueous systems. *Chemical Engineering Journal*, 172(1), 37–46. <http://doi.org/10.1016/j.cej.2011.05.015>
- Shakhashiri. (2011). Water. *General Chemistry*, (Chemical of the Week), 1–7.
- Solomon, F. (2008). Impacts of Metals on Aquatic Ecosystems and Human Health. *Environment and Communities*, (April).
- Suciu, N. (2014). Diffusion in random velocity fields with applications to contaminant transport in groundwater. *Advances in Water Resources*, 69, 114–133. <http://doi.org/10.1016/j.advwatres.2014.04.002>
- Tang, W., Duan, S., Shan, B., Zhang, H., Zhang, W., Zhao, Y., & Zhang, C. (2016). Concentrations, diffusive fluxes and toxicity of heavy metals in pore water of the Fuyang River, Haihe Basin. *Ecotoxicology and*

Environmental Safety, 127, 80–86.

<http://doi.org/10.1016/j.ecoenv.2016.01.013>

Thibodeaux, L., & Mackay, D. (2010). *Handbook of chemical mass transport in the environment*. Retrieved from

https://www.google.com/books?hl=en&lr=&id=dYbLBQAAQBAJ&oi=fnd&pg=PP1&dq=Handbook+of+chemical+mass+transport+in+the+environment&ots=pdAG4m9mRD&sig=CyENVH9_2euVqyEtAYqweG6qKjg

Trivedi R.C. (2003). Effects and source of water pollution. In '*Water quality standards*', *Int. Conf. on water quality Management* (p. 12). New Delhi: Int. Conf. on water quality Management.

Vandas, S. J., Winter, T. C., & Battaglin, W. A. (2002). *Water and the environment*. (U. S. G. S. Bureau of Reclamation , National Park Service, U.S. Army Corps of Engineers, USDA Forest Services, Ed.) (American G). Retrieved from <https://books.google.com.gh/books?id=sWXxAAAAMAAJ>

Vested, H. J., Olesen, W. K., Refsgaard, A., Engesgaard, P., & Malmgren-Homen, A. (1993). Advection - Dispersion Review Rivers and Groundwater. *ISPRA-Institute for Systems Engineering and Information, EUR 15107*(Commission of the European Communities-Joint Research centre).

Vieira, M. E. C., & Bordalo, A. A. . (2000). The Douro estuary (Portugal): a mesotidal salt wedge, 23(0).

Wendy, G., & Sabine, M. (2009). Human Health Effects of Heavy Metals. *Environmental Science and Technology*, (Center for Hazardous Substance Research-Kansas State University), 1–6. Retrieved from www.engg.ksu.edu/CHSR

Wolfram Research, I. (2017). Molar Volume of the elements. Retrieved 9 July

2017, from <http://www.periodictable.com/Properties/A/MolarVolume.html>

Younger, L. P., Banwart, S. A., & Hedin, S. R. (2002). *Mine Water_ Hydrology, Pollution, Remediation*.

Zaporozec, A. (2002). *Ground water contamination inventory* (Serie N° 2).

International Hydrological Programme Project 3.1 (IHP-V)-UNESCO.

Ziemen, G. E., & Castleman, B. I. (1989). Threshold Limit Values Historical Perspectives.pdf. *Journal of Occupational Medicine*, 31(N° 11), 9.

Annexes

Table 10: Dimensions of the pipe and velocity calculation

Mesured dimensions of The Pipe	
Q Exiting Fibrocimento (L/min)	4.5
Q(L/sec)	0.075
Diametre of Fibrocimento Pipe(m)	0.000245103
Calculated dimensions of the Pipe	
S:Section of Fibrocimento Pipe ($\text{Pi} \cdot (\text{D}/2)^2$)(m ²)	0.237582944
Equivelent section(Section/10*) (m ²)	0.023758294
Velocity (Q/S) (m/sec)	0.003156792

*The number 10 for the equivelent section indicate that water occude 1/10 of the pipe

Table 11: Diffisivity calculation (Wolfram Research, 2017)

Element	Φ1	Φ2	η(μPas) at 20°C	η(cP)	M	T	V*	D1	D2
Al	2.26	2.6	1002	1.002	18	293	$9.999 \cdot 10^{-6}$	0.44192042	0.117100381
Cu	2.26	2.6	1002	1.002	18	293	$7.124 \cdot 10^{-6}$	0.541606245	0.142981004
Fe	2.26	2.6	1002	1.002	18	293	$7.0923 \cdot 10^{-6}$	0.543057419	0.143357073
Mn	2.26	2.6	1002	1.002	18	293	$7.354 \cdot 10^{-6}$	0.531356648	0.140324311
Zn	2.26	2.6	1002	1.002	18	293	$9.161 \cdot 10^{-6}$	0.465749375	0.123295824
As	2.26	2.6	1002	1.002	18	293	$1.308 \cdot 10^{-5}$	0.376108825	0.099956641
Ni	2.26	2.6	1002	1.002	18	293	$6.588 \cdot 10^{-6}$	0.56758932	0.149711172
Pb	2.26	2.6	1002	1.002	18	293	$1.827 \cdot 10^{-5}$	0.307784226	0.08209954

Table 12 : Kinetic constant estimation

Element	Kinetic constant (1/min)	Kinetic constant (1/sec)
Al	0,00898	0,000149667
Fe		0,00007
Pb	0,0299	0,000498333
Mn		0,0001
Cu	0,00804	0,000134
Zn	0,00845	0,000140833
As		0,0002
Ni	0,003	0,00005